PHILOSOPHICAL TRANSACTIONS OF THE ROYAL SOCIETY A MATHEMATICAL, PHYSICAL & ENGINEERING SCIENCES

Mechanics of Deep Underground Explosions

P. Chadwick, A. D. Cox and H. G. Hopkins

Phil. Trans. R. Soc. Lond. A 1964 **256**, 235-300
doi: 10.1098/rsta.1964.0006

MECHANICS OF DEEP UNDERGROUND EXPLOSIONS

By P. CHADWICK†

Department of Applied Mathematics, University of Sheffield

A. D. COX and H. G. HOPKINS

Royal Armament Research and Development Establishment, Fort Halstead, Sevenoaks, Kent

(*Communicated by Sir William Penney, F.R.S.—Received* 17 *April* 1963)

CONTENTS

† Formerly at the United Kingdom Atomic Energy Authority, Atomic Weapons Research Establishment, Aldermaston.

Vol. 256. A. 1070. (Price £1. 4*s*.; U.S. $3.60) 29 [Published 23 July 1964

Discussion of the effects of explosions in soils is complicated by many factors, foremost among which are the physical characteristics of natural soils. In this paper, certain aspects of the mechanics of deep underground chemical explosions are treated theoretically in terms of a model of the physical situation. This model refers to the dynamic expansion of a spherical cavity in a plastic-elastic, incompressible, ideal soil of infinite extent, and it is analogous to one which has been used in studies of underwater explosions.

The main predictions of the model studied are as follows. In all cases of practical interest, the expansion of the cavity is large and occurs rapidly, with an extensive region of the surrounding soil undergoing plastic deformation. The amplitudes of any subsequent pulsations are small. The features of the disturbance show much dependence upon the type of soil and upon the depth at which the explosion takes place.

The present model seems to provide an acceptable account of some of the qualitative features of cavity formation due to a deep underground explosion. Furthermore, some quantitative agreement is found between predicted and observed sizes of cavities in one special case.

Notation

A list of symbols is given below. All notation is defined when first introduced in the paper, but it should be noted that a few symbols have different meanings in different contexts.

E	Young's modulus
μ	shear modulus
ν	Poisson's ratio
c	cohesion
ϕ	angle of internal friction
$Y = 2c\cos\phi/(1-\sin\phi)$	yield stress parameter
$\alpha = 2\sin\phi/(1-\sin\phi)$	shear resistance parameter
ρ	density

(the first seven rows: soil physical constants)

S, P, Z, MS	referring to different types of ideal soil (see § 4·2·3)
P	pressure exerted by TNT explosion products on camouflet surface
γ_1, γ_2	adiabatic indices for TNT explosion products
$\mathscr{E}$	energy release of explosive charge
p_a	atmospheric pressure
h	depth of burial of explosive charge
g	acceleration due to gravity
$\Pi = p_a + \rho g h$	initial uniform hydrostatic pressure in ideal soil
$ex, s, a, 0$	subscripts referring to explosion products, soil, atmosphere and initial conditions
r	radial co-ordinate
t	time
u, v	radial displacement and velocity
$\dot{F} \equiv \dfrac{\mathrm{D}F}{\mathrm{D}t} = \dfrac{\partial F}{\partial t} + v\dfrac{\partial F}{\partial r}$	convective derivative of any function F
$\sigma_r, \sigma_\theta, \dot{\epsilon}_r, \dot{\epsilon}_\theta$	radial and tangential components of stress and strain rate tensors
$\dot{\epsilon}_r^e, \dot{\epsilon}_\theta^e, \dot{\epsilon}_r^p, \dot{\epsilon}_\theta^p$	radial and tangential components of elastic and plastic strain rate tensors
f	yield function
$\dot{\lambda}$	plastic flow-rate parameter
$\dot{W}, \dot{W}^e, \dot{W}^p$	total, elastic, and plastic rates of work done on soil (per unit volume)

a radius of camouflet surface

b, d radius of plastic-elastic boundary during first expansion and contraction phases, respectively

U_1 total energy input from explosion products

U_2 potential energy stored at infinity

U_3 total elastic strain energy in soil

U_4 total plastic work done on soil

U_5 total kinetic energy of soil

} components of partition of energy

t_i $(i = 1, 2, \ldots)$ durations of successive expansion and contraction phases of camouflet motion

$t_{i,e}$, $t_{i,p}$ $(i = 1, 2, \ldots)$ durations of elastic and plastic-elastic parts of phases of camouflet motion

1. Introduction

Discussion of the effects of explosions in soils is complicated by many factors, foremost among which are the physical characteristics of natural soils. Progress in understanding the mechanics of the phenomena involved is not easily achieved, and previous investigations have led only to rather limited conclusions. In this paper, attention is confined to the simplest situation, namely that of an underground chemical explosion occurring at such a depth that only effects essentially associated with elastic stress waves are propagated to ground level. This situation is of central importance in the general subject of explosive action in soils. The model of cavity or camouflet motion studied here is an approach to the study of underground explosions. It is believed to provide a realistic account of some of the qualitative features involved, although the interpretation and assessment of the quantitative predictions obtained is uncertain due to the inherent limitations of the model assumed and to a lack of sufficient experimental data.

It should be noted that the term *camouflet* is used in military mining to designate a mine charge which, when exploded, has no disruptive effect at ground level (see, for example, the *Encyclopædia Britannica*). Although the original meaning of *camouflet* was the mine charge itself, it is here used to refer to the cavity produced by the explosion.

The reasons for the present study arise from the failure of Hopkinson's size-scaling law to apply to large explosions and also the need to extend earlier studies of camouflet motion due to G. I. Taylor and W. G. Penney (see § 2). There is no direct concern here with the art of military mining.

The contents of this paper are set out in three parts arranged as follows. Part I is concerned with certain preliminary considerations. It gives a discussion of the effects of explosions in soils and the approaches made to their study, and an account of the dimensional theory of explosions in soils. It also gives an outline of the physical properties of *TNT* explosion products and of *natural* soils such as clays and sands, together with a discussion of the idealization of these properties assumed in the remainder of the paper. In part II, attention is given to the theoretical mechanics of *ideal* soils and the basic equations of spherical plastic-elastic motion are derived. Part III is concerned chiefly with models of camouflet motion due to Taylor and Penney and to the present authors, and detailed theories together with numerical values are given. Finally, concluding remarks on the investigation are made.

PART I. PRELIMINARY CONSIDERATIONS

2. Effects of explosions in soils

2·1. *General background*

The general subject of explosion phenomena in soils embraces a wide range of topics which are of considerable importance from both military and civil viewpoints. The problems which merit attention are generally characterized by complexity and uncertainty of the physical situation and by attendant mathematical difficulties in their theoretical study. In particular, owing to the difficulty of developing satisfactory theoretical studies of crater and camouflet formation, much reliance has perforce been placed upon simple scaling laws. Such laws correlate the results observed for explosions of different sizes and, within their range of validity, enable predictions to be made of the effects of an explosion of any given size.

Until the end of World War II, the largest size of chemical explosion occurring in circumstances where predictions of the effects were needed was about 50 T (T denoting 10^9 cal, the approximate energy release of a ton of *TNT*), and it was found that the size-scaling law due to Bertram Hopkinson (see § 3·1) led to reasonably satisfactory results. However, the development of nuclear devices has greatly extended the size of man-made explosions, up to those having an energy release of the order of 100 MT. Also, tests undertaken in the United States Atomic Energy Commission's series of nuclear and chemical explosions for peaceful purposes ('Project Plowshare') have involved chemical explosions of sizes up to 450 T.

Now Hopkinson's size-scaling law, in the form in which it is usually applied, states, for example, that the diameter and the depth of the crater formed by an explosion at ground level are both directly proportional to the cube-root of the charge volume or, equivalently, to a typical linear dimension of the charge (see § 3·1). Although Hopkinson was concerned solely with chemical explosions, it is only necessary in the proof of his law to confine attention to some particular class of explosions in which the nature of the explosive and the surrounding medium are invariable. Within that class, it is predicted that the shape (say, the quotient of the depth and the diameter) of the crater formed by an explosion at ground level remains the same. However, this prediction that crater shape is independent of explosion size is now known not to be verified by the observed results. Thus craters formed by nuclear explosions become relatively more shallow as the explosion size increases. More precisely, the experimental data (see Glasstone 1962, pp. 289–296) show that, within the range of size of nuclear explosions, the crater diameter and depth increase in proportion approximately to the one-third and one-fourth powers of the total energy released. A similar trend seems likely also to be the case for chemical explosions, although this does not appear to have yet been definitely established. It may also be noted that lunar (and perhaps also terrestrial) craters, the formation of which is attributed by some authorities to the impact of meteorites, show the same trend of increasing relative shallowness with size (see, for example, Hill & Gilvarry 1956).

The failure of Hopkinson's law to correlate the effects of explosions of high energy yield is one reason for renewed interest in theoretical studies of the mechanics of explosions in soils. A likely explanation of this failure follows from the assumption, made in the derivation

of Hopkinson's size-scaling law, that effects due to gravity are negligible (see § 3·1). It is customary, however, in soil mechanics to describe the condition for the onset of plastic flow in a typical natural soil by Coulomb's law of failure (see § 4·2·2). Coulomb's law states that the shear stress at which flow occurs is the sum of a constant cohesive stress and a frictional stress that increases linearly with the normal component of the stress vector. Although this law is based upon experiments carried out at low stresses and strains, a similar trend, not necessarily linear, seems likely under explosion conditions. Thus the resistance to relative movement in a region of soil undergoing plastic deformation will increase, often markedly, with depth. Such an effect invalidates the basis of Hopkinson's size-scaling law, which is therefore expected to fail ultimately for extrapolations to large explosions, certainly in respect of results for quantities associated with the vertical direction, such as crater depth. Hence the applicability of Hopkinson's size-scaling law is limited to relatively small explosions.

2·2. *Previous theoretical studies*

Dimensional analysis provides a qualitative approach to the study of explosion phenomena in soils. This approach was used in the unpublished work, dating from about 1915, of Hopkinson, which led to the size-scaling law discussed in § 2·1.

Taylor (1940) in his work on the theory of one-dimensional, finite amplitude, plastic wave propagation uses a version of this theory to discuss the propagation of earth waves from an explosion; he notes that the governing equations are formally identical with those for the propagation of one-dimensional, finite amplitude waves in a compressible perfect fluid (the pressure being a function only of the density), although the correspondence between the two situations exists only for loading waves, since solid materials exhibit hysteresis in the plastic range. Taylor's work is closely related to analysis by Th. von Kármán, Kh. A. Rakhmatulin and others (see, for example, Craggs 1961 and Hopkins 1961).

Some other work which concerns the propagation of shock waves and the formation of cavities is of general interest in connexion with the present study. The present treatment of camouflet formation in soils is essentially an extension of that of cavity formation in metals, discussed by Hopkins (1960). Some general accounts of work on shock waves, particularly in metals, are given by Rinehart & Pearson (1954, chap. 9 and 10) and Hopkins (1961), primarily from experimental and theoretical viewpoints, respectively (see also Stanyukovich 1960, pp. 568 *et seq.*). There is also extensive Russian work concerning explosions in soils under spherically symmetric conditions. Much of this interesting work is essentially based upon the hypothesis of finite compaction in soils, and it is discussed further in § 7·3 (see also Cristescu 1958, pp. 227 *et seq.*; 1960).

The first step towards a quantitative treatment of the problem of camouflet formation was made by Devonshire & Mott (1944), although no account was taken of the frictional strength of soils. This treatment was based upon earlier work by Bishop, Hill & Mott (1945) concerning static deep-punching in metals (see Hill 1950, p. 104), but important quantitative differences were found as a result of the values of Young's modulus and yield strength being much smaller for soils than for metals. Hill (1948) later derived dynamical equations to describe the formation of spherical camouflets in ideal soils, frictional strength and compressibility being neglected. The main purpose of Hill's work was to discuss the problem

in general terms, and no attempt was made to derive detailed quantitative results from the theory.

The limitations of the above theoretical studies of explosion phenomena in soils were apparently first appreciated by Taylor and Penney, who suggested a new approach for more realistic studies that took account of the frictional as well as the cohesive strength of soils. This approach was applied by Penney (1954, private communication) to a discussion of the mechanics of camouflet formation by underground explosions and of crater formation by surface explosions. In the former case, the object was first to provide predictions of the sizes of camouflet produced by chemical explosions, reasonable agreement being found with observed values (although these are not extensive), and secondly, to afford some general understanding of the mechanics of explosion phenomena in soils. In the latter case, the object was to provide size-scaling laws valid for large explosions to replace Hopkinson's law which, as stated in § 2·1, is valid only for small explosions. Penney's analysis of crater formation by large chemical explosions assumes that the crater and the associated soil deformation are identical with those caused by slowly thrusting a rigid sphere into the ground. It is supposed that the radius of this sphere increases linearly with the cube-root of the total energy release, the constant of proportionality being determined from small-scale experimental data. Then, assuming that the energy available for crater formation is a constant fraction of the total energy released by the chemical explosion, and making plausible assumptions for the non-linear law of resistance to the penetration of the sphere, it is possible to estimate crater sizes. Penney predicts that for sand and clay, and for a range of crater diameter from 20 to 4000 ft., crater diameter and depth vary as the 0·30 and 0·24 powers of the energy release. These results exhibit the same trend as the experimental data quoted in § 2·1.

The agreement achieved between experimental data and the theoretical predictions based upon the approach of Taylor and Penney to crater and camouflet formation gives confidence in the mathematical models that they used. At the same time, the fact that their studies are incompletely developed has needed to be remedied by further work. In this paper the approach made by Taylor and Penney to underground explosions is elaborated and a more comprehensive study of the mechanics of camouflet formation is undertaken. Although the methods of plasticity theory are not universally appropriate to studies of situations involving large deformations in soils caused by explosions, here at least this approach seems to be justified.

2·3. *Sequence of events in underground explosions*

In continuing this account of preliminary considerations, it is appropriate to discuss briefly the essential phenomena characterizing an underground explosion. It should be noted that there are some similarities, and at the same time important differences, between the cognate problems of explosions in condensed media such as soils, metals and water. There is much qualitative information on the sequence of physical events due to an explosion taking place in a solid or liquid medium. For detailed discussions of explosion phenomena in water and soils, Cole (1948) and Glasstone (1962) should be consulted (see also Pokrovskiĭ & Fedorov 1957).

The disturbance created by an explosion that produces a camouflet is primarily the result

of the exchange of energy between the gaseous explosion products and the surrounding soil. The energy source envisaged here is that provided by a spherical charge of chemical high explosive, say, for definiteness, *TNT*.

The physics of the detonation of a spherical charge of *TNT* does not depend upon the nature of the surrounding medium. This process has been described, for example, by Cole (1948, chap. 3). Assuming that initiation takes place at the centre of the charge, the outward motion of the detonation front and the variation of the physical and chemical properties of the gases in its wake are described by the hydrodynamical-chemical theory of spherical detonation waves. The motion is characterized by geometrical similarity, the pressure being of the order of 10^5 atm. and the temperature being about 3000 °C at the detonation front. At the instant of arrival of the detonation wave at the charge surface, where the surrounding soil is at rest, there occurs a sudden and extremely violent blow on the soil face. The immediate effect of the blow is the propagation of a disturbance (normally a shock wave) outwards into the hitherto undisturbed soil. Simultaneously, a rarefaction wave is reflected inwards through the gaseous explosion products, and there is no longer geometrical similarity. Owing to dissipative processes and spherical divergence, the disturbance propagated outwards into the soil is attenuated and ultimately it decays into an elastic wave. The material behind the shock front is heated irreversibly and, at the same time, set in outward motion. Although particle velocities in the wake will not be small, the associated displacements are not comparable with those occurring in the subsequent stages of the motion, when the camouflet first enlarges considerably and later on executes pulsations. Owing to successive wave reflexions at the camouflet surface and centre, there are rapid fluctuations of pressure in the explosion products, but after a very short time the major part of the soil shock wave may be considered to have been emitted. In the process, there will have been a considerable reduction of the total energy retained by the gases, and the repeated passage of waves through them will to some extent have effected more uniform conditions. Earlier, the cohesive and, perhaps, frictional strengths were negligible factors in determining the mechanical behaviour of the soil near the camouflet surface, the soil behaving much like a compressible fluid medium at these high stress intensities. Under the much-reduced stress intensities now prevailing, the mechanical behaviour of the soil is expected to be closer to that normally encountered in civil engineering practice, although some changes associated, for example, with compaction may have occurred (see § 7·3).

The main part of the first expansion phase of camouflet motion may now be considered to have been originated; it takes place behind the soil shock wave. In other words, the outward motion of the camouflet surface can be regarded approximately as being due to the expansion of the gaseous explosion products, the energy of which has been reduced by the transference of energy to the soil shock wave. In the ensuing motion, the inertia of the soil and the mechanical properties of the explosion products and the soil provide the necessary conditions for oscillatory motion with non-linear damping.

Qualitatively, camouflet motion may be expected to exhibit some similarities with underwater bubble motion. Thus, in particular, some oscillatory motion of the camouflet surface is to be expected. However, although this does occur, one prediction of the present model is that, in all practical circumstances, the amplitude of the pulsations subsequent to the first expansion phase is small (see § 7·1·7). Thus there is an important quantitative difference

between the motion of camouflets and of bubbles. The motion in the first expansion phase is damped by plastic deformation, which involves the dissipation of mechanical energy. Although its amplitude is not large, there is some inward motion after the end of this phase. Subsequently, damping is due to the propagation of elastic strain energy to large distances and to dissipative processes in the soil and, to a lesser extent, in the explosion products. Thus the strength of soils and their capacity for dissipating mechanical energy by plastic deformation result in marked differences between the detailed quantitative effects of explosions in soils and in water. In particular, camouflet motion consists almost entirely of one half-period of oscillation, namely the first expansion phase. Penney (1954, private communication) has described this type of motion as *dead-beat*, and although this term has a different meaning in dynamics, it is a convenient one in the present context.

2·4. *Aims and methods of the present investigation*

The purpose of this paper is to give a connected theoretical treatment of a model of the mechanics of camouflet formation. It will be assumed that the motion is spherically symmetrical. This is valid to a sufficient degree of approximation if the region of soil subjected to plastic deformation is reasonably homogeneous and does not extend to ground level, and if appropriate account is taken of soil weight. Thus only effects essentially associated with elastic stress waves are propagated to ground level. This condition means of course that, for a given depth of charge burial, the situation envisaged becomes progressively less realistic with increase in the size of explosion. Moreover, no account can be taken of soil stratification.

Figure 1 is a schematic representation of the soil disturbance associated with an expanding camouflet, and it shows the zones of elastic and plastic deformation and also the zone of fracture. In the present study, the possible occurrence of soil fracture is for convenience ignored, the fracture zone therefore being combined with the plastic zone.

The most important objective of a theory of camouflet motion is to predict the variation with time of the radii of the camouflet surface and the plastic-elastic boundary. Also of interest is the determination of the fractions of the charge energy converted into shock wave energy, elastic strain energy, plastic work and kinetic energy of the soil. Inasmuch as camouflet motion appears to be dead-beat, practical interest is centred largely upon the first expansion phase.

The above quantities depend upon a large number of physical properties of the explosion products and the soil. Simple dimensional analysis (discussed in § 3) provides a qualitative approach and leads to scaling and modelling laws, valid under certain conditions, of particular interest in connexion with the design and interpretation of experiments and with the prediction of results. Although it is possible to include formally in such an analysis all physical properties believed to be of any appreciable significance, such generality is only achieved at the expense of detailed quantitative predictions. A quantitative theoretical study of camouflet motion can only be developed on the basis of mathematical models of underground explosions which portray a simplified description of the complex physical processes involved in practice. The first aim of theoretical investigations is to identify the physical processes which determine the main features of the disturbance. Ultimately, a reasonably simple theory is required which is based upon realistic physical simplifications

PHILOSOPHICAL TRANSACTIONS OF THE ROYAL SOCIETY A MATHEMATICAL, PHYSICAL & ENGINEERING SCIENCES

of the true situation and which leads to quantitative predictions to be judged against experimental data.

A model of underground explosions necessarily requires some simplification of the true mechanical behaviour of both the explosion products and the soil, and this is discussed in § 4. The basic equations governing the model of camouflet motion are developed in § 5, with restriction to spherical motion. One further matter finally requires attention, namely the allowance to be made for the effects of gravity. The simple assumption is made that the soil is initially in a state of *uniform hydrostatic pressure* taken equal to the sum of the atmospheric pressure and the overburden pressure at the position of the charge centre (cf. Cole 1948, chap. 8). In this way some allowance is made for the weight of the soil without violating the restriction to spherical symmetry.

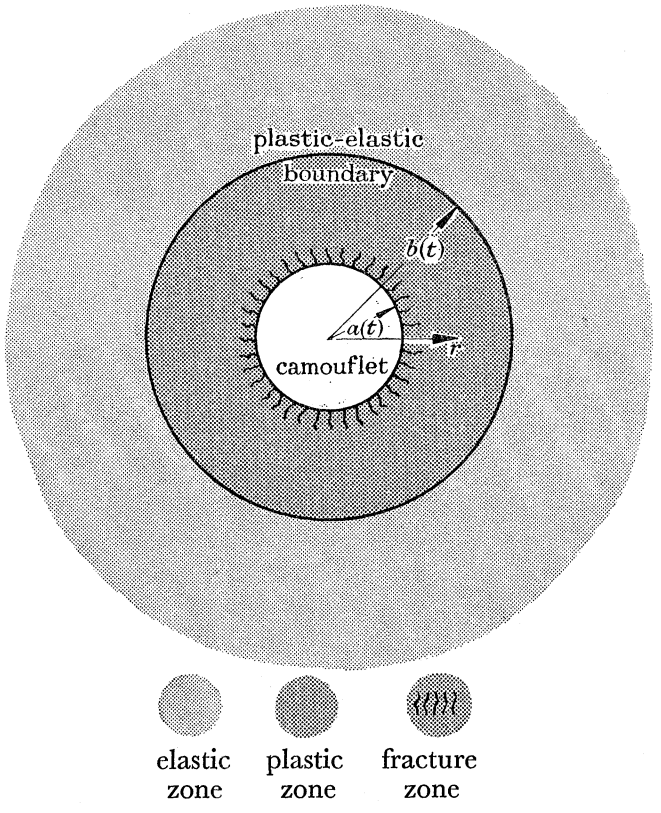

FIGURE 1. Schematic representation of disturbance in soil due to an expanding camouflet.

The above approach to camouflet motion leads to a precise mathematical problem of the propagation of non-linear plastic-elastic waves due to pressure applied at the surface of a spherical cavity in an infinite medium. The complexity of this problem is apparent. Therefore, in order to achieve some simplification of the analysis, it is assumed that there is isochronous motion, as in the analysis of underwater explosions (cf. Cole 1948, chap. 8). This means that all wave propagation phenomena are ignored, either compressibility or inertial effects being everywhere neglected. This assumption is consistent with the absence of a direct treatment of the soil shock wave. It is further assumed that the explosion products are at uniform pressure, that volume changes take place adiabatically, and that the energy has been reduced to one-third of the detonation energy owing to the emission of the shock wave. These assumptions are known to be realistic in studies of underwater bubble motion.

The value of the fraction of the detonation energy carried by the shock wave has no significance in analysis, but it does affect the numerical predictions. The true value, appropriate to given circumstances, is not known. Here, a value fixed at two-thirds is assumed, this being suggested by its validity for underwater explosions. Comparison between experimental data and theoretical predictions may lead to a revision of this provisional estimate.

The above model of camouflet motion is amenable to detailed theoretical analysis, but the computational work required to obtain numerical values in particular cases is beyond the scope of hand calculation. The arithmetic has therefore been done on the I.B.M. computers at Aldermaston. In § 6, the detailed theory of a point source model of an underground explosion, due to Taylor and Penney, is developed. This fictitious situation, which represents essentially an extrapolation of the real one, provides a simple but useful approximate description of the first expansion phase of camouflet formation. In § 7, the detailed theory of a spherical charge model of an underground explosion is developed, and attention is given to the first expansion phase, including its initial stages, and to the pulsations which follow this phase. This latter theory and some other elaborations of the original theory of Taylor and Penney are due to the present authors. The various theories of camouflet motion under isochronous conditions discussed here, although quite closely related, exhibit some important differences. The nature of these differences and the reasons for their existence are connected with the conditions assumed at the initiation of the first expansion phase and with some degree of freedom in the choice both of elastic stress-strain relations and of assumptions necessary for isochronous motion. Numerical values are presented for three typical ideal soils representing a fully saturated clay, a dry sand and a partly saturated clay or mixed soil. In certain cases, numerical values are given for different theories and a comparison between them effected. The values obtained for the final camouflet sizes are compared with the very limited experimental data available. Also included in § 7 is some discussion, appropriate to conditions of camouflet formation, of the changes in the strength of soils due to rate-of-strain effects and of the choice of finite elastic stress-strain relations for soils.

3. Dimensional theory of explosions in soils

Dimensional analysis provides a simple, albeit limited, approach to the study of camouflet formation in soils. Field quantities (such as displacements, velocities, stresses, etc.) associated with the motion all depend upon a large number of physical properties of the explosion products, the soil and the atmosphere, upon the geometrical features of the situation and upon gravity. The important quantities include the variations with time of the camouflet radius, the energy partition and the extent of the region of plastic deformation. The particular values of these quantities at the termination of the first expansion and contraction phases of the motion are of considerable interest. Although it is possible to include formally in a dimensional analysis all the physical properties concerned, or at least those believed to be of any appreciable significance, such generality is only achieved at the expense of quantitative information. However, the importance and usefulness of a dimensional analysis of a physical situation is that it leads directly to scaling and modelling laws, valid of course under certain specified conditions.

3·1. *Hopkinson's size-scaling law*

Scaling and modelling laws for explosions in various media are widely known and used, but unfortunately not always with a proper realization and understanding of their limitations. Of particular interest here is Hopkinson's law of size-scaling, and it is important to understand correctly the bases and limitations of this law in connexion with explosions in soils. Thornhill (1957) has stated Hopkinson's law of size-scaling for explosions as follows: 'If two explosions are identical in all but size, then they are mathematically identical when expressed in units derived from the same fundamental pressure and velocity and a fundamental length proportional to the linear dimensions of the charge.'

The analysis required to establish Hopkinson's size-scaling law for explosions in soils may be given under quite general assumptions. In contrast, it is necessary to recognize the limitations of the models of camouflet formation given later in this paper, which reflect the considerable physical simplifications made. So far as the present discussion is concerned, it is not necessary to specify all the relevant physical properties of the explosion products, the soil and the atmosphere, since these properties remain the same within any one class of explosions. It should be noted, however, that detailed specification of the more important of these physical properties would be necessary in any discussion of modelling laws correlating effects for different classes of explosions involving, say, different types of explosives and soils. Modelling laws are not considered here, attention being confined to Hopkinson's size-scaling law.

Since the relevant physical properties need not be specified in detail, account is taken implicitly of such effects as non-linear compressibility (perhaps resulting in the formation of shock waves), rate of strain and work hardening or softening in the soil, as well as departures from conditions of spherical symmetry. None of these effects is directly included in the later theoretical analysis of this paper. The situation envisaged here is one in which the depth of charge burial is sufficiently great for the camouflet surface not to reach ground level. Nevertheless, if a crater is formed, the main arguments of the present section are not affected. In the case of camouflet formation, the disturbance produced in the air is unlikely to be of appreciable significance, even for quite shallow explosions.

Suppose that, following detonation, the motion depends upon certain sets of quantities which characterize the physical properties and geometrical features of the explosion products, the soil and the atmosphere, together with the bodily effect of gravity. Let q_{ex}, q_s and q_a denote these sets of quantities. Then, for example, q_{ex} would include, on the assumption that the explosion products constitute an ideal polytropic gas, the velocity of sound behind the detonation front, the detonation velocity and the adiabatic index; q_s would include elastic and plastic constants; and q_a would include atmospheric pressure, velocity of sound and adiabatic index. The geometrical features include the size, shape and position of the explosive charge. It is sufficient to define explicitly only the following quantities:

l, h	representative linear dimension for charge size, and depth of charge burial
V_p	velocity of longitudinal elastic waves in soil
p_a	atmospheric pressure at ground level
g	acceleration due to gravity.

Thus, according to the present scheme, the quantities involved are q_{ex}, q_s and q_a (not explicitly described), together with l, h, V_p, p_a and g.

Let the fundamental pressure, velocity and length be p_a, V_p and l. Since no reference is made to thermal properties, the dimensions of temperature are conveniently supposed to be given in terms of the present mechanical system of dimensions. In the above system of units, the fundamental units of mass, length and time are $M = l^3 p_a V_p^{-2}$, $L = l$ and $T = l V_p^{-1}$. Let Q denote any physical quantity which is dependent upon the motion, and $[Q]$ be that combination of the fundamental dimensions (i.e. p_a, V_p and l) having the same dimensions as Q. Then $Q' = Q/[Q]$ is the corresponding non-dimensional (or reduced) physical quantity. In principle, on the basis of known physical laws, the problem of an explosion in a soil could now be completely formulated in terms of a system of equations, together with associated initial, boundary and continuity conditions, all expressed in non-dimensional form. Let x_i $(i = 1, 2, 3)$ be rectangular Cartesian co-ordinates with their origin at the centre of the camouflet, and t be time measured from a convenient instant. Then $x_i' = x_i/l$ and $t' = V_p t/l$ are the corresponding non-dimensional co-ordinates and time. It follows that any quantity Q' is determined as a function of the reduced space and time variables x_i' and t' and of the non-dimensional modelling parameters q_{ex}', q_s', q_a', h/l and gl/V_p^2 (the quantities V_p' and p_a' having been universally reduced to unity). In mathematical terms,

$$Q' = Q'(x_i', t'; q_{ex}', q_s', q_a', h/l, gl/V_p^2). \tag{3·1}$$

On the basis of any assumed mathematical model of the physical problem (such as those considered in later sections of this paper), direct inspection of the governing equations might reveal that not all the modelling parameters occur independently. Although this result would permit some simplification of the form of the function Q', it has no direct significance here.

Suppose now that attention is confined to a particular class of explosions which differ only in charge size l and depth of charge burial h. Suppose further that the relevant quantities included in q_{ex}, q_s and q_a are such that their dimensions can all be expressed in the form $(p_a)^\alpha (V_p)^\beta$ these quantities accordingly being independent of l in the system of fundamental units comprising p_a, V_p and l. This assumption excludes, in particular, any discussion of stratified soils or rate-of-strain effects. The modelling parameters q_{ex}', q_s' and q_a' occurring in equation (3·1) are then constants and need not be explicitly denoted. Thus, for such a class of explosions, equation (3·1) reduces to

$$Q' = Q'(x_i', t'; h/l, gl/V_p^2). \tag{3·2}$$

Now, in general, if the relation (3·2) is to be completely independent of all the modelling parameters, it is necessary first to restrict attention to explosions for which h/l is constant (that is, to explosions which are geometrically similar in every respect), and secondly, as gl/V_p^2 varies with l, the function Q' must be assumed to be sensibly independent of the modelling parameter gl/V_p^2 over some set of explosions falling within the class already defined. Equation (3·2) then becomes

$$Q' = Q'(x_i', t'), \tag{3·3}$$

and this final result, derived under the stated conditions, is the mathematical expression of Hopkinson's size-scaling law. The law is seen to rest, in particular, upon the assumptions

that geometrical similarity between explosions is achieved and that the effects of gravity and rate of strain are negligible. It is therefore at best an approximation to the true state of affairs. The particular importance of this law is that, within the class of explosions considered, and subject to the validity of the assumptions, it co-ordinates results for all explosions. Thus, if experimental data are available for one particular size of explosion, relations of the type (3·3) can be calibrated and results then predicted for different sizes of explosion. More precisely, equation (3·3) shows that, for any assigned values of x_i' and t', the quantity Q' is completely specified, and it follows that $Q \propto [Q]$. Now if Q has dimensions $M^\alpha L^\beta T^\gamma$ when expressed in terms of mass, length and time, then it will have dimensions $p_a^\alpha V_p^{-2\alpha-\gamma} l^{3\alpha+\beta+\gamma}$ in terms of p_a, V_p and l. Thus, for example, if Q is a length or time associated with the motion, then Q is directly proportional to l. It should be noted that, when there is spherical symmetry, equation (3·3) is more simply written as

$$Q' = Q'(r', t'), \tag{3·4}$$

where r' is the reduced radial co-ordinate. Now suppose that, in equation (3·4), Q is taken as a, the radius of the camouflet surface. It is then clear that a' is an invariable function of t', and that the values $a'_{(i)}$ and $t'_{(i)}$ $(i = 1, 2, \ldots)$ of a' and t', corresponding to the termination of successive expansion and contraction phases, are constant, for each value of i, independently of the charge size. In other words, $a_{(i)}$ and $t_{(i)}$ are proportional to l, and, in particular, the radius of the camouflet surface at the end of the first expansion phase and the time of expansion are both proportional to the representative linear dimension of the charge.

Similar results may be derived when the explosive charge is characterized, not by a representative length l, but by either its total mass $\mathscr{M}$ or its total energy release $\mathscr{E}$. Now if p_a, V_p and either $\mathscr{M}$ or $\mathscr{E}$ are taken as fundamental pressure, velocity and mass or energy, then the fundamental units of mass, length and time are $\mathscr{M}$, $\mathscr{M}^{\frac{1}{3}} p_a^{-\frac{1}{3}} V_p^{\frac{2}{3}}$ and $\mathscr{M}^{\frac{1}{3}} p_a^{-\frac{1}{3}} V_p^{-\frac{1}{3}}$ or $\mathscr{E} V_p^{-2}$, $\mathscr{E}^{\frac{1}{3}} p_a^{-\frac{1}{3}}$ and $\mathscr{E}^{\frac{1}{3}} p_a^{-\frac{1}{3}} V_p^{-1}$, respectively. It then follows as above that lengths or times associated with the motion are directly proportional to either $\mathscr{M}^{\frac{1}{3}}$ or $\mathscr{E}^{\frac{1}{3}}$. In particular, $a_{(i)}$ and $t_{(i)}$ are directly proportional to these quantities. Results of this kind are examples of the so-called *cube-root* scaling law, which is the imprecise description commonly given to Hopkinson's size-scaling law. It may be noted that, despite general usage, the cube-root scaling law cannot be formulated in terms of charge *weight*.

It has been shown that Hopkinson's size-scaling law (equation (3·3)) is valid under rather restrictive conditions. Thus, in particular, effects due to gravity, rate of strain and soil stratification (or other inhomogeneities) should be negligible. Apart possibly from rate-of-strain effects, it seems clear on physical grounds that the required conditions may be satisfied quite well when stress intensities are of a much higher order of magnitude than those due to gravity. Thus, for example, because of the high pressures involved, the fraction of charge energy absorbed in the formation of the soil shock wave should be virtually independent of both gravity and the yield strength of the soil. In fact, this fraction should be determined almost entirely by the variation of compressibility of the soil with pressure. However, in the main part of the motion, not all the required conditions for the validity of Hopkinson's law can be satisfied in practice. Coulomb's law of plastic yielding in soils (see equation (4·4)) implies that flow is inhibited by the prevailing pressure, and therefore the resistance to deformation in soils increases with depth. Thus, for a soil exhibiting

PHILOSOPHICAL TRANSACTIONS OF THE ROYAL SOCIETY A MATHEMATICAL, PHYSICAL & ENGINEERING SCIENCES

internal frictional resistance, Q' cannot, in general, be regarded as independent of the modelling parameter gl/V_p^2. Equation (3·3) is then no longer valid, and, for example, the ratio of camouflet size to charge size is no longer constant. Hence, even if Hopkinson's law is found experimentally to be correct over some range of charge size, it will be expected to fail beyond a certain limit.

4. Physical properties of explosion products and soils

This section concerns the mechanical behaviour of explosion products and soils, and the related assumptions made in the theoretical analysis of this paper. Particular attention is given to the choice of numerical values of physical parameters required in the application of the present theory of camouflet motion. For definiteness, attention is confined to *TNT*, but the procedure for other high explosives would be similar.

The term *natural soil* as used in this paper is intended to cover the range of relatively soft, uncemented geological materials of the Earth's crust which, broadly speaking, are comparatively loose aggregates of mineral particles, the voids being filled with water, air or both. The distribution of particle size is within the clay, silt and sand fractions. The limits of the range of soils envisaged are represented by the frictionless, fully saturated clays and the cohesionless dry sands. A partly saturated clay or mixed soil, exhibiting frictional as well as cohesive strength, can be regarded as an intermediate case. Specifically excluded from the present discussion are brittle materials, such as rock.

In contrast, the term *ideal soil* is used in this paper to describe a material which behaves exactly according to the various laws discussed later, which are idealizations of the behaviour of natural soils. The reader should note this distinction carefully.

4·1. *Explosion products*

The detonation process in high explosives is discussed in considerable detail by Cole (1948, chap. 3) and requires only brief mention here. Calculations by Jones & Miller (1948) predict that, for a loading density (i.e. density of solid explosive) of 1·5 g/cm^3 (93·6 lb./ft.^{3}), the detonation velocity in *TNT* is 7720 m/s (25 300 ft./s), in reasonable agreement with the experimental value of 6790 m/s (22 300 ft./s). Furthermore, these authors calculated the adiabatic pressure-density relation for the explosion products, and Taylor (1950) used their data in making a detailed calculation of the properties of detonation waves. It may be noted that the detonation velocity is well in excess of stress wave velocities in soils (see table 2). Also, for a 1 lb. spherical charge of *TNT* (radius 4·2 cm or 0·14 ft.), detonation is completed in about 5 μs, a time much shorter than the predicted duration of the first expansion phase of camouflet formation in situations of practical interest (see table 9).

The condition of geometrical similarity existing behind the detonation front ceases to apply when the detonation wave reaches the charge surface. Initially, the ensuing motion involves a disturbance, which is probably a shock wave, travelling outwards into the soil, and a rarefaction wave travelling inwards through the explosion products. The theory of the propagation of spherical shock waves due to explosions in solid materials, including metals, soils and rocks, has received attention in the U.S.A. and U.S.S.R. and, to a lesser extent, in the U.K. Some theoretical studies are available (see § 7·3), but their application

to explosion phenomena necessitates a knowledge of the appropriate constitutive equations at high stress intensities, and at present this is extremely limited.

For these reasons (see also § 2·4), no direct attention is given in the present paper to the shock wave propagated through the soil. Instead, as in studies of the problem of underwater bubble motion (Cole 1948, chap. 8), it is assumed that the motion is isochronous (see § 5·6), all wave propagation effects being neglected. In order to allow for the induced motion and the energy associated with the shock wave, it is assumed that the detonation energy of the isochronous model (referred to as the *camouflet energy* $\mathscr{E}_{\text{cam.}}$) is a known fraction, here taken as one-third, of the true detonation energy $\mathscr{E}$. Both $\mathscr{E}$ and $\mathscr{E}_{\text{cam.}}$ refer to the energy released in the expansion of the gaseous explosion products to atmospheric pressure. Further, in order to avoid the necessity of discussing the wave motion in the gases, it is assumed that waves have traversed the camouflet a sufficient number of times for it to be possible to treat the volume changes of these products as occurring under conditions of uniform density and pressure.

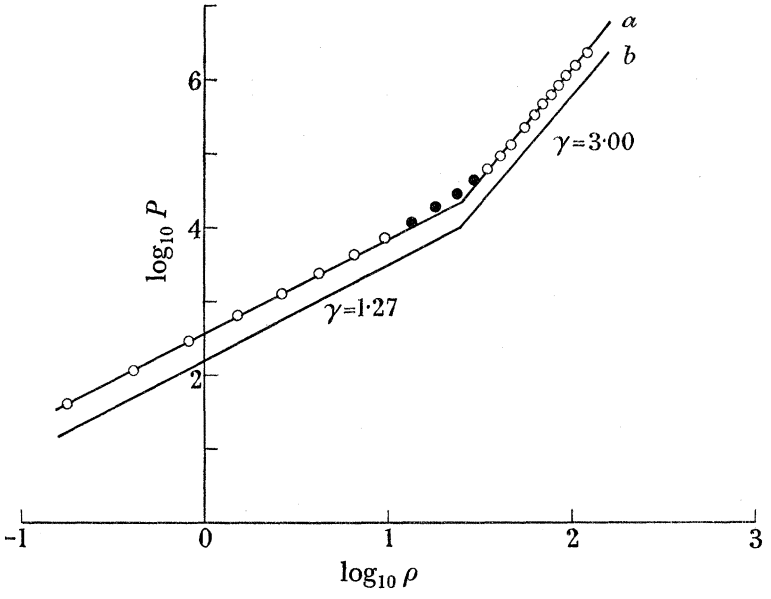

FIGURE 2. Relation between pressure P (Lb./in.^{2}) and density ρ (lb./ft.^{3}) during adiabatic expansion of explosion products of *TNT* at a loading density of 93·6 lb./ft.^{3} (data adapted from Jones & Miller 1948). ○, data from Jones & Miller (1948); (*a*) least-squares fit to these data (●, excluded); (*b*) relation assumed in § 7.

Jones & Miller (1948) have calculated, for a loading density of 93·6 lb./ft.^{3}, the relation between temperature, pressure and density during the adiabatic expansion of the gaseous explosion products of *TNT*. Their numerical values are set out in table 1, and the variation of pressure with density is shown in figure 2. It is clear that the curve expressing this can be approximated by two straight line segments, intersecting at a point corresponding to a critical density. The relation expressed by these two lines refers to an explosion of total energy release $\mathscr{E}$, whereas here a relation is required which pertains to a model explosion of energy release $\mathscr{E}_{\text{cam.}} = \frac{1}{3}\mathscr{E}$. The assumption is made that this latter relation is also represented by two straight lines, with the same slopes and critical density as before but now occupying a position corresponding to an energy release $\mathscr{E}_{\text{cam.}}$. In other words, the new

curve is obtained by a bodily translation, parallel to the pressure axis, of the original curve (see figure 2).

Since uniform conditions are assumed within the explosion products, the law of variation of gas pressure P with camouflet radius a is

$$P = \begin{cases} P_0(a/a_0)^{-3\gamma_1} & \text{if} \quad 1 \leqslant a/a_0 \leqslant a^*/a_0, \\ P_0(a^*/a_0)^{-3\gamma_1}(a/a^*)^{-3\gamma_2} & \text{if} \quad a/a_0 \geqslant a^*/a_0, \end{cases} \tag{4·1}$$

where a_0 is the initial value of a, and a^* is the value of a corresponding to the critical density. The constants a^*/a_0, γ_1 and γ_2 may be determined from the data in table 1, and then the modified initial pressure P_0 is so chosen that the work done by the explosion products in expanding adiabatically from pressure P_0 to atmospheric pressure is equal to $\mathscr{E}_{\text{cam.}}$. On the basis of the data given in the last column of table 1, γ_1 and γ_2 are given the exact values 3·00 and 1·27, respectively. Then, from a least-squares fit to the data given in table 1, the values in the range 1200 to 1500 °K being ignored (see table 1 and figure 2), it is found that

$$a^*/a_0 = 1{\cdot}530. \tag{4·2}$$

For *TNT* ($C_7H_5O_6N_3$), the detonation energy is 247·9 kcal/mole (see Jones & Miller 1948) and the molecular weight is 227·141. It is then found that

$$P_0 = 4{\cdot}882 \times 10^5 \text{ Lb./in.}^2, \tag{4·3}$$

if the atmospheric pressure is taken to be 14·7 Lb./in.^{2}.

TABLE 1. TEMPERATURE T, PRESSURE P, DENSITY ρ AND ADIABATIC INDEX $\gamma = \mathrm{d}(\ln P)/\mathrm{d}(\ln \rho)$ DURING ADIABATIC EXPANSION OF EXPLOSION PRODUCTS OF *TNT* AT A LOADING DENSITY OF 93·6 LB./FT.^{3}

Data adapted from Jones & Miller (1948).

T (°K)	P (Lb./in.^{2})	ρ (lb./ft.^{3})	γ
3400	$2{\cdot}303 \times 10^6$	$1{\cdot}215 \times 10^2$	3·36
3200	$1{\cdot}562$	$1{\cdot}056$	2·63
3000	$1{\cdot}133$	$9{\cdot}351 \times 10^1$	2·76
2800	$8{\cdot}460 \times 10^5$	$8{\cdot}412$	2·93
2600	$6{\cdot}340$	$7{\cdot}623$	3·10
2400	$4{\cdot}696$	$6{\cdot}920$	3·27
2200	$3{\cdot}334$	$6{\cdot}230$	3·30
2000	$2{\cdot}200$	$5{\cdot}495$	3·05
1800	$1{\cdot}291$	$4{\cdot}607$	2·76
1700	$9{\cdot}058 \times 10^4$	$4{\cdot}054$	2·39
1600	$6{\cdot}263$	$3{\cdot}474$	2·09
1500*	$4{\cdot}251$	$2{\cdot}888$	1·86
1400*	$2{\cdot}824$	$2{\cdot}318$	1·68
1300*	$1{\cdot}833$	$1{\cdot}792$	1·54
1200*	$1{\cdot}157$	$1{\cdot}329$	1·44
1100	$7{\cdot}081 \times 10^3$	$9{\cdot}449 \times 10^0$	1·37
1000	$4{\cdot}177$	$6{\cdot}424$	1·32
900	$2{\cdot}358$	$4{\cdot}170$	1·29
800	$1{\cdot}263$	$2{\cdot}570$	1·27
700	$6{\cdot}324 \times 10^2$	$1{\cdot}494$	1·27
600	$2{\cdot}899$	$8{\cdot}071 \times 10^{-1}$	1·27
500	$1{\cdot}183$	$3{\cdot}976$	1·27
400	$4{\cdot}087 \times 10^1$	$1{\cdot}721$	1·27

* Data omitted in least-squares fit for determining constants in equation (4·1).

4·2. *Soils*

The theoretical treatment of problems of soil mechanics is difficult even when attention is confined to the constructional problems of civil engineering. This is because the mechanical behaviour of natural soils under the action of applied loading is complicated, varied and incompletely understood. Further, as Terzaghi (1943, chap. 1) has remarked, the inhomogeneity of soil deposits of any appreciable extent precludes the possibility of completely specifying the physical data in problems of soil mechanics. Thus the interpretation of theoretical predictions requires the exercise of experience and judgement.

It follows from the above remarks that theoretical studies in soil mechanics necessarily relate to ideal soils, the physical properties of which are an approximation to those of natural soils. Such a procedure can lead to useful information provided that the uncertainties of the true situation are kept in mind. Refinements which attempt to take account of the physical properties in more detail will lead to complications of the analysis, and improvement in approximation will be achieved only at the expense of considerable labour, perhaps unwarranted in civil engineering problems, but possibly essential in explosion problems.

The subject of the mechanical behaviour of natural soils has an extensive literature, some discussion of which is essential for an appreciation of the bases and limitations of the definition of an ideal soil adopted in the present study. For additional information, the reader is referred to the textbook by Terzaghi (1943) and the review article by Skempton & Bishop (1954).

Any analysis of camouflet formation involves the use of constitutive equations valid over much wider ranges of stress, strain and rate of strain than are ever encountered in civil engineering. The appropriateness of a mathematical model of the physical situation can therefore only be assessed *a posteriori* by the direct comparison of experimental data and theoretical predictions. The ideal soil considered in this paper is defined to be a solid that obeys Hooke's law within the elastic range and Coulomb's criterion at yield under the restriction of perfectly plastic flow. It is expected that this idealized material will provide a reasonable model of natural soils so far as mechanical behaviour under conventional conditions of low stress, etc., is concerned, but it is not known how closely ideal soils represent natural soils under explosion conditions. The hypothesis, made in this paper, that an ideal soil gives a reasonable account of the mechanical behaviour of natural soils under all conditions, is therefore to be regarded as tentative and subject to revision in the light of further evidence from experiments. The assumption of perfect plasticity implies direct neglect of all physical effects, such as work hardening or softening and rate of strain, which may influence the yield strength of the soil. However, once average strains and rates of strain are known or have been estimated, an approximate account of such effects may be taken by ascribing a suitable nominal value to the yield strength.

Even under conventional conditions, the physical properties of natural soils, as measured in the field and in the laboratory, and those of ideal soils are by no means the same thing. For this reason, divergencies are inevitable between theory and practice in soil mechanics (see Terzaghi 1943, vii–viii).

PHILOSOPHICAL TRANSACTIONS OF THE ROYAL SOCIETY A MATHEMATICAL, PHYSICAL & ENGINEERING SCIENCES

4·2·1. *Strength characteristics and structure of natural soils under conventional conditions*

As interpreted here, the term *soil* includes clays, silts and sands, in increasing coarseness of texture. A soil is thus a relatively loose aggregate of mineral particles, the voids being filled with water, air or both.

In terms of strength, a fundamental division exists between cohesive soils, such as clays, and cohesionless particle aggregates, such as dry sands. The properties of cohesion and friction in soils are due to essentially different kinds of interaction between the constituent particles. Suppose that a sample of soil contains a mixture of mineral particles ranging in size from, say, 0·002 to 2 mm. Then, for all particle sizes, frictional forces are set up at interparticle contacts. Furthermore, there are interparticle cohesion forces which become more important as the particle size diminishes. In general, both these effects are present, and the size distribution of soil particles and the intensity of the applied stresses will determine their relative contributions to the bulk mechanical behaviour of the soil.

The above discussion treats a soil essentially as a granular structure, but the resistance to deformation also depends upon the water and air content of the voids and upon the external conditions imposed during deformation. Now consider the strength characteristics of a sample of fully saturated soil in which, initially at least, the pore space is completely occupied by water. The water is much less compressible than the soil structure and hence, under *undrained* conditions, when the natural water content is retained, the applied load is supported mainly by the water. Since practically no pressure is then exerted at the interparticle contacts, no frictional forces are brought into play, and the soil behaves as a frictionless material. On the other hand, under *fully drained* conditions, the natural water content is allowed to escape freely from the sample as the deformation proceeds. The applied forces are then supported by the granular skeleton, and the soil exhibits both cohesion and internal friction.

A theoretical and experimental investigation of the strength characteristics of saturated soils has been made by Bishop & Eldin (1950), and the effective vanishing of frictional strength for a range of saturated soils may be taken to be established. Suppose that a soil sample is initially almost completely saturated. Then, under the action of sufficiently high pressure, the air within the pore space is compressed and driven into solution with the water, and, with contraction of the voids, a state of complete saturation may be achieved. Under these conditions the frictional strength of the sample, although perhaps originally quite high, falls to zero.

It may be noted that it is usual in soil mechanics to deal with *effective* rather than *actual* stresses. The components, in some rectangular Cartesian co-ordinate system, of the effective stress tensor are defined to be $\sigma'_{ij} = \sigma_{ij} + u\delta_{ij}$, where u is the pore water pressure and σ_{ij} are the actual stress components. The concept of interparticle friction is then formulated in terms of the components σ'_{ij}. The question of drainage does not now arise since it is found, for example, that under zero drainage conditions the normal component of the effective stress vector at an interparticle contact is zero, and therefore no frictional resistance occurs. Such a formulation of the present problem would, however, involve separate consideration of the motion of the soil skeleton and the pore water, and an equation expressing the flow of pore water through the skeleton would also be required (see Skempton & Bishop 1954).

A model of soil mechanical behaviour which represents a natural soil as a two-phase system, consisting of a porous elastic solid through which fluid can percolate, has been proposed by Biot (1941*a*, 1955). The resulting theory has been applied to a number of situations characterized by small deformations; in particular, to problems of soil consolidation (Biot 1941*b*, 1956*a*; Biot & Clingan 1941, 1942) and of wave propagation (Biot 1956*b*, *c*). The present treatment, in which the soil is regarded as a single-phase system, is mathematically more flexible than Biot's theory, and furthermore the duration of the first expansion phase of camouflet motion is so small that the migration of pore water through the mineral skeleton seems unlikely to have a significant effect upon the bulk motion of the soil.

(*a*) *Clays*. Clay soils have been widely studied because of their importance in civil engineering. A clay is basically an aggregate of fine mineral particles, together with water and air, both normally present in the interparticle voids. The presence of these fine particles implies that clays exhibit cohesion. Clays are also relatively impermeable, which means that all but the slowest deformations of a fully saturated sample may be regarded as taking place under undrained conditions, the movement of the pore water being restrained by the structure of the clay. Thus, fully saturated clays normally behave as though they were frictionless. This effect is evident in results obtained by K. Terzaghi (see Bishop & Eldin 1950, p. 14) who found, in tests made on identical samples of a clay, that the angle of internal friction was about $\frac{1}{2}^\circ$ at normal rates of loading and about 23° at extremely slow ones, when precautions were taken to ensure that drainage occurred.

(*b*) *Sands*. The basic structure of a dry sand is very much simpler than that of a clay. The average particle size for sands is still small, although it is larger by an order of magnitude than the average for clays, and the voids in a dry sand are entirely filled with air. The material has practically no cohesion and is virtually incompressible, apart possibly from slight compaction and so long as no crushing of individual grains occurs. When a sample of dry sand is compressed, the external forces are supported entirely by forces set up over interparticle contacts. The tangential components of these forces account for the overall resistance to deformation. A completely saturated sand has no apparent frictional strength under undrained conditions and then offers negligible resistance to deformation. A partly saturated sand offers frictional resistance and has in addition some cohesion.

(*c*) *Other soils*. The foregoing remarks provide a broad qualitative description of the structure and physical properties affecting the resistance to deformation of clays and sands. Silts may be regarded as intermediate to clays and sands, and most natural soils are mixtures of these basic types. In general, soils possess both cohesive and frictional strengths, but, in view of the sensitiveness of these properties to external conditions, physical parameters rather than constants must be taken to represent them.

4·2·2. *Mechanical behaviour of ideal soils*

Suppose that a natural soil sample is being deformed under the action of an increasing uniaxial compressive stress. Once this stress satisfies a certain yield criterion, characteristic of the material and depending upon the test conditions, the soil exhibits flow. Under the action of an increasing uniaxial tensile stress, failure occurs at an even lower stress, but by fracture rather than flow. The stresses set up in the ground during the expansion of a camouflet are predominantly compressive, and under these conditions soils undergo

PHILOSOPHICAL TRANSACTIONS OF THE ROYAL SOCIETY A MATHEMATICAL, PHYSICAL & ENGINEERING SCIENCES

deformation mainly by flow. It is true that fractures do occur in the immediate vicinity of the camouflet surface, but this effect cannot readily be included in theoretical studies. In the present paper, soil regions undergoing deformation are assumed to remain continuous, their mechanical behaviour accordingly being governed by field and constitutive equations which, with appropriate initial, boundary and continuity conditions, determine the distributions of density, stress, velocity and displacement.

It is assumed that the condition for flow to take place in an ideal soil is obtainable from Coulomb's (1773) law, which states that the critical value of the shear stress depends upon two physical parameters, namely the cohesion stress c and the angle of internal friction ϕ. Let σ and τ be respectively the normal and shear stresses exerted across a plane surface element drawn through a typical point of a region of soil. Coulomb's law states that the onset of plastic flow at that point occurs when

$$|\tau| = c - \sigma \tan\phi \tag{4·4}$$

for some orientation of the surface element. When equation (4·4) is used to describe the behaviour of natural soils, it is found that the quantities c and ϕ must be regarded as empirical parameters, the values of which depend upon test conditions (such as drainage) and also upon such factors as rate of strain and volume change; but for ideal soils c and ϕ are, by definition, constant. The shear strength of natural soils can be analyzed in relation to their true cohesion and angle of internal friction (see Skempton & Bishop 1954), but for most practical purposes the strength is more conveniently expressed in terms of the empirical parameters defined above.

Although there is a reasonably close correspondence between natural soils and ideal soils under conventional conditions, the behaviour of natural soils under explosion conditions is not known. Therefore the use of a model based upon ideal soils to predict results for camouflet formation in natural soils involves a considerable extrapolation. However, rather than omit altogether the effects of friction, for example, it seems better to include these on a provisional basis, which may later be modified in the light of further information about their precise nature.

Before Coulomb's law (equation (4·4)) is incorporated into a theory of continuum mechanics, it is convenient to restate it in invariant form. Let $\sigma_1, \sigma_2, \sigma_3$ be the three principal components of stress. Then Shield (1955) has shown that the required form is

$$\sigma_3 - \sigma_1 = 2c\cos\phi - (\sigma_3 + \sigma_1)\sin\phi \quad \text{if} \quad \sigma_1 \leqslant \sigma_2 \leqslant \sigma_3, \tag{4·5}$$

with similar results for the other possible relations between the principal stresses. It should be noted that Coulomb's law for the onset of plastic flow in a soil is a generalization of Tresca's law for such flow in a metal. In principal stress space, restricting attention to stress states for which none of $\sigma_1, \sigma_2, \sigma_3$ exceeds $c\cot\phi$, equations (4·5) represent a set of six planes enclosing the hexagonal pyramid shown in figure 3. For a given point within a region of soil (taken to be isotropic, but not necessarily homogeneous), the position and shape of this pyramid are determined by the values of c and ϕ, and the state of stress must correspond to a point lying either inside or on the pyramid. If the representative point lies on the pyramid, then the condition for the onset of plastic flow is satisfied. It should be noted in passing that plastic behaviour of natural soils does not necessarily involve any actual yield of the constituent particles, permanent deformation in soils being mainly the result of particle

reorientation accompanied by sliding at interparticle contacts. There may be some slight initial volume changes and perhaps failure in the larger grains.

Natural soils appear to exhibit initially a linear type of deformation, as described by Hooke's law, although there is generally some dependence upon rate of strain, the so-called elastic constants then varying with the rate of loading. However, it is not true that all soils exhibit full elastic recovery, this depending upon the past history of the soil. It will be seen later that analysis is complicated by the fact that finite strain may occur below yield in circumstances when the soil strength is considerably enhanced by high stress intensities, so that linear elasticity theory is not adequate.

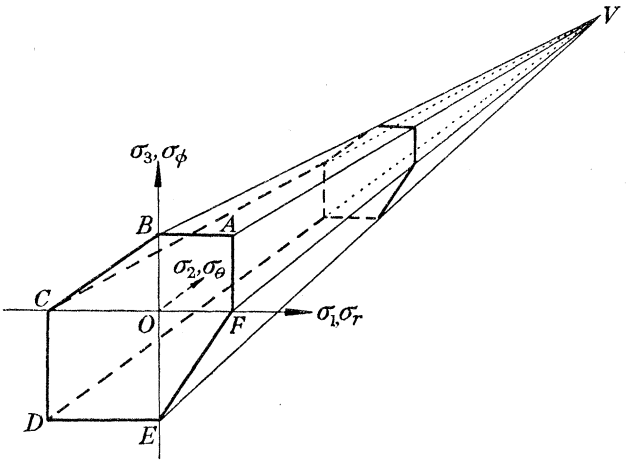

FIGURE 3. Coulomb yield surface in principal stress space.

In statically determinate problems (see Hill 1950, p. 131), Coulomb's failure condition (4·5), when combined with the condition of equilibrium, is sufficient to determine possible stress distributions in regions of soil about to undergo plastic flow. Although this approach is adopted in the classical theory of earth pressure (see Prager 1955*b*), it is applicable only in certain situations. The deficiencies of this theory, which were first appreciated from developments in the theory of metal plasticity, arise from the failure of Coulomb's law to specify either the changes in deformation following the onset of plastic flow or the possible changes in resistance to deformation as flow proceeds. In the terminology of metal plasticity theory (see, for example, Hill 1950, chap. 2), equation (4·5) defines an *initial yield surface*. Immediate analogy then suggests that points lying inside this surface correspond to *elastic* stress states and that those lying on it correspond to *initial plastic* stress states. Furthermore, it suggests that flow of an ideal soil may be described by the *associated* flow rule (see Prager 1953). It then becomes possible to contruct formally a complete plastic-elastic theory for ideal soils which differs from metal plasticity theory only in the form of the initial yield function (now dependent upon the mean value of the principal stresses). So far as problems of incipient plastic flow in soils are concerned, this approach seems reasonable. However, in problems of continued plastic flow, the adoption of a *non-associated* flow rule is indicated, since, as shown in § 5, use of the associated flow rule implies the physically unrealistic possibility of unlimited dilatancy. Thus, arguments based upon the foregoing supposed analogy are subject to certain qualifications. The ability of a soil to resist further deformation once plastic flow has occurred depends to some extent, as with

ductile metals, upon the rate and magnitude of deformation, and the concept of perfect plasticity accordingly has similar limitations for both soils and metals. At the present time, theoretical soil plasticity is restricted mainly to perfectly plastic behaviour with the additional requirement that, in continued plastic flow, the condition of plastic incompressibility is satisfied. Consistent theories of soil plasticity, with due account of compatibility between stress and velocity fields, originated with work of Drucker & Prager (1952) and Drucker (1953), later extended by Shield (1955), Chadwick (1959, 1962), Haythornthwaite (1960*a*), Cox, Eason & Hopkins (1961) and Cox (1962). A recent discussion of the yield and flow properties of natural soils has been given by Haythornthwaite (1960*b*). There is also much Russian work on this subject, to which the above papers give some references.

The above discussion has been confined to the behaviour of soils when being loaded. It is necessary, however, when discussing the contraction phases of camouflet formation, to consider unloading behaviour. There are even less data available in this case, and the assumed behaviour is taken by analogy with metal plasticity. This unloading behaviour, which is discussed in more detail in §§ 6·1·2 and 7·1·7, is believed to represent a limiting case in the sense that natural soils will recover less than is predicted by the theory. As will be seen, the main conclusion that arises from consideration of the contraction phase is that for ideal soils the extent of the contraction is generally negligible. In view of the above remarks, this conclusion is likely to hold *a fortiori* for natural soils.

A continuum theory of elastic, perfectly plastic deformation of ideal soil has now been formulated. This theory involves five physical quantities: two elastic constants, say, Young's modulus E and Poisson's ratio ν, two plastic constants, cohesion stress c and angle of internal friction ϕ, and the initial density ρ_0. The properties of this continuum, as described by soil plasticity theory, are very much simpler than those of a region of natural soil, even when this latter is reasonably homogeneous. The theory is thus necessarily an approximation, and the accuracy of its predictions must be checked by direct comparison with experimental data in situations where these can be obtained.

4·2·3. *Values of physical constants*

The task of choosing numerical values of the above-mentioned elastic and plastic constants appropriate to particular problems of soil mechanics is not simple. Basically, this is due to the fact that a given soil is normally made up of three components (solid, liquid and gaseous), and this situation is concealed in the phenomenological continuum approach outlined above. In order to simplify theoretical studies it is assumed that the soil is isotropic and homogeneous. Extensive and fairly uniform regions of natural soils do occur, for example, in clay deposits and sand deserts, but generally there are a number of factors which cause appreciable departure from uniform conditions, much depending upon the size of the region considered. Among these factors are anisotropy within single strata brought about by non-uniformities in the process of deposition and by pressure exerted by the overburden, surfaces of discontinuity arising from faults and from juxtaposition of different strata, and variability of water content, as occurs normally near ground level due to changing weather conditions and also where the influence of a water-table is felt. Thus the physical properties of soils in their natural state are seldom likely to be known to any high degree of accuracy, for, even if the relevant physical properties of given soil samples can

be determined with reasonable accuracy under laboratory conditions, considerable uncertainty is introduced in estimating from such measurements the overall physical properties of regions of soils *in situ*. There is the further difficulty of extrapolating values of physical constants to much higher strains and rates of strain than are ordinarily encountered in experimental studies of soil mechanical behaviour. In view of these difficulties, it is usually advisable, whenever convenient, to consider a series of values extending over the probable range of conditions present in a particular application.

The following discussion of numerical values of the five physical quantities taken above to characterize ideal soils is intended to be sufficiently general to cover the soil types defined at the outset, and also to be specific in respect of certain soils. Thus, detailed physical data are proposed for particular soils falling within the following three basic classes: fully saturated clays with $c > 0$ and $\phi = 0$ (soil S), partly saturated clays or mixed soils with $c > 0$ and $\phi > 0$ (soil P), and dry sands with $c = 0$ and $\phi > 0$ (soil Z). It is also found necessary later to consider a slightly frictional clay (soil MS, see § 7·1·7). So far as large-scale features of camouflet formation are concerned, it turns out that the most important soil constants are c and ϕ. For this reason, for each pair of values of c and ϕ corresponding to a soil of one of the above types, only one pair of values of E and ν is assigned, this being taken as typical for all soils of that type.

(*a*) *Elastic constants*. In general, the elastic constants E and ν occur independently in theoretical analyses. However, the shear modulus $\mu = E/\{2(1+\nu)\}$ is the only elastic constant occurring in Penney's work, and only E occurs in the incompressible theory given in this paper.

Let V_p and V_s be the velocities of propagation of longitudinal and transverse elastic waves. Then

$$V_p^2 = E(1-\nu)/\{\rho_0(1+\nu)\,(1-2\nu)\}, \quad V_s^2 = E/\{2\rho_0(1+\nu)\} = \mu/\rho_0, \tag{4·6}$$

and ν is expressed in terms of the quotient V_s/V_p (< 1) by

$$\nu = 1 - \tfrac{1}{2}(1 - V_s^2/V_p^2)^{-1}. \tag{4·7}$$

Thus the values of ν and μ are readily calculated from experimental values of the elastic wave velocities V_p and V_s. Values of V_p in clay deposits are often obtained from seismic refraction experiments, but values of V_s are only rarely measured in the field. Illustrative values of elastic wave velocities and other data for some types of clay soils given in table 2 are due to J. K. Wright (1958, private communication).

It will be observed that, for the soils listed in table 2, the values of ν are close to $\frac{1}{2}$. In Chadwick's (1959) investigation of the quasi-static expansion of a spherical cavity in an ideal soil, the neglect of the compressibility of the soil is found to have only a small influence on numerical values. This conclusion should remain true in the dynamical theory so far as motion of the camouflet surface is concerned, but the elimination of the elastic wave motion makes the results of energy-partition calculations difficult to interpret.

The numerical values of Young's modulus adopted for the three basic soil types are given in table 3.

It appears from experimental data that the behaviour of soils is viscoelastic rather than elastic, since the values of E and ν are frequency-dependent. Therefore theoretical work in soil mechanics should strictly take account of the variation of these quantities. In respect

of camouflet formation, however, preliminary calculations indicate that the large-scale features of the motion are only weakly dependent upon the values of the elastic parameters. Constant values, derived from stress-wave measurements and therefore relevant to the correct range of frequency, are accordingly adopted here.

TABLE 2. VALUES OF ELASTIC WAVE VELOCITIES AND OTHER DATA FOR SOME TYPES OF CLAY SOILS

soil	V_p (ft./s)	V_s (ft./s)	ν	μ (Lb./in.^{2})	ρ_0 (lb./ft.^{3})
very soft clay (Dersingham)	5000	1500	0·45	$4{\cdot}9\times10^4$	101
unconsolidated clay (Foulness)	5000	1500	0·45	$5{\cdot}8\times10^4$	119
Oxford clay (Stewartby)	5000	2000	0·40	$9{\cdot}4\times10^4$	109

(*b*) *Plastic constants.* Experimental values of the cohesion and angle of internal friction of soils have been extensively reported, but these refer mainly to static tests. For fully saturated soils, $\phi = 0$ under undrained conditions. For clay soils, values of the cohesion c normally lie in the range 0 to 20 Lb./in.^{2}, but for exceptionally stiff clays c may be as high as 40 Lb./in.^{2}. At the other extreme of the range of soil types considered here, dry sands have zero cohesion and angles of internal friction ϕ within the range 30 to 45°, depending upon the size distribution and the shape of the constituent particles. Over the complete range of soils, most combinations of values of c and ϕ, falling within the ranges mentioned above for sands and clays, are known to occur.

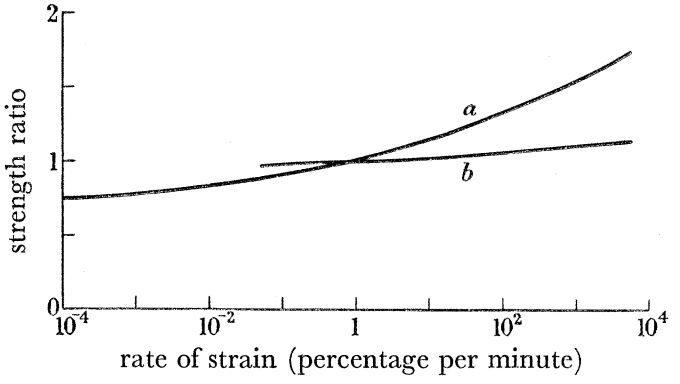

FIGURE 4. Relation between strength and rate of strain for (*a*) clay and (*b*) sand (data of D. W. Taylor and A. Casagrande & W. L. Shannon, from Skempton & Bishop 1954). Strength at rate of strain 1% per minute taken as standard.

Only a limited number of measurements of c and ϕ have been made under dynamic conditions. Of particular value are data reported by D. W. Taylor and by A. Casagrande & W. L. Shannon (see Skempton & Bishop 1954) which show that, as the rate of strain increases from zero to about $1{\cdot}5\,s^{-1}$, the strengths of clays and sands increase by factors of about 2 and 1·2, respectively. These data are summarized in figure 4. The rates of strain involved in camouflet motion are, at certain places and times, very much higher than $1{\cdot}5\,s^{-1}$. However, the discussion given in § 7·1·6 shows that the average value, taken over both space and time, is very much smaller than these maximum values, being of the order of 5 to $10\,s^{-1}$ for 1 lb. explosive charges (and still less for larger sizes), and it is feasible to extrapolate strength data obtained under moderate transient loading conditions to rates

of strain of this order of magnitude. Rate-of-strain effects in soils are not well understood, but in clays the resistance to the flow of pore water is probably one reason for their existence.

The numerical values of cohesion and angle of internal friction adopted for the three basic soil types are given in table 3.

TABLE 3. NUMERICAL VALUES OF PHYSICAL PARAMETERS FOR BASIC TYPES OF IDEAL SOILS

S, frictionless, fully saturated clay; *P*, partly saturated clay or mixed soil; *Z*, cohesionless dry sand; *MS*, slightly frictional clay (compare soil *S* and see §7·1·7).

soil	E (Lb./in.^{2})	c (Lb./in.^{2})	ϕ (deg)	ρ_0 (lb./ft.^{3})
S	$1{\cdot}5\times10^5$	20	0	125
P	8×10^4	15	10	125
Z	2×10^4	0	30	100
MS	$1{\cdot}5\times10^5$	20	1	125

(*c*) *Density*. Many accurate measurements of the densities of soil samples have been made. For the most part, these give results in the range 100 to 140 lb./ft.^{3}.

The numerical values of density adopted for the three basic soil types are given in table 3.

It is clear from the foregoing discussion that the choice of numerical values of physical data for use in theoretical studies of the mechanics of camouflet motion is not simple. However, so far as general information is concerned, the data proposed for the ideal counterparts of the three basic types of natural soils are thought to be realistic. When results for particular soils are required, the appropriate values of soil constants should be carefully chosen with reference to whatever experimental data are available.

It should be noted finally that it is normal in soil mechanics to deal with excess stresses above atmospheric pressure. Thus, quoted values of the cohesion of a soil generally refer to the relative cohesion $c^* = c + p_a \tan\phi$ (see Cox *et al.* 1961, p. 33). Care must be taken in any application of the present theory to ascertain whether this is in fact the case. To illustrate the differences which may arise from the use of c^* in place of c, note that most soils have values of c and ϕ in the ranges $0 \leqslant c \leqslant 20$ Lb./in.^{2} and $0 \leqslant \phi \leqslant 40°$, whereas $p_a = 15$ Lb./in.^{2} approximately. The two terms in c^* can therefore be of comparable magnitude. For sands, when c is very small and ϕ is about 40°, the second term $p_a \tan\phi$ predominates.

PART II. THEORETICAL MECHANICS OF IDEAL SOILS

5. SPHERICAL PLASTIC-ELASTIC FLOW

In this section a general theory of spherical plastic-elastic flow in ideal soils is developed which provides the basis for the present treatment of camouflet formation under spherically symmetric conditions. Subject to certain stated assumptions, which correspond to simplifications of the true physical situation (see §§ 2·4 and 4), the analysis given is exact, being based upon laws of conservation of mass and momentum and upon equations describing plastic-elastic flow without fracture.

5·1. *Preliminary assumptions*

The camouflet is formed by the expansion of confined gases at high temperature and pressure. In the numerical investigations given in later sections, the law of variation of

PHILOSOPHICAL TRANSACTIONS OF THE ROYAL SOCIETY A MATHEMATICAL, PHYSICAL & ENGINEERING SCIENCES

gas pressure at the camouflet surface is assumed to be given by equations (4·1) to (4·3), except in one special case discussed in § 6·1·3. The motion envisaged involves large plastic-elastic deformations which take place rapidly under conditions of spherical symmetry in an infinite region of homogeneous isotropic soil. The mechanical behaviour of the soil is that of an ideal material which obeys Hooke's law within the elastic range and Coulomb's criterion and associated flow rule at yield (although this latter condition is later modified) under the restriction of perfectly plastic flow. The soil is accordingly characterized by five physical constants: Young's modulus E, Poisson's ratio ν, cohesion stress c, angle of internal friction ϕ and initial density ρ_0 (see § 4·2·2). It may be noted that Coulomb's yield criterion and associated flow rule for soils reduce, in the particular case of zero internal friction, to Tresca's yield condition and associated flow rule for ductile metals. Accordingly, the present analysis applies to metals as well as to soils. However, the former case is the simpler, and the values of corresponding physical constants for soils and metals are widely different, so that the two cases are better treated separately. A detailed survey of work on the dynamic expansion of spherical cavities in metals has been given by Hopkins (1960).

5·2. *General equations*

Let r be distance measured from the centre of the camouflet, a be the current camouflet radius, and t be time measured from the instant when the camouflet first starts to expand. The soil is supposed initially to be at rest but not free from stress (see § 5·4). All field quantities are functions only of the independent variables r and t.

Large deformations of the material are involved, and here an Eulerian description of the motion is chosen. The aim is to establish equations sufficient for the determination of the distributions of displacement, velocity, stress and density at all times.

Let r, θ, ϕ be spherical polar co-ordinates with origin at the centre of the camouflet. The condition of spherical symmetry requires that only the radial velocity component v, the principal components of stress σ_r, σ_θ and $\sigma_\phi \equiv \sigma_\theta$ and the principal components of strain rate $\dot{\epsilon}_r$, $\dot{\epsilon}_\theta$ and $\dot{\epsilon}_\phi \equiv \dot{\epsilon}_\theta$ are not identically zero. In general, the use in this paper of a superior dot, or of $\mathrm{D}/\mathrm{D}t$, denotes differentiation following the motion of a material point, i.e. $\dot{F} \equiv \mathrm{D}F/\mathrm{D}t = \partial F/\partial t + v(\partial F/\partial r)$ for any given function F. However, it should be noted that strictly speaking the use of the conventional notation $\dot{\epsilon}_r$, $\dot{\epsilon}_\theta$, $\dot{\epsilon}_\phi$ $(\equiv \dot{\epsilon}_\theta)$ to denote strain rates violates this definition, since these quantities are defined in their own right, by equations (5·1), rather than as rates of change of other quantities. The strain tensor components ϵ_r, ϵ_θ, ϵ_ϕ $(\equiv \epsilon_\theta)$ do not explicitly appear in the analysis of this paper and are only defined implicitly by equation (5·1) and the foregoing definition of the meaning of the superior dot.

The total strain rates are defined in terms of v by

$$\dot{\epsilon}_r = \partial v/\partial r, \quad \dot{\epsilon}_\theta = v/r. \tag{5·1}$$

The elastic strain rates $\dot{\epsilon}_r^e$ and $\dot{\epsilon}_\theta^e$ are assumed to be given by

$$E\dot{\epsilon}_r^e = \dot{\sigma}_r - 2\nu\dot{\sigma}_\theta, \quad E\dot{\epsilon}_\theta^e = (1-\nu)\,\dot{\sigma}_\theta - \nu\dot{\sigma}_r. \tag{5·2}$$

For obvious reasons, ideal materials satisfying these equations are said to be *convective Hookean* (see also § 7·2). The plastic strain rates $\dot{\epsilon}_r^p$ and $\dot{\epsilon}_\theta^p$ are then defined by

$$\dot{\epsilon}_r^p = \dot{\epsilon}_r - \dot{\epsilon}_r^e, \quad \dot{\epsilon}_\theta^p = \dot{\epsilon}_\theta - \dot{\epsilon}_\theta^e. \tag{5·3}$$

For any particular material point, the state of stress at any time may be represented by a point in a three-dimensional space in which the principal stresses σ_1, σ_2, σ_3 are taken as rectangular Cartesian co-ordinates. In this so-called principal stress space, the Coulomb yield surface has the shape of a pyramid, with vertex at the point V ($c\cot\phi$, $c\cot\phi$, $c\cot\phi$), which intersects the plane $\sigma_2 = 0$ in the irregular hexagon $ABCDEF$ as shown in figure 3 (see Shield 1955 and Cox *et al.* 1961). The stress history of a material point may be represented by a path in principal stress space, no part of which lies outside the yield surface. If the representative stress point lies inside the yield surface, then any immediate stress changes are elastic. If, on the other hand, this point lies on the yield surface, then such changes are elastic when the stress path proceeds inwards from the yield surface, but otherwise these are plastic. For definiteness, let $\sigma_1 = \sigma_r$, $\sigma_2 = \sigma_\theta$, $\sigma_3 = \sigma_\phi$. Then, as $\sigma_\theta \equiv \sigma_\phi$ here, it follows from the shape of the yield surface that plastic flow occurs only for stress states represented by points on the lines passing through V and either one of the points C $(-b, 0, 0)$ and F $(a, 0, 0)$, where

$$\left.\begin{aligned} a/2c &= \cos\phi/(1+\sin\phi) = \tan(\tfrac{1}{4}\pi - \tfrac{1}{2}\phi), \\ b/2c &= \cos\phi/(1-\sin\phi) = \tan(\tfrac{1}{4}\pi + \tfrac{1}{2}\phi). \end{aligned}\right\} \tag{5·4}$$

The Coulomb *flow rule* (i.e. the equations for the plastic strain rates) requires the vector with components $\dot\epsilon_r^p$, $\dot\epsilon_\theta^p$, $\dot\epsilon_\phi^p$ to be directed along the outward normal to the yield surface at the stress point in question. Denote the yield function by $f(\sigma_r, \sigma_\theta, \sigma_\phi)$, the sign of f being so chosen that $f < 0$ for stress states below yield and $f = 0$ for stress states at yield. The flow rule is then

$$\dot\epsilon_r^p = \dot\lambda \frac{\partial f}{\partial \sigma_r}, \quad \dot\epsilon_\theta^p = \dot\lambda \frac{\partial f}{\partial \sigma_\theta}, \quad \dot\epsilon_\phi^p = \dot\lambda \frac{\partial f}{\partial \sigma_\phi}, \tag{5·5}$$

where $\dot\lambda(r, t) \geqslant 0$ is a scalar function. It should be noted that the condition $\dot\lambda \geqslant 0$ is a consequence of the more fundamental condition $\dot W^p \geqslant 0$, where $\dot W^p$ is the plastic rate of work per unit volume. In equations (5·5), f is to be interpreted appropriately (i.e. in the manner proposed by Koiter 1953 and Prager 1953) at singular points. Since $\dot\epsilon_\theta^p \equiv \dot\epsilon_\phi^p$, a particular combination of the plastic flow mechanisms for either one of the pairs of plastic régimes (*VBC*, *VCD*) and (*VEF*, *VFA*) applies. The yield functions involved are

$$\left.\begin{aligned} f_{VBC} &= -\sigma_r/b + \sigma_\phi/a - 1, \quad f_{VCD} = -\sigma_r/b + \sigma_\theta/a - 1, \\ f_{VEF} &= \sigma_r/a - \sigma_\phi/b - 1, \quad f_{VFA} = \sigma_r/a - \sigma_\theta/b - 1. \end{aligned}\right\} \tag{5·6}$$

Then, from equations (5·5), remembering the restriction $\dot\epsilon_\theta^p \equiv \dot\epsilon_\phi^p$, it follows that the required flow rule is

$$\left.\begin{aligned} \dot\epsilon_r^p &= -\dot\lambda/b, \quad \dot\epsilon_\theta^p = \dot\epsilon_\phi^p = \dot\lambda/2a \quad \text{for plastic régime } VC, \\ \dot\epsilon_r^p &= \dot\lambda/a, \quad \dot\epsilon_\theta^p = \dot\epsilon_\phi^p = -\dot\lambda/2b \quad \text{for plastic régime } VF, \end{aligned}\right\} \quad (\dot\lambda \geqslant 0). \tag{5·7}$$

The yield conditions and flow rules for both plastic régimes may be written more simply in the single form

$$\left.\begin{aligned} \dot\epsilon_r^p &= -\dot\lambda(\varpi - \sin\phi)/2c\cos\phi, \quad \dot\epsilon_\theta^p = \dot\epsilon_\phi^p = \dot\lambda(\varpi + \sin\phi)/4c\cos\phi, \\ \sigma_\theta &= \{(\varpi - \sin\phi)\,\sigma_r + 2c\cos\phi\}/(\varpi + \sin\phi), \quad \sigma_\phi = \sigma_\theta, \end{aligned}\right\} \quad (\dot\lambda \geqslant 0), \tag{5·8}$$

where ϖ is equal to $+1$ or -1 according as plastic régime *VC* or *VF* applies. Since

$$\varpi = \operatorname{sgn}(-\dot\epsilon_r^p) = \operatorname{sgn}(\dot\epsilon_\theta^p),$$

PHILOSOPHICAL TRANSACTIONS OF THE ROYAL SOCIETY A MATHEMATICAL, PHYSICAL & ENGINEERING SCIENCES

it may be expected that plastic régimes *VC* and *VF* will apply to the expansion and contraction phases of motion, respectively.

The stress rate, strain rate relations and the yield condition are therefore

$$\left.\begin{aligned} E(\partial v/\partial r) &= \dot{\sigma}_r - 2\nu\dot{\sigma}_\theta - E\dot{\lambda}(\varpi - \sin\phi)/2c\cos\phi, \\ E(v/r) &= (1-\nu)\,\dot{\sigma}_\theta - \nu\dot{\sigma}_r + E\dot{\lambda}(\varpi + \sin\phi)/4c\cos\phi, \\ f &= \varpi\sigma_\theta - \{(\varpi - \sin\phi)\,\sigma_r + 2c\cos\phi\}/(1+\varpi\sin\phi) = 0, \\ \dot{\lambda} &\begin{cases} = 0 & \text{if either } f<0 \text{ or } f=0 \text{ and } \dot{f}<0, \\ \geqslant 0 & \text{if } f=\dot{f}=0. \end{cases} \end{aligned}\right\} \quad (5{\cdot}9)$$

with

Equations (5·9) describe not only loading behaviour, but also unloading, which may involve either purely elastic behaviour or reverse plastic flow.

The complete system of basic equations consists of equations (5·9) together with the equations of motion and of conservation of mass, namely

$$\frac{\partial\sigma_r}{\partial r} + \frac{2(\sigma_r - \sigma_\theta)}{r} = \rho\left(\frac{\partial v}{\partial t} + v\frac{\partial v}{\partial r}\right), \quad (5{\cdot}10)$$

$$\dot{\rho} + \frac{\rho}{r^2}\frac{\partial}{\partial r}(r^2 v) = 0, \quad (5{\cdot}11)$$

where ρ is the density. If the displacement undergone by a material point at radius r and time t is u, then $v = \dot{u}$, and hence

$$v = \frac{\partial u}{\partial t}\Big/\left(1 - \frac{\partial u}{\partial r}\right). \quad (5{\cdot}12)$$

Equations $(5{\cdot}9_{1,2})$ and (5·11) show that

$$\dot{\rho}/\rho = \dot{p}/k - (\dot{\lambda}\tan\phi)/c, \quad (5{\cdot}13)$$

where $p = -\frac{1}{3}(\sigma_r + 2\sigma_\theta)$, and $k = E/\{3(1-2\nu)\}$ is the elastic bulk modulus. Since $\dot{\lambda} = 0$ prior to yield, equation (5·13) may be integrated to give

$$\rho = \rho_0 \exp\{(p - \Pi)/k - (\lambda\tan\phi)/c\}, \quad (5{\cdot}14)$$

where ρ_0 is the initial density and Π is the initial value of p (see equations (5·27)). Thus, since $\lambda > 0$, plastic strain always produces a decrease in density unless $\phi = 0$. This result is not physically acceptable under conditions of continued plastic flow (see Jenike & Shield 1959, and § 5·7).

Now consider a material element of volume $\mathrm{d}\tau$. The rate of performance of work on this element exceeds the rate of increase of kinetic energy by $W\mathrm{d}\tau$, where

$$\dot{W} = \sigma_r\dot{\epsilon}_r + 2\sigma_\theta\dot{\epsilon}_\theta \quad (5{\cdot}15)$$

is the contribution to the rate of increase of internal energy per unit volume of the element (see, for example, Jeffreys 1931, p. 75). In the theory of metal plasticity, it is customary to treat $\dot{W}$ as the sum of the elastic strain energy rate $\dot{W}^e$ and the plastic strain energy rate $\dot{W}^p = \dot{W} - \dot{W}^e$. This theory also involves the assumption that W^e is the recoverable contribution to the rate of increase of internal energy and that $\dot{W}^p$ is the irrecoverable one, the latter being associated with changes in heat and in atomic arrangement and motion (see Hill

1950, p. 5). The validity of the above procedure, which is also implicit in the theory of soil plasticity, has not been established from thermodynamical principles. Thus

$$\left.\begin{aligned} \dot{W} &= \dot{W}^e + \dot{W}^p, \\ \text{where, from equations (5·2), (5·8}_{1,2}\text{) and (5·9}_3\text{),} \\ \dot{W}^e &= \sigma_r \dot{\epsilon}_r^e + 2\sigma_\theta \dot{\epsilon}_\theta^e = \frac{1}{2E}\frac{\mathrm{D}}{\mathrm{D}t}\{\sigma_r^2 - 4\nu\sigma_r\sigma_\theta + 2(1-\nu)\,\sigma_\theta^2\}, \\ \dot{W}^p &= \sigma_r \dot{\epsilon}_r^p + 2\sigma_\theta \dot{\epsilon}_\theta^p = \dot{\lambda} \geqslant 0, \end{aligned}\right\} \tag{5·16}$$

$\dot{W}^e$ and $\dot{W}^p$ (here identical with $\dot{\lambda}$) being the recoverable elastic and the irrecoverable plastic components of the (excess) rate of work $\dot{W}$.

The parameter $\dot{\lambda}$ may be entirely eliminated from the equations. First, for purely elastic deformation, $\dot{\lambda} = 0$. Secondly, for plastic-elastic deformations (see equations (5·9$_{1,2}$)), $\dot{\lambda}$ may be eliminated from the stress rate, strain rate relations to give

$$\begin{aligned} \{1-2\nu+\varpi(1+2\nu)\sin\phi\}\,\dot{\sigma}_r + 2\{1-2\nu-\varpi\sin\phi\}\,\dot{\sigma}_\theta \\ = E\left\{(1+\varpi\sin\phi)\frac{\partial v}{\partial r} + 2(1-\varpi\sin\phi)\frac{v}{r}\right\}. \end{aligned} \tag{5·17}$$

The necessary second equation follows from the condition of continued yield, which (see equation (5·9$_3$)) requires that

$$\dot{\sigma}_\theta = (1-\varpi\sin\phi)\,\dot{\sigma}_r/(1+\varpi\sin\phi). \tag{5·18}$$

Then, from equations (5·9$_{1,2}$) and (5·18),

$$\begin{aligned} \dot{\lambda} = 4\varpi c\cos\phi\left[\{1-2\nu+\varpi(1+2\nu)\sin\phi\}\frac{v}{r} - \{1-2\nu-\varpi\sin\phi\}\frac{\partial v}{\partial r}\right] \\ \times\{(1-2\nu)\,(3-2\varpi\sin\phi) + (3+2\nu)\sin^2\phi\}^{-1}, \end{aligned} \tag{5·19}$$

so that $\dot{\lambda}$ is expressed in terms of v only, and the condition for non-negative plastic rate of work is

$$\{\varpi(1-2\nu)+(1+2\nu)\sin\phi\}\frac{v}{r} - \{\varpi(1-2\nu)-\sin\phi\}\frac{\partial v}{\partial r} \geqslant 0. \tag{5·20}$$

It should be noted that the present analysis incorporates convective terms which are neglected in the classical theory of infinitesimal elasticity. This procedure has the advantage of removing certain inconsistencies between the equations governing elastic and plastic deformations. Furthermore, it anticipates the fact that for ideal soils it is possible for finite deformations to occur even within the elastic range (see tables 8 and 12). The description of large elastic deformations in ideal soils is discussed in §§ 7·1·1 and 7·2.

5·3. *Discontinuity relations*

The analysis of § 5·2 implicitly assumes certain conditions of continuity and differentiability on the various field quantities such as stress and velocity. In fact it is assumed there that only *weak* discontinuities occur. On a *strong* discontinuity surface, finite discontinuity relations hold which may be regarded as replacing some of the differential equations there.

In the present analysis, any possible discontinuity surface must be spherical and concentric with the camouflet surface. Let S denote such a spherical surface, say, $r = r_1(t)$, and suppose

that a discontinuity in at least one field quantity, say $G(r,t)$, occurs across S. This discontinuity is to be regarded as the limit of the variation of a continuous distribution across a thin spherical shell enclosing S as this shell shrinks up about S. The discontinuity in G across S is defined as

$$\left.\begin{aligned} [G] &= G^+ - G^-, \\ \text{where} \quad G^\pm &= \lim_{r \to r_1 \pm 0} G(r,t). \end{aligned}\right\} \tag{5·21}$$

The position of S will generally vary with the time, and this variation may be represented by the curve C whose equation is

$$g(r,t) \equiv r - r_1(t) = 0, \tag{5·22}$$

drawn in a plane in which r and t are taken as rectangular Cartesian co-ordinates.

It should be remarked that certain discontinuities in field quantities cannot be precisely realized in real materials. Certain features of true physical behaviour, such as work-hardening and rate-of-strain effects, tend to diffuse sharp discontinuities into continuous transitions over narrow regions. For general discussions of discontinuity relations in the mechanics of solids, see Prager (1955*a*), Hill (1961) and Thomas (1961, chap. 2).

The arguments now developed are formal, the statement of analytical conditions sufficient for the validity of the results being omitted.

The kinematical restriction on permissible discontinuities in the derivatives of a continuous field quantity is first considered. Suppose that G is continuous across S throughout some time interval. Let P_1, P, P_2 be points, taken in order, on a small segment of C. Then $[G]_{P_1} = [G]_{P_2} = 0$, and hence $([G]_{P_1} - [G]_{P_2})/\delta s = [(G_{P_1} - G_{P_2})/\delta s] = 0$, where δs is the distance P_1P_2. Proceeding to the limit as $\delta s \to 0$, $[\partial G/\partial s]_P = 0$ or, from equation (5·22),

$$\left.\begin{aligned} V[\partial G/\partial r] + [\partial G/\partial t] &= 0, \\ \text{where} \quad V &= \mathrm{d}r_1/\mathrm{d}t \end{aligned}\right\} \tag{5·23}$$

is the velocity of propagation of S. Two different cases arise in connexion with equation (5·23): (i) $V = 0$ when $[\partial G/\partial t] = 0$ but $\partial G/\partial r$ may or may not be continuous, and (ii) $V \neq 0$ when either $[\partial G/\partial r] = 0$ *and* $[\partial G/\partial t] = 0$ or $[\partial G/\partial t] = -V[\partial G/\partial r] \neq 0$.

Even in ideal materials a number of continuity requirements on field quantities must hold. First, in plastic-elastic flow without fracture,

$$[u] = 0. \tag{5·24}$$

Secondly, from the laws of conservation of mass and of momentum,

$$[\rho(v - V)] = 0, \tag{5·25}$$

$$[\sigma_r - \rho v(v - V)] = 0. \tag{5·26}$$

5·4. *Initial and boundary conditions*

It is supposed that initially ($t = 0$) the region $r \geqslant a(0) = a_0$ is at rest and under a uniform hydrostatic pressure Π, and that subsequently ($t > 0$) the known pressure $P(a)$ acts on the camouflet surface $r = a(t)$. Then the initial and boundary conditions are

$$\left.\begin{aligned} &u = v = 0, \quad \sigma_r = \sigma_\theta = -\Pi, \quad \rho = \rho_0 \quad \text{for} \quad r \geqslant a_0 \quad \text{at} \quad t = 0, \\ &\sigma_r = -P(a) \quad \text{at} \quad r = a(t), \\ &\left.\begin{aligned} u, v &\to 0, \quad \sigma_r, \sigma_\theta \to -\Pi, \quad \rho \to \rho_0 \quad \text{as} \quad r \to \infty \end{aligned}\right\} \quad \text{for} \quad t > 0. \end{aligned}\right\} \tag{5·27}$$

As stated in § 2·4, the value of Π is chosen to be the sum of atmospheric pressure p_a and the overburden pressure $\rho_0 gh$ at the depth of the charge centre, i.e.

$$\Pi = p_a + \rho_0 gh. \tag{5·28}$$

5·5. *Statement of mathematical problem*

The mathematical problem is to determine the quantities ρ, u, v, σ_r, σ_θ as functions of r and t subject to the field and constitutive equations (5·9) to (5·12), the discontinuity relations (5·24) to (5·26), the initial and boundary conditions (5·27), and the assumption that the yield function is continuous at plastic-elastic boundaries.

Suppose that the variables ρ, u, v, σ_r, σ_θ are known up to some time t. Then it is required to determine the incremental changes $\delta\rho$, δu, δv, $\delta\sigma_r$, $\delta\sigma_\theta$ occurring in the increment of time δt. In the case of a local elastic deformation, there are available the kinematic relation (5·12), the two convective-Hookean stress rate, strain rate relations ($5·9_{1,2}$) with $\dot{\lambda} = 0$, the equation of motion (5·10) and the equation of conservation of mass (5·11). In the case of a local plastic deformation, there are available the equations (5·10) to (5·12) as before, together with the single plastic-elastic relation between stress rate and strain rate (5·17) and the yield condition on the stress rates (5·18). Thus, in each case, five equations are available for the five unknowns. In principle, the problem is therefore a determinate one, but it should be observed that the positions of any discontinuity surfaces are not known *a priori*, and they must therefore be found as part of the solution. However, under spherically symmetric conditions, and in simplified procedures based upon the neglect of wave propagation effects (see § 5·6), the determination of the nature of discontinuity surfaces presents no difficulties. Finally, the solution must satisfy the conditions $f < 0$ or $f = 0$ *and* $\dot{f} < 0$ in elastically deforming regions, and $f = \dot{f} = 0$ *and* $\dot{W}^p \geqslant 0$ in plastically deforming regions.

5·6. *Simplified procedures*

The present problem is one of non-linear plastic-elastic wave propagation. It might reasonably be supposed that the analysis is essentially concerned with the integration of a system of hyperbolic partial differential equations, the complexity of which obviously renders a direct solution feasible only by purely numerical techniques. Here, however, the complications due to wave propagation effects are avoided by using simplified procedures based on one or other of two assumptions. First, in § 6, it is assumed that the plastic region is incompressible and the elastic region is compressible, all inertial effects in the latter being neglected. Secondly, in § 7, the entire soil region is assumed incompressible. Motion governed by either of these assumptions will be described here by the term *isochronous*. These procedures enable a more far-reaching analytical treatment of the basic equations to be made.

Taylor and Penney (1954, private communication), whose analysis is confined to the first expansion phase of camouflet motion, assume that the material in the plastic region is incompressible, and that the material in the elastic region is in equilibrium. These assumptions lead to mathematical inconsistencies at the plastic-elastic boundary, as observed by E. P. Hicks (1954, private communication). In the present work, following the earlier approach proposed by Hill (1948), these inconsistencies, which arise from the violation of conditions (5·25) and (5·26) at the plastic-elastic boundary, are avoided by assuming

that the material is everywhere incompressible and including inertial effects in both the plastic and elastic regions. The form of the governing equations of completely incompressible motion is derived in the next section, but the development of detailed analysis and presentation of numerical values is deferred to § 7.

5·7. *Equations for incompressible flow*

Under the assumption of completely incompressible motion,

$$\rho = \rho_0 = \text{constant}, \tag{5·29}$$

and the equation of conservation of mass (5·11) now shows that $\partial(r^2 v)/\partial r = 0$. The particle velocity is therefore given by

$$v = a^2\dot{a}/r^2, \tag{5·30}$$

where $\dot{a}$ is the velocity of the camouflet surface.

The strain rates are now

$$\dot{\epsilon}_r = -2a^2\dot{a}/r^3, \quad \dot{\epsilon}_\theta = a^2\dot{a}/r^3, \tag{5·31}$$

and the equation of motion (5·10) becomes

$$\frac{\partial \sigma_r}{\partial r} + \frac{2(\sigma_r - \sigma_\theta)}{r} = \rho_0 \left\{ \frac{a^2\ddot{a} + 2a\dot{a}^2}{r^2} - \frac{2a^4\dot{a}^2}{r^5} \right\}. \tag{5·32}$$

Since assumption (5·29) applies to both elastic and plastic deformation, it is necessary first to put $\nu = \frac{1}{2}$ and then, in order to achieve consistency with equation (5·14), to set $\phi = 0$ in the Coulomb flow rule ($5·8_{1,2}$). Thus the stress rate, strain rate relations and yield condition are taken to be

$$\left.\begin{aligned} E(\partial v/\partial r) &= \dot{\sigma}_r - \dot{\sigma}_\theta - E\varpi\dot{\lambda}/2c, \\ E(v/r) &= \tfrac{1}{2}(\dot{\sigma}_\theta - \dot{\sigma}_r) + E\varpi\dot{\lambda}/4c, \\ f &= \varpi\sigma_\theta - \{(\varpi - \sin\phi)\,\sigma_r + 2c\cos\phi\}/(1 + \varpi\sin\phi) = 0, \\ \dot{W}^p &\begin{cases} = 0 & \text{if either} \quad f < 0 \quad \text{or} \quad f = 0 \quad \textit{and} \quad \dot{f} < 0, \\ \geqslant 0 & \text{if} \quad f = \dot{f} = 0. \end{cases} \end{aligned}\right\} \tag{5·33}$$

with

The relation between the fundamental condition $\dot{W}^p \geqslant 0$ and the derived condition $\dot{\lambda} \geqslant 0$ is discussed later (see remarks following equations (5·36)).

Chadwick (1959) has shown that the effect of elastic compressibility is small when a camouflet is expanded quasi-statically, but no corresponding investigation has been made for dynamic expansion. The use of a non-associated flow rule represents a departure from current methods of plasticity theory. There is some fundamental evidence supporting the admissibility of associated flow rules for metals, but not for soils. At large plastic strain, when λ is large, equation (5·14) implies considerable reductions in ρ if ϕ is non-zero. This result is physically unacceptable because soils exhibit only limited dilatancy, and the associated density changes are relatively small. The modified flow rule is therefore physically more realistic under conditions of large strain. However, when $\nu = \frac{1}{2}$ the longitudinal elastic wave velocity is infinite and some assessment of the error that this incurs needs to be made.

For convenience, the forms taken by certain of the equations in § 5·2 under conditions of incompressible flow are given below.

Equation (5·15) still holds, but $\dot{W}^e$ and $\dot{W}^p$ are now given by

$$\dot{W}^e = \frac{1}{2E}\frac{\mathrm{D}}{\mathrm{D}t}\{(\sigma_r-\sigma_\theta)^2\}, \quad \dot{W}^p = \frac{\varpi\dot{\lambda}}{2c}(\sigma_\theta-\sigma_r). \tag{5·34}$$

It is no longer possible or necessary to eliminate $\dot{\lambda}$ from the stress rate, strain rate equations, as in equation (5·17), since equations ($5{\cdot}33_{1,2}$) are dependent and serve only to determine $\dot{\lambda}$. It should be noted from the yield condition ($5{\cdot}33_3$) that

$$\sigma_\theta-\sigma_r = 2\varpi(c\cos\phi-\sigma_r\sin\phi)/(1+\varpi\sin\phi). \tag{5·35}$$

Thus

$$\dot{W}^p = \dot{\lambda}(\cos\phi-\sin\phi\,\sigma_r/c)/(1+\varpi\sin\phi), \tag{5·36}$$

and hence $\dot{W}^p \geqslant 0$ implies that $\dot{\lambda} \geqslant 0$ only if $\sigma_r < c\cot\phi$. However, this restriction has already been made in relation to the yield surface defined by equations (4·5), and the equivalence of the two conditions is therefore established.

The condition for non-negative plastic rate of work is not now expressible in terms of v only, but, with use of equations (5·30), ($5{\cdot}33_2$) and (5·35), it can be written as

$$\frac{2a^2\dot{a}}{r^3}(\sigma_r-\sigma_\theta)-\frac{1}{2E}\frac{\mathrm{D}}{\mathrm{D}t}\{(\sigma_r-\sigma_\theta)^2\} \geqslant 0. \tag{5·37}$$

Equations (5·24) to (5·26) simplify to

$$[u]=0, \quad [v]=0, \quad [\sigma_r]=0, \tag{5·38}$$

and, since the yield function is assumed to be continuous across a plastic-elastic boundary,

$$[\sigma_\theta]=0. \tag{5·39}$$

Finally, the initial and boundary conditions (5·27) remain unaltered.

PART III. MODELS OF CAMOUFLET MOTION

6. Point source models

In this section, the theory of spherical plastic-elastic flow in ideal soils, developed in § 5, is applied to a point source model of camouflet motion. For such a model the given energy release $\mathscr{E}_{\mathrm{cam.}}$ is concentrated at a single point. A comparison between numerical values obtained for point source and spherical charge models of explosions is made in § 7·1·7.

The discussion now proceeds according to the assumptions made in regard to isochronous motion. In § 6·1, the plastic region is assumed to be incompressible, and inertial effects are neglected in the elastic region, as proposed by Taylor and Penney (1954, private communication) in their similarity theory of the first expansion phase. Hicks's (1954, private communication) modification of the Penney–Taylor theory is discussed in § 6·2. This theory includes inertial effects in the elastic region, now taken to be incompressible.

The analysis given in this section relates only to the first expansion phase of the motion. However, a preliminary argument is applied to the discussion of the subsequent pulsations, precise discussion being deferred to §§ 7·1·2 and 7·1·3.

PHILOSOPHICAL TRANSACTIONS OF THE ROYAL SOCIETY A MATHEMATICAL, PHYSICAL & ENGINEERING SCIENCES

6·1. *Penney–Taylor similarity theory*

The theory of spherically symmetric camouflet formation due to Taylor and Penney is developed here in its original form, save for certain extensions and corrections concerning the law of variation of the pressure of the explosion products and the nature of the energy partition. The analysis of camouflet formation was developed by Taylor for quasi-static deformation and extended by Penney to dynamic deformation. The theory has the characteristic feature of geometrical similarity, so that, in particular, the radius of the plastic-elastic boundary is a constant multiple of the radius of the expanding camouflet surface. It should be noted, however, that the condition of geometrical similarity, which is a structural feature of the theory and not a consequence of dimensional arguments, ceases to apply at the end of the first expansion phase. The present model provides a useful approximation to the more elaborate solution obtained in § 7 when a sufficiently large expansion occurs, although, since the camouflet is assumed to expand from zero radius, the problem of the initiation of plastic flow is indeterminate.

Let $a(t)$ and $b(t)$ be the radii of the camouflet surface and the plastic-elastic boundary respectively (see figure 1). Thus the region $a \leqslant r < b$ is deforming plastically, the boundary $r = b$ is at yield, and the region $r > b$ is deforming elastically.

6·1·1. *First expansion phase*

From equation $(5{\cdot}9_3)$, setting $\varpi = 1$ for expansion conditions, the yield condition may be written in the form

$$(1+\alpha)\,\sigma_\theta - \sigma_r - Y = 0, \tag{6·1}$$

where

$$Y = 2c\cos\phi/(1-\sin\phi), \quad \alpha = 2\sin\phi/(1-\sin\phi) \tag{6·2}$$

are respectively referred to as the *yield strength* and *friction coefficient* of the soil. Equation (6·1) was used by Taylor and Penney, but they did not derive equations (6·2) showing the dependence of Y and α upon the soil parameters c and ϕ.

In the elastic region, inertial effects are neglected, but compressibility effects are included. Let the strain be defined to be zero in the initial state. Then, taking Hooke's law to connect changes of stress and strain, it follows that

$$\left.\begin{aligned} E(\partial u/\partial r) &= \sigma_r + \Pi - 2\nu(\sigma_\theta + \Pi), \\ E(u/r) &= (1-\nu)\,(\sigma_\theta + \Pi) - \nu(\sigma_r + \Pi), \\ \frac{\partial \sigma_r}{\partial r} &+ \frac{2(\sigma_r - \sigma_\theta)}{r} = 0. \end{aligned}\right\} \tag{6·3}$$

It should be noted that, as mentioned above, the point source model due to Taylor and Penney is developed here essentially in its original form. For this reason Hooke's law is used in its normal form, relating stresses and strains, rather than in its convective form, equation (5·2). Since the law is only used in the elastic region where, according to the Penney–Taylor similarity theory, only small strains occur, no significant error is thereby incurred.

With the use of the boundary conditions (5·27), the appropriate solution of equations (6·3) is

$$\left.\begin{aligned} \sigma_r &= -\Pi - 4\mu C/r^3, \\ \sigma_\theta &= -\Pi + 2\mu C/r^3, \\ u &= C/r^2, \end{aligned}\right\} \quad (r > b), \tag{6·4}$$

where C is a function of time determined below. Although the material is not assumed to be incompressible in the elastic region, the form of this solution shows that no density changes occur there (see equation (5·14)). Since the material in the plastic region is assumed to be incompressible and $a_0 = 0$, the condition of conservation of mass gives $r^3 - r_0^3 = a^3$, where r_0 is the initial radius of the material point currently at radius r. In particular, when $r = b$ and $r_0 = b - (u)_{r=b}$, then

$$(u)_{r=b} \approx a^3/3b^2, \tag{6·5}$$

where $(u)_{r=b}$ is assumed small. From equations $(6·4_3)$ and (6·5) it therefore follows that

$$C = \tfrac{1}{3}a^3. \tag{6·6}$$

Since the material at the plastic-elastic boundary is at yield, equations (6·1), $(6·4_{1,2})$ and (6·6) give

$$(b/a)^3 = 2\mu(3+\alpha)/\{3(Y+\alpha\Pi)\} = \text{constant} = n^3, \quad \text{say}, \tag{6·7}$$

where, under practical conditions, n is of the order of 10. Thus the radius of the plastic-elastic boundary is a constant multiple n of the radius of the camouflet surface. Also, since

$$-(\sigma_r)_{r=b+0} = \{2Y + 3(1+\alpha)\,\Pi\}/(3+\alpha), \tag{6·8}$$

the radial (and tangential) stresses at the plastic-elastic boundary are constant.

In the plastic region, the equation of motion (5·32) holds and, with use of the yield condition (6·1), it follows that σ_r satisfies the equation

$$\frac{\partial\sigma_r}{\partial r} + \frac{2\alpha}{(1+\alpha)\,r}\sigma_r = \frac{2Y}{(1+\alpha)\,r} + \rho_0\left\{\frac{a^2\ddot{a} + 2a\dot{a}^2}{r^2} - \frac{2a^4\dot{a}^2}{r^5}\right\}. \tag{6·9}$$

Hence

$$\sigma_r = \frac{Y}{\alpha} - \rho_0(1+\alpha)\left\{\frac{a^2\ddot{a} + 2a\dot{a}^2}{(1-\alpha)\,r} - \frac{a^4\dot{a}^2}{(2+\alpha)\,r^4}\right\} + F(t)\,r^{-2\alpha/(1+\alpha)}, \tag{6·10}$$

where $F(t)$ is a disposable function. Since the density is constant, it follows from equations (5·25) and (5·26) that σ_r is continuous at $r = b$. Hence, with the use of equation (6·8), $F(t)$ is determined, and then

$$\sigma_r = \frac{Y}{\alpha} - \rho_0(1+\alpha)\left\{\frac{a^2\ddot{a} + 2a\dot{a}^2}{(1-\alpha)\,r} - \frac{a^4\dot{a}^2}{(2+\alpha)\,r^4}\right\}$$
$$- \left\{\frac{na}{r}\right\}^{2\alpha/(1+\alpha)}\left[\frac{3(1+\alpha)\,(Y+\alpha\Pi)}{\alpha(3+\alpha)} - \rho_0(1+\alpha)\left\{\frac{a\ddot{a} + 2\dot{a}^2}{(1-\alpha)\,n} - \frac{\dot{a}^2}{(2+\alpha)\,n^4}\right\}\right] \quad (a \leqslant r < b). \tag{6·11}$$

The particular cases $\alpha = 0$ and 1, corresponding to $\phi = 0$ (frictionless material) and $\phi \approx 19\frac{1}{2}°$, are treated by finding the limiting form of equation (6·11) as $\alpha \to 0$ and 1, respectively. These results are not set down here, but it may be noted that logarithmic terms appear. The relation between the camouflet pressure $P(a)$ and the camouflet radius a, which follows at once from equation (6·11), is

$$P = n^{2\alpha/(1+\alpha)}\left[\frac{3(1+\alpha)\,(Y+\alpha\Pi)}{\alpha(3+\alpha)} - \rho_0(1+\alpha)\left\{\frac{a\ddot{a} + 2\dot{a}^2}{(1-\alpha)\,n} - \frac{\dot{a}^2}{(2+\alpha)\,n^4}\right\}\right]$$
$$+ \rho_0(1+\alpha)\left\{\frac{a\ddot{a} + 2\dot{a}^2}{1-\alpha} - \frac{\dot{a}^2}{2+\alpha}\right\} - \frac{Y}{\alpha}. \tag{6·12}$$

This equation will be referred to as *Penney's camouflet equation*. If $P(a)$ is known, equation (6·12) is a non-linear second-order ordinary differential equation for $a(t)$ which is to be

integrated subject to suitable initial conditions. The substitution of this solution into the other equations completes the analysis. The numerical integration of Penney's camouflet equation is discussed in § 6·1·3, and illustrative numerical results are given in § 6·1·4.

6·1·2. *First contraction phase and subsequent pulsations*

Since, in general, $\ddot{a} \neq 0$ at the end of the first expansion phase, further motion will occur. Detailed analysis is required to determine the exact nature of this motion and, in particular, the change in the camouflet radius during the first contraction phase. It is useful to anticipate here certain results which are obtained in § 7·1. The further motion of the camouflet varies with the type of ideal soil and also with the value of the initial uniform hydrostatic pressure Π. In general, for an ideal soil exhibiting any appreciable internal friction, it appears that further changes in the camouflet radius are small. For frictionless ideal soils, the amplitude of motion during the first contraction phase increases markedly with Π. Ultimately, plastic deformation will cease and any further motion then consists of elastic pulsations.

The first contraction phase involves preliminary elastic motion, generally followed by further plastic-elastic motion. The yield condition, now given by equation $(5{\cdot}9_3)$ with $\varpi = -1$, is

$$(1+\alpha)\,\sigma_r - \sigma_\theta - Y = 0, \tag{6·13}$$

where the soil parameters Y and α are defined in equations (6·2). Because of the elastic unloading, a repetition of the argument of § 6·1·1, with interchange of equations (6·1) and (6·13), would afford no basis for linking the states of motion in the first expansion and contraction phases, and a complete plastic-elastic analysis of the first contraction phase is hence unavoidable. However, in certain cases it can be shown, by appeal to energy considerations, that the motion of the camouflet surface subsequent to the first expansion phase is small. Consider the energy partition at the end of the first expansion phase. The total kinetic energy is zero. In the plastic region, the plastic work and the elastic strain energy can be evaluated from equations (5·16), care being taken to change ν from its actual value to $\frac{1}{2}$ as material becomes plastic. The remaining part of the work done by the explosion products in expanding the camouflet is stored reversibly as elastic strain energy in the elastic region and, due to work done against the uniform hydrostatic pressure, as potential energy at infinity. Let the radii of the camouflet surface and the plastic-elastic boundary at the end of the first expansion phase (when $t = t_1$) be a_1 and b_1. Then the total work done on the final elastic region by forces at the final plastic-elastic boundary is

$$4\pi b_1^2 \int_0^{t_1} (-\sigma_r v)_{r=b_1}\,\mathrm{d}t = 4\pi b_1^2 \int_0^{a_1} \left(\Pi + \frac{4\mu a^3}{3b_1^3}\right)\frac{a^2}{b_1^2}\,\mathrm{d}a = \tfrac{4}{3}\pi a_1^3 \left\{\Pi + \frac{Y+\alpha\Pi}{3+\alpha}\right\}, \tag{6·14}$$

with use of equations (5·30), $(6{\cdot}4_1)$, (6·6) and (6·7). The total work done on the same region by the stress at infinity is

$$\lim_{R\to\infty}\left\{4\pi R^2 \int_0^{t_1} (\sigma_r v)_{r=R}\,\mathrm{d}t\right\} = \lim_{R\to\infty}\left\{4\pi R^2 \int_0^{a_1} \left(-\Pi - \frac{4\mu a^3}{3R^3}\right)\frac{a^2}{R^2}\,\mathrm{d}a\right\} = -\tfrac{4}{3}\pi a_1^3 \Pi, \tag{6·15}$$

with use of equations (5·30), $(6{\cdot}4_1)$ and (6·6). Hence, from equations (6·14) and (6·15), the total strain energy stored in the elastic region is

$$\tfrac{4}{3}\pi a_1^3 \frac{Y+\alpha\Pi}{3+\alpha}, \tag{6·16}$$

and potential energy of amount $\frac{4}{3}\pi a_1^3 \Pi$ (6·17)

is stored at infinity. The work done by the camouflet pressure is

$$\left.\begin{aligned} 4\pi\int_0^{a_1} a^2 P(a)\,\mathrm{d}a &= \tfrac{4}{3}\pi a_1^3 P_m, \\ P_m &= \frac{1}{V_1}\int_0^{V_1} P(V)\,\mathrm{d}V \end{aligned}\right\} \quad (6\cdot18)$$

where

is the mean value of P, regarded as a function of camouflet volume V, during the first expansion phase. Now if

$$P_m \gg \Pi + \frac{Y+\alpha\Pi}{3+\alpha}, \quad (6\cdot19)$$

then, assuming that the elastic strain energies of the plastic and elastic regions are of the same order of magnitude, the sum of the recoverable strain energy and the potential energy at infinity is much smaller than the work done by the camouflet pressure. Therefore this work must be only slightly greater than the irrecoverable plastic work. In this case the energy available to enforce compression of the gaseous explosion products is small, so that the amplitude of any further motion must be small. It seems, however, that the strong inequality (6·19) does not hold in most practical situations and therefore the above argument is generally inconclusive.

6·1·3. *Numerical procedures*

Penney's camouflet equation can be written in the form

$$\frac{1+\alpha}{1-\alpha}\rho_0(a\ddot{a}+2\dot{a}^2)\{1-n^{-(1-\alpha)/(1+\alpha)}\}-\frac{1+\alpha}{2+\alpha}\rho_0\dot{a}^2\{1-n^{-2(2+\alpha)/(1+\alpha)}\}$$
$$+\left(\Pi+\frac{Y}{\alpha}\right)\left\{3\frac{1+\alpha}{3+\alpha}n^{2\alpha/(1+\alpha)}-1\right\}+\Pi-P=0. \quad (6\cdot20)$$

It is convenient to reduce equation (6·20) to non-dimensional form. Let the velocity c_0 be defined by

$$c_0^2 = E/\rho_0, \quad (6\cdot21)$$

and introduce a non-dimensional time τ and distance x defined by

$$\tau = c_0 t/a_0, \quad x = a/a_0, \quad (6\cdot22)$$

where a_0 is an arbitrary length specified later. Then equation (6·20) reduces to

$$K_1 x x'' + 2(K_1 - K_2)\,x'^2 + K_3 - \Theta(x) = 0, \quad (6\cdot23)$$

where

$$\left.\begin{aligned} K_1 &= \frac{1+\alpha}{1-\alpha}\{1-n^{-(1-\alpha)/(1+\alpha)}\}, \\ K_2 &= \frac{1+\alpha}{2(2+\alpha)}\{1-n^{-2(2+\alpha)/(1+\alpha)}\}, \\ K_3 &= \frac{1}{E}\left(\Pi+\frac{Y}{\alpha}\right)\left\{3\frac{1+\alpha}{3+\alpha}n^{2\alpha/(1+\alpha)}-1\right\} \end{aligned}\right\} \quad (6\cdot24)$$

are constants,

$$\Theta(x) = \frac{P(a)-\Pi}{E}, \quad (6\cdot25)$$

and the primes denote differentiation with respect to τ.

Initially, $t = 0$ and $a = 0$, i.e. $\tau = 0$ and $x = 0$. If xx'' is zero when $\tau = 0$, then equation (6·23) shows that

$$x' = \left\{\frac{\Theta_0 - K_3}{2(K_1 - K_2)}\right\}^{\frac{1}{2}} \quad \text{when} \quad \tau = 0, \tag{6·26}$$

where $\Theta_0 = \Theta(0)$. It can be shown that if $n > 1$, then $K_1 - K_2 > 0$. Thus the initial value of x' will be real if

$$P_0 \geqslant \Pi + \left(\Pi + \frac{Y}{\alpha}\right)\left\{3\frac{1+\alpha}{3+\alpha}n^{2\alpha/(1+\alpha)} - 1\right\}, \tag{6·27}$$

and this minimum value of P_0 is seen from equation (6·20) to be the pressure needed to expand the camouflet quasi-statically.

Once $\Theta(x)$ is known, equation (6·23) can be integrated, subject to the known initial conditions, in order to determine x as a function of τ. The discussion of the camouflet pressure given in § 4·1 must now be extended to cover the case when the energy release $\mathscr{E}_{\text{cam.}}$ is confined to a single point, the length a_0 in equation (4·1) then being undefined. A plausible way of overcoming this difficulty is to choose a_0 in equations (4·1) and (6·22) to be equal to the radius of a spherical charge which has an effective energy release $\mathscr{E}_{\text{cam.}}$ equal to that of the point source, and then to assume that equation (4·1) is valid in the range $a \geqslant 0$. However, if this is done, no solution of equation (6·23) can be obtained because, due to the behaviour of $\Theta(x)$ near $x = 0$, various integrals diverge. This procedure is therefore valueless. From the wide range of mathematically acceptable assumptions which can be made, two will be chosen here, being referred to as *assumptions A and B*. The numerical values given later show that the main features of camouflet motion are not critically dependent upon the precise assumptions made.

Assumption A is that the camouflet pressure has a constant value P_1 for $a \leqslant a_0$, where a_0 is the radius of a spherical charge having effective energy release $\mathscr{E}_{\text{cam.}}$. The law of variation of $P(a)$ when $a > a_0$ is supposed to be given by equations (4·1) with P_0 replaced by P_1. Thus

$$P(a) = \begin{cases} P_1 & \text{if} \quad 0 \leqslant a/a_0 \leqslant 1, \\ P_1(a/a_0)^{-9} & \text{if} \quad 1 \leqslant a/a_0 \leqslant 1{\cdot}530, \\ P_1(1{\cdot}530)^{-5{\cdot}19}\,(a/a_0)^{-3{\cdot}81} & \text{if} \quad a/a_0 \geqslant 1{\cdot}530. \end{cases} \tag{6·28}$$

It is found, on equating the energy release to $\mathscr{E}_{\text{cam.}}$ as in § 4·1, that

$$P_1 = 1{\cdot}991 \times 10^5 \text{ Lb./in.}^2. \tag{6·29}$$

The growth of the camouflet up to radius a_0 (i.e. for $0 \leqslant x \leqslant 1$) is governed by the equation

$$K_1 xx'' + 2(K_1 - K_2)\,x'^2 + K_3 - \Theta_0 = 0, \tag{6·30}$$

where $\Theta_0 = (P_1 - \Pi)/E$ is a constant. This equation can be written as

$$\frac{\mathrm{d}}{\mathrm{d}x}\{x^{4(1-K_2/K_1)}x'^2\} = \frac{2}{K_1}(\Theta_0 - K_3)\,x^{3-4K_2/K_1},$$

and, on integration subject to the initial condition (6·26), it follows that

$$x' = \left\{\frac{\Theta_0 - K_3}{2(K_1 - K_2)}\right\}^{\frac{1}{2}}. \tag{6·31}$$

Thus the camouflet expands at constant velocity. Since $x = 0$ when $\tau = 0$, the complete solution of equation (6·30) is therefore

$$x = \left\{\frac{\Theta_0 - K_3}{2(K_1 - K_2)}\right\}^{\frac{1}{2}}\tau. \tag{6·32}$$

From equation (6·32), the time taken for the camouflet to expand to radius a_0 ($x = 1$) is

$$t_0 = \frac{a_0}{c_0}\left\{\frac{2(K_1 - K_2)}{\Theta_0 - K_3}\right\}^{\frac{1}{2}}. \tag{6·33}$$

If t_0 is now taken as a new time-origin, the new initial conditions for the integration of equation (6·23) are

$$x = 1, \quad x' = \left\{\frac{\Theta_0 - K_3}{2(K_1 - K_2)}\right\}^{\frac{1}{2}} \quad \text{when} \quad \tau = 0. \tag{6·34}$$

The growth of the camouflet beyond radius a_0 is governed by equations (6·23) and (6·34), the camouflet pressure being given by equations (6·28) and (6·29).

Assumption B is that $a = a_0$ and $\dot{a} = 0$ at $t = 0$, and that $P(a)$ is given by equations (4·1) to (4·3), where a_0 is again the radius of a spherical charge having effective energy release $\mathscr{E}_{\text{cam.}}$. Although this assumption cannot be reconciled with the analysis underlying equation (6·12), it involves no mathematical inconsistencies and has the virtue of being sufficiently different from assumption *A* to lend some weight to the conclusion that the solution of equation (6·12) is not too critically dependent upon the precise form of law of variation of gas pressure $P(a)$.

Assumptions *A* and *B* are seen to differ only in respect of the initial velocity of the camouflet surface and the constant of proportionality for the relation between camouflet pressure and radius, and the procedure for the numerical integration of equation (6·12) is the same in both cases.

It is found convenient to replace equation (6·23) by a set of simultaneous first-order differential equations. Thus, define the variables

$$\left.\begin{aligned} x_0 &= \tau = c_0 t/a_0, \\ x_1 &= x = a/a_0, \\ x_2 &= x' = \dot{a}/c_0, \\ x_3 &= \{P(a) - \Pi\}/E = \Theta(x), \end{aligned}\right\} \tag{6·35}$$

which satisfy the equations

$$\left.\begin{aligned} \mathrm{d}x_0/\mathrm{d}\tau &= 1, \\ \mathrm{d}x_1/\mathrm{d}\tau &= x_2, \\ \mathrm{d}x_2/\mathrm{d}\tau &= \{x_3 - K_3 - 2(K_1 - K_2)\, x_2^2\}/K_1 x_1, \\ \mathrm{d}x_3/\mathrm{d}\tau &= x_2 \Theta'(x_1). \end{aligned}\right\} \tag{6·36}$$

The appropriate initial conditions are then

$$x_0 = 0, \quad x_1 = 1, \quad x_2 = \{(\Theta_0 - K_3)/2(K_1 - K_2)\}^{\frac{1}{2}} \quad x_3, = (P_1 - \Pi)/E \quad \text{for assumption } A, \tag{6·37}$$

$$x_0 = 0, \quad x_1 = 1, \quad x_2 = 0, \quad x_3 = (P_0 - \Pi)/E \quad \text{for assumption } B. \tag{6·38}$$

Although the systems of equations (6·36), (6·37) and (6·36), (6·38) are simple, they serve to illustrate the procedure adopted for the integration of camouflet equations throughout this paper, the method used being a fourth-order Runge–Kutta process due to Gill (1951). Numerical values are given in § 6·1·4.

It may be noted that, for frictionless ideal soils ($\alpha = 0$), equations (6·24) become

$$K_1 = 1 - n^{-1}, \quad K_2 = \tfrac{1}{4}(1 - n^{-4}), \quad K_3 = \tfrac{4}{9}(1 + 3\ln n)\, n^{-3}. \tag{6·39}$$

PHILOSOPHICAL TRANSACTIONS OF THE ROYAL SOCIETY A MATHEMATICAL, PHYSICAL & ENGINEERING SCIENCES

Penney's camouflet equation may be written in the general form

$$P = A + Ba\ddot{a} + C\dot{a}^2, \tag{6·40}$$

where $A = EK_3 + \Pi$, $B = \rho_0 K_1$ and $C = 2\rho_0(K_1 - K_2)$. An integrating factor of equation (6·40) is $\dot{a}a^{(2C/B)-1}$, and hence, if $a = \dot{a} = 0$ when $t = 0$ are taken as initial conditions, it follows that

$$\int_0^a P(a)\, a^{(2C/B)-1}\, \mathrm{d}a = \tfrac{1}{2}Ba^{2C/B}\left(\frac{A}{C} + \dot{a}^2\right). \tag{6·41}$$

Thus $\dot{a}$ is determined, and a second quadrature would determine a. Setting $\dot{a} = 0$ $(a \neq 0)$ in equation (6·41), the camouflet radius a_1 at the end of the first expansion phase is given implicitly by

$$\int_0^{a_1} P(a)\, a^{(2C/B)-1}\, \mathrm{d}a = \frac{AB}{2C} a_1^{2C/B}. \tag{6·42}$$

An important special case arises when $3B = 2C$ (i.e. $K_1 = 4K_2$). Except for a factor 4π, the left-hand side of equation (6·42) is then recognized as the work done by the camouflet pressure during the first expansion phase, and if W_{ex} is the work done by the camouflet pressure in expanding the camouflet to radius a, then equations (6·41) and (6·42) simplify to

$$(1/4\pi)\, W_{ex}(a) = a^3(\tfrac{1}{3}A + \tfrac{1}{2}B\dot{a}^2), \tag{6·43}$$

$$(1/4\pi)\, W_{ex}(a_1) = \tfrac{1}{3}Aa_1^3. \tag{6·44}$$

Now if $P(a_1) \approx p_a$, then $W_{ex}(a_1) \approx \mathscr{E}_{\mathrm{cam.}}$, and equation (6·44) yields the approximation

$$a_1 = (3\mathscr{E}_{\mathrm{cam.}}/4\pi A)^{\frac{1}{3}}. \tag{6·45}$$

The *duration* of the first expansion phase, however, depends upon the *rate* at which work is done by the camouflet pressure as well as upon $\mathscr{E}_{\mathrm{cam.}}$, and no corresponding approximate formula can be obtained.

For any given soil, the condition $K_1 = 4K_2$ will, in general, be satisfied at only one particular depth of charge burial. However, it is of more interest that this condition is approximately satisfied for a frictionless soil at all depths, provided only that n is large (see equations (6·39)). In this case, equation (6·45) can be written explicitly in the form

$$a_1 = \left[\frac{3}{4\pi}\mathscr{E}_{\mathrm{cam.}} \Big/ \left\{\Pi + \tfrac{2}{3}Y\left(1 + \ln\frac{2E}{3Y}\right)\right\}\right]^{\frac{1}{3}}. \tag{6·46}$$

Hill (1948), discussing camouflet formation in soils (see § 2·2), and Hunter (1958), discussing cavity formation in metals, have obtained results similar to equation (6·46).

6·1·4. *Numerical values*

As stated above, the camouflet equation (6·23) has been integrated subject to two different sets of initial conditions. Thus, the computer program CAM 1 A assumes that conditions (6·37) apply at $t = 0$ and that $P(a)$ is given by equations (6·28) and (6·29), and program CAM 1 B assumes that conditions (6·38) apply at $t = 0$ and that $P(a)$ is given by equations (4·1) to (4·3). Numerical values are given in table 4 for the three ideal soils S, P and Z (see § 4·2·3), and for a depth of charge burial of 100 ft. Values of ν for these ideal soils were not assigned in § 4·2·3: it is assumed here for simplicity that $\nu = \frac{1}{2}$ in each case, so that $\mu = \frac{1}{3}E$. It is seen that the numerical values given by the two programs are in good

agreement. In addition to these large-scale features of the motion, the programs compute x as a function of τ. These results are presented in graphical form in figure 5, where, for comparison, results derived from the theory developed in § 7·1 are also displayed. Detailed discussion of numerical values is deferred to § 7·1·7.

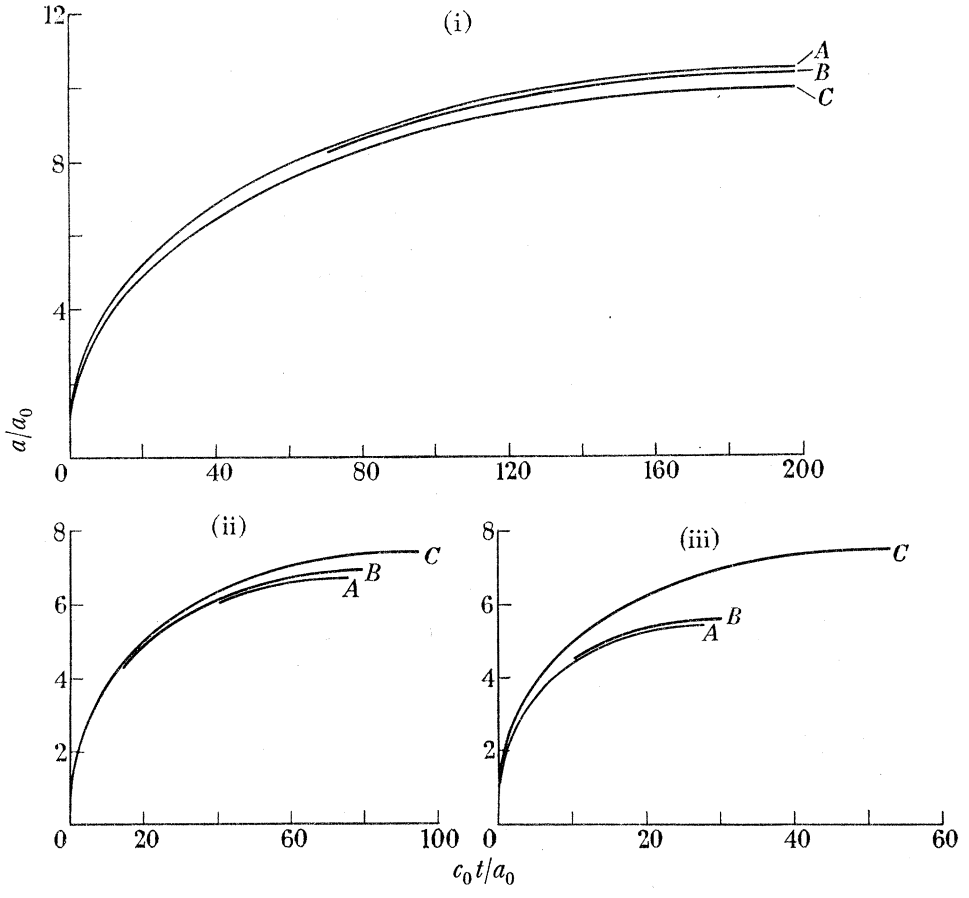

FIGURE 5. Variation of camouflet radius with time during first expansion phase for explosions at depth 100 ft. in soils (i) *S*, (ii) *P* and (iii) *Z*. (*A*) point source model, assumption *A*, (*B*) point source model, assumption *B* and (*C*) spherical charge model.

It should be noted that, in view of the apparently quite unambiguous and relatively simple features of the plastic zones predicted by the models of camouflet formation discussed in this paper, a direct numerical check on the condition of non-negative plastic rate of work has not been undertaken. The condition is known to be satisfied in related problems and, as it is tedious to check, it has been assumed to be true here.

The numerical values in table 4 are presented in dimensionless form. In order to obtain results for a given energy release $\mathscr{E}$, it is necessary first to determine the radius a_0 of the equivalent spherical charge. Then, to determine dimensional values of quantities, all dimensionless lengths and times are multiplied by a_0 and a_0/c_0, respectively. There is, however, an important proviso to be noted. All the present results are based upon an assumed law of variation of $\Theta(x)$ which must be the same for all values of a_0. This means that the pressure Π is to be treated as constant, which implies that the depth of charge burial h does not change. Thus the family of results corresponding to a range of values of a_0 pertains to charges

of different sizes all detonated at the same depth. Accordingly, the present dimensionless formulation of the problem, although apparently conforming to Hopkinson's size-scaling law, does not in fact do so, since complete geometrical similarity is not preserved.

TABLE 4. NUMERICAL VALUES FOR POINT SOURCE MODELS

Depth of charge burial, 100 ft.

$\tau_1 = c_0 t_1/a_0$, scaled time to end of first expansion phase.
a_1/a_0, scaled radius of camouflet surface at end of first expansion phase.
n, constant quotient of radii of plastic-elastic boundary and camouflet surface.
A, B refer to calculations made under assumptions A and B (for the former, τ_1 then includes time of initial expansion under constant pressure).

soil	assumption	τ_1	a_1/a_0	n
S	A	199·5	10·55	13·57
	B	198·7	10·42	13·57
P	A	76·64	6·773	9·187
	B	79·27	6·919	9·187
Z	A	28·66	5·422	5·092
	B	29·90	5·590	5·092

Furthermore, it follows that a_0 cannot realistically be increased without limit, because the plastic-elastic boundary must not extend to ground level if the assumed condition of spherical symmetry is to be reasonably well met (see §2·4). As a_0 is increased, b increases but h remains constant. This implies a maximum value for a_0 beyond which the theory cannot be expected to apply. Table 5 gives some numerical values for this restriction expressed in terms of charge mass. These values are such that for a charge of the mass shown, the radius of the plastic-elastic boundary at the end of the first expansion phase is just equal to the depth of charge burial, 100 ft. In §7·1·7 this question is further discussed and more general results derived (see table 11).

TABLE 5. RESTRICTION ON CHARGE MASS

Depth of charge burial, 100 ft.

soil	maximum mass (lb.)
S	$1{\cdot}4 \times 10^2$
P	$1{\cdot}6 \times 10^3$
Z	$1{\cdot}8 \times 10^4$

6·2. *Other theories*

The Penney–Taylor theory of explosions in soils has the distinctive feature of geometrical similarity. This is a direct consequence of the fact that inertial terms are neglected in the elastic region, whether or not incompressibility is also assumed. Hicks (1954, private communication) has modified the Penney–Taylor theory by including these inertial terms. In order to eliminate effects due to wave propagation, it is then necessary to assume incompressibility throughout the soil. Two simultaneous non-linear second-order ordinary differential equations follow for the radii $a(t)$ and $b(t)$. These camouflet equations contain terms, involving products of the soil friction coefficient with the inertial stresses, which result in the monotonic increase, as the camouflet expands, of the quotient b/a. Except when the material is frictionless, the complexity of Hicks's camouflet equations approaches that of the equations obtained in §7·1·1 for spherical charge models of explosions, and the

similarity feature present in the Penney–Taylor theory is lost. The theory of § 7, which is not restricted to point source models, is therefore preferable to Hicks's theory, although the latter does have a useful application in the simpler case of frictionless materials.

7. Spherical charge models

In this section the general theory of spherical plastic-elastic flow in ideal soils, developed in § 5 and specialized to incompressible flow in § 5·7, is applied to a spherical charge model of camouflet motion. Attention is confined to the case in which the material is incompressible, and inertial effects are everywhere included. Alternative theories are discussed in § 7·3.

7·1. *Incompressible flow theory*

Let t_i $(i = 1, 2, \ldots)$ be the durations of successive expansion and contraction phases. Let $t_i = t_{i,e} + t_{i,p}$, where $t_{i,e}$ and $t_{i,p}$ are respectively the durations of the elastic and the plastic-elastic parts of the ith phase.

7·1·1. *First expansion phase*

In the first expansion phase, the mechanical behaviour is elastic for a time $t_{1,e}$ and is plastic-elastic for a further time $t_{1,p}$. It is normally expected that $t_{1,e} \ll t_{1,p}$.

(*a*) *Elastic deformations.* Initially, the motion involves only elastic deformation of the soil surrounding the expanding camouflet surface. The deformation is governed by the equation of motion (5·32) and the convective-Hookean relations ($5{\cdot}33_{1,2}$) in which $\dot{\lambda}$ is to be taken as zero. For convenience, these equations are restated here in the forms

$$\frac{\partial \sigma_r}{\partial r} + \frac{2(\sigma_r - \sigma_\theta)}{r} = \rho_0 \left\{ \frac{a^2\ddot{a} + 2a\dot{a}^2}{r^2} - \frac{2a^4\dot{a}^2}{r^5} \right\}, \tag{7·1}$$

$$\dot{\sigma}_\theta - \dot{\sigma}_r = 2Ea^2\dot{a}/r^3. \tag{7·2}$$

Now define

$$\Sigma = \sigma_\theta - \sigma_r - 2E \ln (r/a_0). \tag{7·3}$$

Then, since $\dot{r} = a^2\dot{a}/r^2$, equation (7·2) gives

$$\dot{\Sigma} = 0. \tag{7·4}$$

Thus, Σ is constant for any material point during elastic deformation. Now at $t = 0$, $\sigma_r = \sigma_\theta$ on physical grounds and the co-ordinate of a material point, currently at radius r, is $r - u$. Thus initially $\Sigma = -2E \ln \{(r-u)/a_0\}$, and hence

$$\sigma_\theta - \sigma_r = -2E \ln (1 - u/r) \quad (\geqslant 0). \tag{7·5}$$

It follows from the incompressibility condition that

$$r^3 - a^3 = (r-u)^3 - a_0^3, \tag{7·6}$$

and equation (7·5) now becomes

$$\sigma_r - \sigma_\theta = \frac{2E}{3} \ln \left\{ 1 - \frac{a^3 - a_0^3}{r^3} \right\}. \tag{7·7}$$

The elimination of σ_θ between equations (7·1) and (7·7) gives the following differential equation for σ_r,

$$\frac{\partial \sigma_r}{\partial r} + \frac{4E}{3r} \ln \left\{ 1 - \frac{a^3 - a_0^3}{r^3} \right\} = \rho_0 \left\{ \frac{a^2\ddot{a} + 2a\dot{a}^2}{r^2} - \frac{2a^4\dot{a}^2}{r^5} \right\}. \tag{7·8}$$

PHILOSOPHICAL TRANSACTIONS OF THE ROYAL SOCIETY A MATHEMATICAL, PHYSICAL & ENGINEERING SCIENCES

Now introduce the dilogarithm

$$\mathrm{Li}_2(x) = -\int_0^x \ln(1-\xi)\frac{\mathrm{d}\xi}{\xi}. \tag{7·9}$$

The definition (7·9) is the one suggested by Lewin (1958, p. 1) who has given a detailed discussion of the properties of this function. Of the numerous functional relations satisfied by the dilogarithm, note should be taken at this stage of Landen's result

$$\mathrm{Li}_2\{x/(x-1)\}+\mathrm{Li}_2\{x\} = -\tfrac{1}{2}\ln^2(1-x) \quad (x<1) \tag{7·10}$$

(see Lewin 1958, p. 5), which will be used in the later analysis of this section.

The solution of equation (7·8) satisfying the stress boundary condition at infinity (equations (5·27)) can now be stated in the form

$$\sigma_r = -\Pi - \frac{4E}{9}\mathrm{Li}_2\left\{\frac{a^3-a_0^3}{r^3}\right\} - \rho_0\left\{\frac{a^2\ddot{a}+2a\dot{a}^2}{r} - \frac{a^4\dot{a}^2}{2r^4}\right\}. \tag{7·11}$$

Finally, with the use of the stress boundary condition at the camouflet surface (equations (5·27)), a is found to satisfy the equation

$$P(a) = \Pi + \frac{4E}{9}\mathrm{Li}_2\left\{1-\frac{a_0^3}{a^3}\right\} + \rho_0(a\ddot{a}+\tfrac{3}{2}\dot{a}^2). \tag{7·12}$$

The three terms on the right-hand side of equation (7·12) correspond in turn to uniform hydrostatic pressure, elastic stress and inertial stress. It may be noted that, when $E = 0$, equation (7·12) applies to underwater bubble motion. Integration of equation (7·12) shows that

$$\int_{a_0}^{a} P(a)\,a^2\mathrm{d}a = \tfrac{1}{3}\Pi(a^3-a_0^3) + \tfrac{1}{2}\rho_0 a^3\dot{a}^2 + \frac{4E}{27}\left[a^3\,\mathrm{Li}_2\left\{1-\frac{a_0^3}{a^3}\right\} + a_0^3\,\mathrm{Li}_2\left\{1-\frac{a^3}{a_0^3}\right\}\right]. \tag{7·13}$$

Now, except for a factor 4π, the left-hand side of equation (7·13) represents the work done by the camouflet pressure, and the terms on the right-hand side represent in turn the potential energy stored at infinity, and the kinetic energy and the elastic strain energy of the soil. Equation (7·13) must be integrated numerically in order to determine $a(t)$. The distributions of stress and velocity are then found from previous equations.

The above analysis applies only until the yield condition is first satisfied. Now, from equation (7·5), $\sigma_\theta - \sigma_r \geqslant 0$, whence the appropriate yield condition is obtained by taking $\varpi = 1$ in equation ($5{\cdot}9_3$) and is

$$(1+\alpha)\,\sigma_\theta - \sigma_r - Y = 0, \tag{7·14}$$

where

$$Y = 2c\cos\phi/(1-\sin\phi), \quad \alpha = 2\sin\phi/(1-\sin\phi). \tag{7·15}$$

Plastic yield occurs first at the camouflet surface when, by definition, $t = t_{1,e}$ and $a = a_{1,e}$. Then, from equations (7·7) and (7·14), setting $r = a$ and $\sigma_r = -P(a)$, it follows that $a_{1,e}$ is given by

$$2E(1+\alpha)\ln(a_{1,e}/a_0) = Y + \alpha P(a_{1,e}). \tag{7·16}$$

In general, $Y/E \ll 1$, and in the simpler and more familiar situation of a frictionless material ($\alpha = 0$), $(a_{1,e}/a_0) - 1$ is therefore small. However, in the general case this need not be so,

since $P(a_{1,e}) \gg Y$, and, even for quite small values of α, the deformations can no longer be considered small. Illustrative numerical values are given in table 8, and further discussion of this question is given in § 7·2.

(*b*) *Plastic-elastic deformation.* When the camouflet radius increases beyond $a_{1,e}$, a plastic region spreads outwards from the camouflet surface. Separate analyses for the elastic and plastic regions are now required, with appropriate matching of results at the plastic-elastic boundary. At time $t\,(\geqslant t_{1,e})$, the radius of the plastic-elastic boundary will be denoted by $b(t)$, so that the regions $a(t) \leqslant r < b(t)$ and $r > b(t)$ are plastic and elastic, respectively, and the boundary $r = b(t)$ is at yield (see figure 1).

(i) *The elastic region* $(r > b)$. In the elastic region, equations (7·1) to (7·8) and (7·11) still hold, and so

$$\left.\begin{aligned} \sigma_\theta - \sigma_r &= -\frac{2E}{3}\ln\left\{1-\frac{a^3-a_0^3}{r^3}\right\}, \\ \sigma_r &= -\Pi - \frac{4E}{9}\mathrm{Li}_2\left\{\frac{a^3-a_0^3}{r^3}\right\} - \rho_0\left\{\frac{a^2\ddot{a}+2a\dot{a}^2}{r} - \frac{a^4\dot{a}^2}{2r^4}\right\}, \end{aligned}\right\} \quad (r > b(t)). \tag{7·17}$$

(ii) *The plastic region* $(a \leqslant r < b)$. In the plastic region, the yield condition (7·14) is satisfied, and so

$$\sigma_r - \sigma_\theta = (\alpha\sigma_r - Y)/(1+\alpha) \quad (a(t) \leqslant r < b(t)), \tag{7·18}$$

which, when substituted into the equation of motion (7·1), gives the differential equation

$$\frac{\partial\sigma_r}{\partial r} + \frac{2\alpha}{(1+\alpha)\,r}\sigma_r = \frac{2Y}{(1+\alpha)\,r} + \rho_0\left\{\frac{a^2\ddot{a}+2a\dot{a}^2}{r^2} - \frac{2a^4\dot{a}^2}{r^5}\right\} \quad (a(t) \leqslant r < b(t)). \tag{7·19}$$

Hence, with use of the condition at the camouflet surface (equations (5·27)), it follows on integration of equation (7·19) that

$$\begin{aligned} \sigma_r = \frac{Y}{\alpha} - \left\{P(a) + \frac{Y}{\alpha}\right\}\left\{\frac{a}{r}\right\}^{2\alpha/(1+\alpha)} &+ \frac{1+\alpha}{1-\alpha}\rho_0\,(a\ddot{a}+2\dot{a}^2)\left[\left\{\frac{a}{r}\right\}^{2\alpha/(1+\alpha)} - \frac{a}{r}\right] \\ &- \frac{1+\alpha}{2+\alpha}\rho_0\dot{a}^2\left[\left\{\frac{a}{r}\right\}^{2\alpha/(1+\alpha)} - \left\{\frac{a}{r}\right\}^4\right] \quad (a(t) \leqslant r < b(t)). \end{aligned} \tag{7·20}$$

Here and elsewhere, results for the special cases $\alpha = 0$ $(\phi = 0)$ and $\alpha = 1$ $(\phi \approx 19\frac{1}{2}^\circ)$ are derived by a limiting process. These results are not given here, but it may be noted that logarithmic terms are involved.

The solution must now be completed by the matching of results at the plastic-elastic boundary. The stresses σ_r and σ_θ must be continuous at $r = b(t)$ (see equations $(5{\cdot}38_3)$ and (5·39)), and it may then be shown that $a(t)$ and $b(t)$ satisfy the two simultaneous non-linear differential equations

$$\begin{aligned} \{Y+\alpha P(a)\}\left\{\frac{a}{b}\right\}^{2\alpha/(1+\alpha)} &+ \frac{2E}{3}(1+\alpha)\ln\left\{1-\frac{a^3-a_0^3}{b^3}\right\} - \alpha\frac{1+\alpha}{1-\alpha}\rho_0\,(a\ddot{a}+2\dot{a}^2)\left[\left\{\frac{a}{b}\right\}^{2\alpha/(1+\alpha)} - \frac{a}{b}\right] \\ &+ \alpha\frac{1+\alpha}{2+\alpha}\rho_0\dot{a}^2\left[\left\{\frac{a}{b}\right\}^{2\alpha/(1+\alpha)} - \left\{\frac{a}{b}\right\}^4\right] = 0, \end{aligned} \tag{7·21}$$

$$Y + \alpha\Pi + \frac{2E}{3}\left[(1+\alpha)\ln\left\{1-\frac{a^3-a_0^3}{b^3}\right\} + \frac{2\alpha}{3}\mathrm{Li}_2\left\{\frac{a^3-a_0^3}{b^3}\right\}\right] + \alpha\rho_0\left\{\frac{a^2\ddot{a}+2a\dot{a}^2}{b} - \frac{a^4\dot{a}^2}{2b^4}\right\} = 0. \tag{7·22}$$

PHILOSOPHICAL TRANSACTIONS OF THE ROYAL SOCIETY A MATHEMATICAL, PHYSICAL & ENGINEERING SCIENCES

The initial conditions for the integration of equations (7·21) and (7·22) are

$$a = a_{1,e}, \quad \dot{a} = \dot{a}_{1,e}, \quad b = a = a_{1,e} \quad \text{when} \quad t = t_{1,e}. \tag{7·23}$$

The first expansion phase terminates at time $t = t_1$ given by

$$\dot{a}(t_1) = 0. \tag{7·24}$$

7·1·2. *First contraction phase*

Owing to the assumed incompressibility of the material, the motion everywhere reverses direction at time $t = t_1$. The further motion will initially involve elastic unloading of the elastic and plastic regions present at the end of the first expansion phase. Thus, for a further time $t_{2,e}$, the entire soil undergoes elastic deformation. This elastic motion is usually terminated by the onset of plastic yield, and a new plastic region then spreads outwards from the camouflet surface. The deformation is now plastic-elastic, and the first contraction phase terminates when the camouflet surface comes to rest for the second time. Two cases can thus arise according as the first contraction phase is or is not solely one of elastic deformation. In the former case, all deformations following the termination of the first expansion phase are likely to be elastic, and then a single analysis formally completes the solution. In the latter case, separate analysis is required for each of the two stages of the motion during the first contraction phase, and further analysis of the motion after the end of this phase is also required. This is the more general case and will now be considered.

(*a*) *Elastic deformation.* Initially, the motion involves only elastic deformation, and this situation persists for a time $t_{2,e}$. The motion is governed by equations (7·1) to (7·4), but their application is complicated by the presence of a plastically deformed region at the end of the first expansion phase.

Let the co-ordinate of any particular material point at the end of the first expansion phase ($t = t_1$) be r_1, and at a subsequent time t ($> t_1$) be r ($< r_1$). Then $r_1^3 - a_1^3 = r^3 - a^3$, by the incompressibility condition. After the end of the first expansion phase, the boundary separating plastically and elastically deformed material will be *convected* and at time t ($> t_1$) its radius will be denoted by $X(a)$, the camouflet radius still being denoted by a. Then $X^3(a) - a^3 = b_1^3 - a_1^3$, by the incompressibility condition. In the subsequent motion the regions $a \leqslant r < X(a)$ and $r > X(a)$ must be separately considered. The previous result that Σ, defined in equation (7·3), is constant for any material point still applies, but its value is now necessarily determined by reference to conditions at time t_1. In this way it is found that

$$\sigma_0 - \sigma_r = \begin{cases} -\dfrac{2E}{3}\ln\left\{1+\dfrac{a_1^3-a^3}{r^3}\right\} + \dfrac{Y+\alpha P(a_1)}{1+\alpha}\left\{1+\dfrac{r^3-a^3}{a_1^3}\right\}^{-2\alpha/\{3(1+\alpha)\}} \\ \quad -\dfrac{\alpha}{1-\alpha}\rho_0 a_1 \ddot{a}_1\left[\left\{1+\dfrac{r^3-a^3}{a_1^3}\right\}^{-2\alpha/\{3(1+\alpha)\}} - \left\{1+\dfrac{r^3-a^3}{a_1^3}\right\}^{-\frac{1}{3}}\right] & (a \leqslant r < X(a)), \\ -\dfrac{2E}{3}\ln\left\{\dfrac{r_1^3-a_1^3+a_0^3}{r^3}\right\} = -\dfrac{2E}{3}\ln\left\{1-\dfrac{a^3-a_0^3}{r^3}\right\} & (r > X(a)), \end{cases} \tag{7·25}$$

equations ($7·25_2$) and (7·7) being identical since elastic deformations are recoverable. The equation of motion (7·1) holds in both regions, and integration, with use of equations (7·25)

and the stress boundary conditions at the camouflet surface and at infinity (equations (5·27)), shows that

$$\sigma_r = \left\{ \begin{aligned} &-P(a)+\frac{4E}{9}\left[\mathrm{Li}_2\left\{1-\frac{a_1^3}{a^3}\right\}-\mathrm{Li}_2\left\{\frac{a^3-a_1^3}{r^3}\right\}\right] \\ &\quad+\frac{2\alpha}{1-\alpha}\rho_0 a_1\ddot{a}_1\int_a^r\left\{1+\frac{x^3-a^3}{a_1^3}\right\}^{-\frac{1}{3}}\frac{\mathrm{d}x}{x} \\ &\quad+2\left\{\frac{Y+\alpha P(a_1)}{1+\alpha}-\frac{\alpha}{1-\alpha}\rho_0 a_1\ddot{a}_1\right\}\int_a^r\left\{1+\frac{x^3-a^3}{a_1^3}\right\}^{-2\alpha/\{3(1+\alpha)\}}\frac{\mathrm{d}x}{x} \\ &\quad+\rho_0\left[a\ddot{a}+\tfrac{3}{2}\dot{a}^2-\left\{\frac{a^2\ddot{a}+2a\dot{a}^2}{r}-\frac{a^4\dot{a}^2}{2r^4}\right\}\right] \qquad (a\leqslant r<X(a)), \\ &-\Pi-\frac{4E}{9}\mathrm{Li}_2\left\{\frac{a^3-a_0^3}{r^3}\right\}-\rho_0\left\{\frac{a^2\ddot{a}+2a\dot{a}^2}{r}-\frac{a^4\dot{a}^2}{2r^4}\right\} \qquad (r>X(a)). \end{aligned} \right\} \tag{7·26}$$

The continuity of σ_r and σ_θ is required at the boundary $r=X(a)$. Evaluation of equation (7·21) when $t=t_1$ shows at once, from equations (7·25), that $\sigma_r-\sigma_\theta$ is continuous. The continuity of σ_r shows, from equations (7·26), that $a(t)$ satisfies the equation

$$\left.\begin{aligned} P(a)-\Pi-\rho_0(a\ddot{a}+\tfrac{3}{2}\dot{a}^2) &= \frac{2\alpha}{1-\alpha}\rho_0 a_1\ddot{a}_1\int_a^{X(a)}\left\{1+\frac{x^3-a^3}{a_1^3}\right\}^{-\frac{1}{3}}\frac{\mathrm{d}x}{x} \\ &\quad+2\left\{\frac{Y+\alpha P(a_1)}{1+\alpha}-\frac{\alpha}{1-\alpha}\rho_0 a_1\ddot{a}_1\right\}\int_a^{X(a)}\left\{1+\frac{x^3-a^3}{a_1^3}\right\}^{-2\alpha/\{3(1+\alpha)\}}\frac{\mathrm{d}x}{x} \\ &\quad+\frac{4E}{9}\left[\mathrm{Li}_2\left\{1-\frac{a_1^3}{a^3}\right\}-\mathrm{Li}_2\left\{\frac{a^3-a_1^3}{X^3(a)}\right\}+\mathrm{Li}_2\left\{\frac{a^3-a_0^3}{X^3(a)}\right\}\right], \end{aligned}\right\} \tag{7·27}$$

which is to be integrated under the initial conditions

$$a=a_1, \quad \dot{a}=\dot{a}_1=0 \quad \text{when} \quad t=t_1. \tag{7·28}$$

The above analysis remains valid until such time as the yield condition is again satisfied. It is to be expected that $\sigma_\theta-\sigma_r<0$, and hence, from equation ($5·9_3$), the appropriate yield condition, obtained by taking $\varpi=-1$, is

$$(1+\alpha)\,\sigma_r-\sigma_\theta-Y=0, \tag{7·29}$$

where Y and α are defined in equation (7·15). Plastic yield occurs first at the camouflet surface, when $t=t_1+t_{2,e}$ and $a=a_{2,e}$. Then, from equations ($7·25_1$) and (7·29), setting $r=a$ and $\sigma_r=-P(a)$, it follows that $a_{2,e}$ is given by

$$2E(1+\alpha)\ln(a_1/a_{2,e})-\alpha P(a_1)-\alpha(1+\alpha)\,P(a_{2,e})-(2+\alpha)\,Y=0. \tag{7·30}$$

(*b*) *Plastic-elastic deformation.* When the camouflet radius decreases below $a_{2,e}$ a new plastic region spreads outwards from the camouflet surface into a region which has previously undergone plastic deformation. Separate analyses are now required for the elastic and plastic regions, and account must also be taken of the plastic deformation already undergone by part of the soil. At time $t\geqslant t_1+t_{2,e}$, the radius of the new plastic-elastic boundary will be denoted by $d(t)$, so that the regions $a(t)\leqslant r<d(t)$ and $r>d(t)$ are currently undergoing plastic and elastic deformation respectively, and the boundary $r=d(t)$ is at yield. Three regions are considered: (i) $a\leqslant r<d$, which is currently undergoing, and has previously undergone,

plastic deformation; (ii) $d < r < X(a)$, which is currently undergoing elastic, but has previously undergone plastic, deformation; and (iii) $r > X(a)$, which is continuing to undergo elastic deformation. This analysis will be valid until the second region is completely engulfed by the first, when $d = X$, but later argument suggests that this stage is not likely to be reached.

The stresses in the three regions are obtainable from the equations

$$\left.\begin{aligned}
&\sigma_r - \sigma_\theta = Y - \alpha\sigma_r,\\
&\sigma_r = \frac{Y}{\alpha} - \left\{P(a) + \frac{Y}{\alpha}\right\}\left\{\frac{a}{r}\right\}^{-2\alpha} + \rho_0\frac{a\ddot{a}+2\dot{a}^2}{1+2\alpha}\left[\left\{\frac{a}{r}\right\}^{-2\alpha} - \frac{a}{r}\right]\\
&\qquad\qquad - \rho_0\frac{\dot{a}^2}{2+\alpha}\left[\left\{\frac{a}{r}\right\}^{-2\alpha} - \left\{\frac{a}{r}\right\}^{4}\right] \quad (a(t) \leqslant r < d(t)),
\end{aligned}\right\} \tag{7·31}$$

$$\left.\begin{aligned}
&\sigma_r - \sigma_\theta = \frac{2E}{3}\ln\left\{1 + \frac{a_1^3 - a^3}{r^3}\right\} - \frac{Y + \alpha P(a_1)}{1+\alpha}\left\{1 + \frac{r^3 - a^3}{a_1^3}\right\}^{-2\alpha/\{3(1+\alpha)\}}\\
&\qquad + \frac{\alpha}{1-\alpha}\rho_0 a_1\ddot{a}_1\left[\left\{1 + \frac{r^3 - a^3}{a_1^3}\right\}^{-2\alpha/\{3(1+\alpha)\}} - \left\{1 + \frac{r^3 - a^3}{a_1^3}\right\}^{-\frac{1}{3}}\right],\\
&\sigma_r = G(t) + \frac{4E}{9}\left[\mathrm{Li}_2\left\{\frac{a^3 - a_1^3}{X^3(a)}\right\} - \mathrm{Li}_2\left\{\frac{a^3 - a_1^3}{r^3}\right\}\right]\\
&\qquad + \frac{2\alpha}{1-\alpha}\rho_0 a_1\ddot{a}_1\int_{X(a)}^{r}\left\{1 + \frac{x^3 - a^3}{a_1^3}\right\}^{-\frac{1}{3}}\frac{\mathrm{d}x}{x}\\
&\qquad + 2\left\{\frac{Y + \alpha P(a_1)}{1+\alpha} - \frac{\alpha}{1-\alpha}\rho_0 a_1\ddot{a}_1\right\}\int_{X(a)}^{r}\left\{1 + \frac{x^3 - a^3}{a_1^3}\right\}^{-2\alpha/\{3(1+\alpha)\}}\frac{\mathrm{d}x}{x}\\
&\qquad - \rho_0\left\{\frac{a^2\ddot{a} + 2a\dot{a}^2}{r} - \frac{a^4\dot{a}^2}{2r^4}\right\} \quad (d(t) < r < X(a)),
\end{aligned}\right\} \tag{7·32}$$

$$\left.\begin{aligned}
&\sigma_r - \sigma_\theta = \frac{2E}{3}\ln\left\{1 - \frac{a^3 - a_0^3}{r^3}\right\},\\
&\sigma_r = -\Pi - \frac{4E}{9}\mathrm{Li}_2\left\{\frac{a^3 - a_0^3}{r^3}\right\} - \rho_0\left\{\frac{a^2\ddot{a} + 2a\dot{a}^2}{r} - \frac{a^4\dot{a}^2}{2r^4}\right\} \quad (r > X(a)),
\end{aligned}\right\} \tag{7·33}$$

where $G(t)$ is a disposable function determined below. The stresses σ_r and σ_θ (or equivalently σ_r and $\sigma_r - \sigma_\theta$) must be continuous at the boundaries $r = d(t)$ and $r = X(a)$. It follows as before, from equations (7·21) and (7·25), that $\sigma_r - \sigma_\theta$ is continuous at $r = X(a)$. The other three conditions show that $a(t)$, $d(t)$ and $G(t)$ are to be determined as functions of t from the equations

$$G(t) = -\Pi - \frac{4E}{9}\mathrm{Li}_2\left\{\frac{a^3 - a_0^3}{X^3(a)}\right\}, \tag{7·34}$$

$$\left.\begin{aligned}
&\{Y + \alpha P(a)\}\left\{\frac{a}{d}\right\}^{-2\alpha} - \alpha\rho_0\frac{a\ddot{a}+2\dot{a}^2}{1+2\alpha}\left[\left\{\frac{a}{d}\right\}^{-2\alpha} - \frac{a}{d}\right] + \alpha\rho_0\frac{\dot{a}^2}{2+\alpha}\left[\left\{\frac{a}{d}\right\}^{-2\alpha} - \left\{\frac{a}{d}\right\}^{4}\right]\\
&\qquad = \frac{2E}{3}\ln\left\{1 + \frac{a_1^3 - a^3}{d^3}\right\} - \frac{\alpha}{1-\alpha}\rho_0 a_1\ddot{a}_1\left\{1 + \frac{d^3 - a^3}{a_1^3}\right\}^{-\frac{1}{3}}\\
&\qquad\qquad - \left\{\frac{Y + \alpha P(a_1)}{1+\alpha} - \frac{\alpha}{1-\alpha}\rho_0 a_1\ddot{a}_1\right\}\left\{1 + \frac{d^3 - a^3}{a_1^3}\right\}^{-2\alpha/\{3(1+\alpha)\}},
\end{aligned}\right\} \tag{7·35}$$

$$\left.\begin{aligned}\frac{Y}{\alpha}-\left\{P(a)+\frac{Y}{\alpha}\right\}\left\{\frac{a}{d}\right\}^{-2\alpha}+\rho_0\frac{a\ddot{a}+2\dot{a}^2}{1+2\alpha}\left[\left\{\frac{a}{d}\right\}^{-2\alpha}+\frac{2\alpha a}{d}\right]-\rho_0\frac{\dot{a}^2}{2+\alpha}\left[\left\{\frac{a}{d}\right\}^{-2\alpha}+\frac{\alpha a^4}{2d^4}\right]\\ =-\Pi+\frac{2\alpha}{1-\alpha}\rho_0 a_1\ddot{a}_1\int_{X(a)}^{d}\left\{1+\frac{x^3-a^3}{a_1^3}\right\}^{-\frac{1}{3}}\frac{\mathrm{d}x}{x}\\ +2\left\{\frac{Y+\alpha P(a_1)}{1+\alpha}-\frac{\alpha}{1-\alpha}\rho_0 a_1\ddot{a}_1\right\}\int_{X(a)}^{d}\left\{1+\frac{x^3-a^3}{a_1^3}\right\}^{-2\alpha/\{3(1+\alpha)\}}\frac{\mathrm{d}x}{x}\\ +\frac{4E}{9}\left[\mathrm{Li}_2\left\{\frac{a^3-a_1^3}{X^3(a)}\right\}-\mathrm{Li}_2\left\{\frac{a^3-a_0^3}{X^3(a)}\right\}-\mathrm{Li}_2\left\{\frac{a^3-a_1^3}{d^3}\right\}\right].\end{aligned}\right\}\quad(7\cdot36)$$

Equations (7·35) and (7·36) are to be integrated under the initial conditions

$$a=a_{2,e},\quad \dot{a}=\dot{a}_{2,e},\quad d=a_{2,e}\quad\text{when}\quad t=t_1+t_{2,e}.\qquad(7\cdot37)$$

The above analysis is valid only while $d(t)<X(t)$ and, as $\dot{d}(t)>0$ and $\dot{X}(t)<0$, this inequality may be violated. However, for frictionless soils it can be proved, with use of equations (7·21) and (7·35), that this cannot happen. For frictional soils, since the amplitude of the return motion is reduced by internal friction, the same is still likely to be true, in which case the above analysis is valid for all soils until the end of the first contraction phase. This is henceforth assumed, but it may be noted that the analysis of any situation in which the above conjecture is false requires attention only to two regions: $a\leqslant r<d$, which is undergoing plastic deformation, and $r>d$, which is continuing to undergo elastic deformation.

The first contraction phase terminates at time $t=t_1+t_2$ given by

$$\dot{a}(t_1+t_2)=0.\qquad(7\cdot38)$$

7·1·3. *Subsequent pulsations*

The formal analysis of the motion following the end of the first contraction phase is straightforward. However, so long as the motion continues to involve plastic deformation, each of its successive phases must be considered separately. Ultimately a state of elastic oscillation is attained.

7·1·4. *Numerical procedures*

The basic analysis of the camouflet motion during the first expansion and contraction phases is given in §§ 7·1·1 to 7·1·3. Some discussion is now given of the numerical solution of the camouflet equations (7·12); (7·21), (7·22); (7·27); and (7·35), (7·36). In comparison with the analysis for point source models, the present equations are more complicated, since b/a does not remain constant. In general, it is now necessary to integrate two simultaneous non-linear second-order ordinary differential equations for the functions $a(t)$ and $b(t)$ *or* $d(t)$. The numerical procedure adopted is again the Runge–Kutta method due to Gill (1951), which applies to any number of simultaneous ordinary differential equations. As in § 6·1·3, the appropriate camouflet equations are first reduced to non-dimensional form by introducing a non-dimensional time τ and distance x defined by

$$\tau=c_0 t/a_0,\quad x=a/a_0,\quad\text{where}\quad c_0^2=E/\rho_0,\qquad(7\cdot39)$$

and they are then rewritten as a set of simultaneous first-order differential equations after the introduction of suitable subsidiary variables. The particular systems of equations used were chosen for convenience in computation and are not given here. Numerical values

have been obtained by means of two computer programs, CAM 2A and CAM 2B, which apply to frictionless and frictional soils, respectively. Both programs also calculate the energy partition, which will now be discussed. Numerical values are given in § 7·1·7 for the three soils *S*, *P* and *Z*.

7·1·5. *Partition of energy*

The work done by the camouflet pressure is converted into elastic strain energy, kinetic energy and plastic work in the soil, and also into potential energy stored at infinity.

The following notation is now introduced:

U_1 total energy input (work done by explosion products)
U_2 potential energy stored at infinity
U_3 total elastic strain energy of soil
U_4 total plastic work performed on soil
U_5 total kinetic energy of soil.

Therefore
$$U_1 = U_2 + U_3 + U_4 + U_5, \tag{7·40}$$
where U_2, U_3 and U_5 correspond to the recoverable, and U_4 to the irrecoverable, energy components.

At any stage the total energy input is
$$U_1 = 4\pi \int_{a_0}^{a} P(a)\, a^2 \,\mathrm{d}a, \tag{7·41}$$
and, with use of equations (4·1) to (4·3), it follows that
$$U_1 = \begin{cases} \frac{2}{3}\pi a_0^3 P_0\{1-(a/a_0)^{-6}\} & (a/a_0 \leqslant 1{\cdot}530), \\ \frac{4}{3}\pi a_0^3 P_0\{0{\cdot}7497 - 0{\cdot}4073(a/a_0)^{-0{\cdot}81}\} & (a/a_0 \geqslant 1{\cdot}530). \end{cases} \tag{7·42}$$
Also, the potential energy stored at infinity is
$$U_2 = \lim_{R\to\infty} \int_0^t 4\pi R^2 \left\{ H + O\left(\frac{1}{R}\right)\right\} \frac{a^2\dot{a}}{R^2}\,\mathrm{d}t = \tfrac{4}{3}\pi(a^3 - a_0^3)\, H, \tag{7·43}$$
and the total kinetic energy of the soil is
$$U_5 = 2\pi\rho_0 \int_a^\infty v^2 r^2 \,\mathrm{d}r = 2\pi\rho_0 a^4 \dot{a}^2 \int_a^\infty \frac{\mathrm{d}r}{r^2} = 2\pi\rho_0 a^3 \dot{a}^2, \tag{7·44}$$
by the incompressibility assumption.

The remaining energy components, U_3 and U_4, must be evaluated separately for each successive stage of the camouflet motion. It would be advantageous to have numerical values for all the components individually, as the energy integral (7·40) would then provide a numerical check. However, for frictional soils U_4 cannot be expressed in closed form, and it is then simplest to compute values of U_3 and to use the identity
$$U_4 = U_1 - U_2 - U_3 - U_5 \tag{7·45}$$
to obtain U_4. It is not proposed to give a complete discussion of formulae for U_3 and U_4, but certain simple results will be stated.

The elastic strain energy of the soil per unit volume is

$$(\sigma_\theta-\sigma_r)^2/2E, \tag{7·46}$$

since the material is incompressible (see equation $(5{\cdot}34_1)$). Hence the total elastic strain energy of the soil is

$$U_3=\frac{2\pi}{E}\int_a^\infty(\sigma_\theta-\sigma_r)^2r^2\,\mathrm{d}r, \tag{7·47}$$

which may be evaluated with use of the formulae obtained for the stresses. In particular, during the elastic part of the first expansion phase, $\sigma_r-\sigma_\theta$ is given by equation (7·7), and it is found that

$$U_3=\frac{16\pi}{27}Ea_0^3\left[\left(\frac{a^3}{a_0^3}-1\right)\mathrm{Li}_2\left\{1-\frac{a_0^3}{a^3}\right\}-\tfrac{1}{2}\ln^2\left\{\frac{a^3}{a_0^3}\right\}\right]. \tag{7·48}$$

Frictionless soils. Further simple results are obtainable only for frictionless soils, to which attention will now be confined. The yield condition reduces to the form $|\sigma_\theta-\sigma_r|=Y$. The elastic strain energy per unit volume throughout any plastic region is therefore

$$Y^2/2E, \tag{7·49}$$

and the total elastic strain energy of the plastic region during the first expansion phase is then

$$\frac{2\pi Y^2}{3E}(b^3-a^3). \tag{7·50}$$

The total elastic strain energy of the elastic region is given by an expression similar to the right-hand side of equation (7·48). The total plastic work done per unit volume of the soil is

$$W^p=\int(\sigma_r\,\mathrm{d}\epsilon_r^p+2\sigma_\theta\,\mathrm{d}\epsilon_\theta^p), \tag{7·51}$$

where the integral is evaluated along the strain path of material points being plastically deformed. Now, from equation $(5{\cdot}34_2)$, $\dot{W}^p=\varpi\dot{\lambda}(\sigma_\theta-\sigma_r)/2c$, where $\dot{\lambda}$ is given in terms of $\dot{\sigma}_r$, $\dot{\sigma}_\theta$ and v by equation $(5{\cdot}33_2)$. In particular, since $\phi=0$ here, it may be shown that

$$\dot{W}^p=\frac{2Ya^2\dot{a}}{r^3}=2Y\frac{\mathrm{D}}{\mathrm{D}t}\left\{\ln\left(\frac{r}{a_0}\right)\right\} \tag{7·52}$$

during the first expansion phase. Accordingly, the total plastic work done per unit volume is

$$W^p=2Y\ln\left(\frac{r}{r_*}\right) \tag{7·53}$$

for material at co-ordinate r at time t which first became plastic at co-ordinate $r_*(r)$ at time $t_*(r)$. Now if $a(t_*)=a_*$ and $b(t_*)=b_*$, then $r_*=b_*$, and the incompressibility condition shows that

$$r^3-a^3=b_*^3-a_*^3. \tag{7·54}$$

From equation (7·22), taking $\alpha=0$, the quotient $(a^3-a_0^3)/b^3$ is seen to be constant during the first expansion phase. Hence, in particular,

$$(a_*^3-a_0^3)/b_*^3=1-a_0^3/a_{1,e}^3. \tag{7·55}$$

The elimination of a_* between equations (7·54) and (7·55) determines $b_*\equiv r_*$, and hence equation (7·53) becomes

$$W^p=\frac{2Y}{3}\ln\left\{\frac{a_0^3r^3}{a_{1,e}^3(r^3-a^3+a_0^3)}\right\}. \tag{7·56}$$

Finally, the total plastic work done on the plastic region is

$$U_4 = \frac{8\pi}{9} Y\left[(a^3-a_0^3)\ln\left\{\frac{a^3-a_0^3}{a_{1,e}^3-a_0^3}\right\}+a^3\ln\left\{\frac{a_{1,e}^3}{a^3}\right\}\right]. \tag{7·57}$$

7·1·6. *Effect of rate of strain*

In § 4·2·3, attention is drawn to the fact that the strength of a soil is dependent upon the rate of strain, and discussion given there shows that this effect is likely to be of significance in the mechanics of camouflet formation. Some estimate of its importance is therefore necessary. That this question can only be answered in largely qualitative terms seems clear for two reasons. First, reliable data concerning the effect of rate of strain on the strength of soils are limited and are confined to relatively low rates of strain at low stress. Secondly, any theoretical treatment attempting to take account of this effect would be difficult. Therefore the inclusion of a rate-of-strain effect in a simplified theory of camouflet motion must make use of *average* values of rates of strain. Although very high rates of strain do occur near the camouflet surface, it will now be shown that average values, taken throughout the plastic region during the first expansion phase and over the duration of this phase, are much lower.

In incompressible deformation, all material is being sheared at the rate

$$\dot\gamma = \tfrac{1}{2}(\dot\epsilon_\theta - \dot\epsilon_r) = 3a^2\dot a/2r^3 \tag{7·58}$$

(see equations (5·31)). Thus $\dot\gamma$ is large when $\dot a$ is large and r is small, as in the early stage of expansion and near the camouflet surface. Attention is now confined to the plastic region during the first expansion phase. At any time t $(t_{1,e} \leqslant t \leqslant t_1)$, the space average of $\dot\gamma(r,t)$ throughout this region is

$$\dot\gamma^*(t) = \frac{1}{\frac{4}{3}\pi(b^3-a^3)}\int_a^b 4\pi r^2\dot\gamma(r,t)\,\mathrm{d}r = \frac{9a^2\dot a}{2(b^3-a^3)}\ln\left(\frac{b}{a}\right), \tag{7·59}$$

and the time average of $\dot\gamma^*(t)$ over the interval $t_{1e} \leqslant t \leqslant t_1$ is

$$\Gamma = \frac{1}{t_{1,p}}\int_{t_{1,e}}^{t_1}\dot\gamma^*(t)\,\mathrm{d}t. \tag{7·60}$$

The numerical value of Γ is taken as a measure of the overall importance of rate of strain during the first expansion phase. The integral (7·60) must, in general, be evaluated numerically, although, when $\alpha = 0$, Γ is given explicitly by

$$\begin{aligned}\Gamma &= \frac{9Y}{4Et_{1,p}}\int_{a_{1,e}}^{a_1}\ln\left[\frac{2E}{3Y}\left\{1-\frac{a_0^3}{a^3}\right\}\right]\frac{a^2\mathrm{d}a}{a^3-a_0^3}\\ &= \frac{3Y}{4Et_{1,p}}\left[\ln\left\{\frac{2E}{3Y}\right\}\ln\left\{\frac{a_1^3-a_0^3}{a_{1,e}^3-a_0^3}\right\}+\mathrm{Li}_2\left\{\frac{a_0^3}{a_0^3-a_{1,e}^3}\right\}-\mathrm{Li}_2\left\{\frac{a_0^3}{a_0^3-a_1^3}\right\}\right],\end{aligned} \tag{7·61}$$

where it has been assumed that $Y/E \ll 1$, and use has been made of equation (7·22). Alternatively, the Penney–Taylor similarity theory, coupled with assumption B of § 6·1·3, gives as an approximation to the formula (7·60) the result, valid for all types of soil,

$$\Gamma = \frac{9\ln(n)\ln(a_1/a_0)}{2(n^3-1)\,t_1}, \tag{7·62}$$

where the constant n is given by equation (6·7). For a frictionless soil, the approximation (6·46) may further be substituted into equation (7·62) to give a more explicit formula for Γ.

It may be noted from the formulae (7·61) and (7·62) that $\Gamma t_{1,p}$ (or Γt_1) is independent of the charge size. Since, according to the present theory, $t_{1,p}$ (or t_1) varies linearly with a_0, it follows that Γ increases without limit as the charge size decreases. With use of equations (7·58) and (7·62), approximate values of Γ and $\dot{\gamma}_{\max.}$, calculated from numerical values given in § 6·1·4 for a 1 lb. charge buried at a depth of 100 ft. in soils S, P and Z, are given in table 6. For other sizes of charge these values scale inversely with a_0. It is apparent that although very high rates of strain do occur during camouflet motion, their overall mean value is much lower but still appreciable. For the mean rates of strain Γ given in table 6, the dynamic strengths of clays and sands are increased from their static values by factors of about 2 and 1·2, respectively (see § 4·2·3 and figure 4). Therefore, for charge masses of 1 lb. and over, suitable average values of c and ϕ can be chosen, although it is clear that, in general, an iterative procedure would have to be used to take account of rate-of-strain effects on the present basis.

In obtaining the numerical results discussed in the next section, the foregoing procedure has not, however, been followed. Instead, for simplicity, it has been assumed that the values of c and ϕ shown in table 3 refer directly to any particular dynamic situation under consideration. Given a particular set of results, together with a value of a_0, it is then possible to determine the static properties of the soil to which they refer. Although this inverse method has the disadvantage that results for different values of a_0 thus correspond to soils with different static properties, the general trends of variation of soil strength with rate of strain discussed in § 4·2·3 are not thought to be sufficiently well defined for the more elaborate procedure to be justified here.

TABLE 6. NUMERICAL VALUES OF AVERAGE AND MAXIMUM RATES OF STRAIN DURING THE FIRST EXPANSION PHASE OF EXPLOSIONS FROM 1 LB. CHARGES BURIED AT DEPTH OF 100 FT.

soil	Γ (s^{-1})	$\dot{\gamma}_{\max.}$ (s^{-1})
S	7·3	$1·5 \times 10^4$
P	4·0	$1·2 \times 10^4$
Z	22·7	$1·1 \times 10^4$

7·1·7. *Numerical values*

Calculations, based upon the numerical procedures outlined in § 7·1·4, have been made for the three soils S, P and Z (see § 4.2.3) and for the four depths of charge burial of 50, 100, 250 and 500 ft. The computer programs determine the radii of the camouflet surface and the plastic-elastic boundary during the first expansion and contraction phases, and the components of energy partition during the first expansion phase only. It is only possible to give here, in tabular and graphical form, a selection of the numerical values obtained. A concise summary of the types of results is provided for reference in table 7. These results are given mainly in non-dimensional form so that they apply to any charge size (but see tables 5 and 11). Table 9 gives some results in dimensional form for a 1 lb. charge.

It is apparent that certain features of the disturbance, such as, for example, the variation with time of the radii of the camouflet surface and the plastic-elastic boundary, show much dependence in detail upon the type of soil and the depth of charge burial. However, a

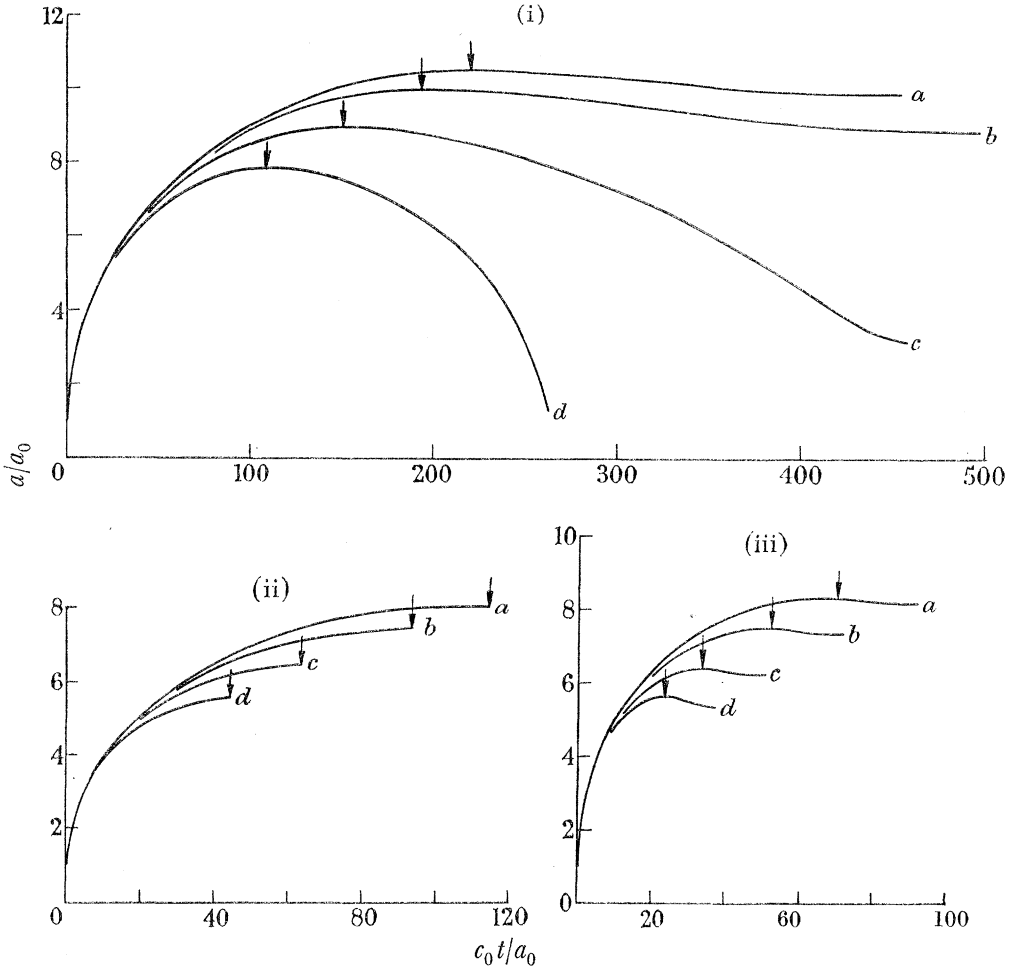

FIGURE 6. Variation of camouflet radius with time during first expansion and contraction phases, according to the spherical charge model. Explosions at depths (*a*) 50 ft., (*b*) 100 ft., (*c*) 250 ft. and (*d*) 500 ft. in soils (i) *S*, (ii) *P* and (iii) *Z*. Arrows indicate maximum expansion (contraction is negligible for soil *P*).

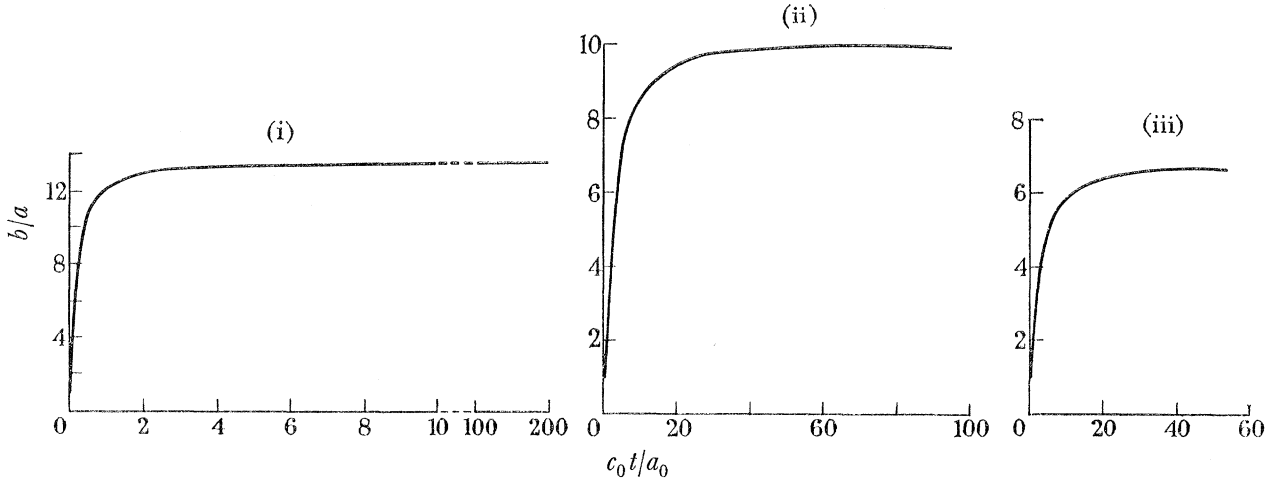

FIGURE 7. Variation of ratio of radius of plastic-elastic boundary to radius of camouflet surface with time during first expansion phase, according to spherical charge model. Explosions at depth 100 ft. in soils (i) *S*, (ii) *P* and (iii) *Z*.

number of general conclusions concerning camouflet motion can be drawn from the results given in the tables and figures of this paper.

Discussing camouflet formation, Devonshire & Mott (1944) conjectured that 'the initial high pressure of the expanding gases sets the surrounding soil into such rapid motion outwards that its kinetic energy carries it on long after the pressure of the gases has fallen to a

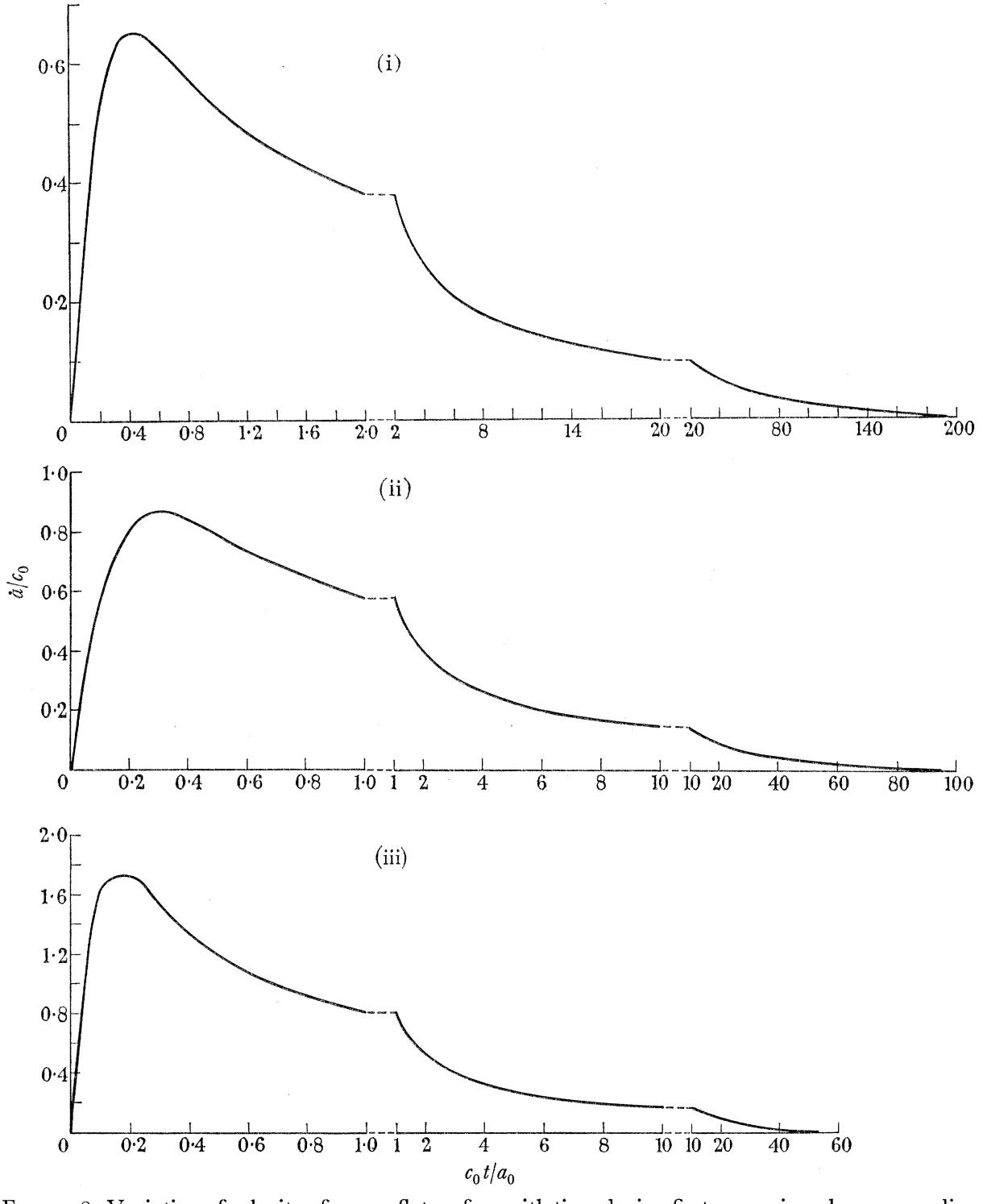

FIGURE 8. Variation of velocity of camouflet surface with time during first expansion phase, according to spherical charge model. Explosions at depth 100 ft. in soils (i) *S*, (ii) *P* and (iii) *Z*.

negligible value'. This conjecture is amply verified by the results obtained in the present study. Thus, for example, in the typical case of an explosion at a depth of 100 ft. in soil S, figures 9 and 10 show that, after a time equal to one-twentieth of the duration of the first expansion phase, the pressure of the gases has dropped by a factor of one thousand from its initial value and the combined total energy of the gases and the soil is largely in the form of kinetic energy of the soil. Subsequently, the other energy components of the soil increase mainly at the expense of this kinetic energy, only very little being provided by the gases.

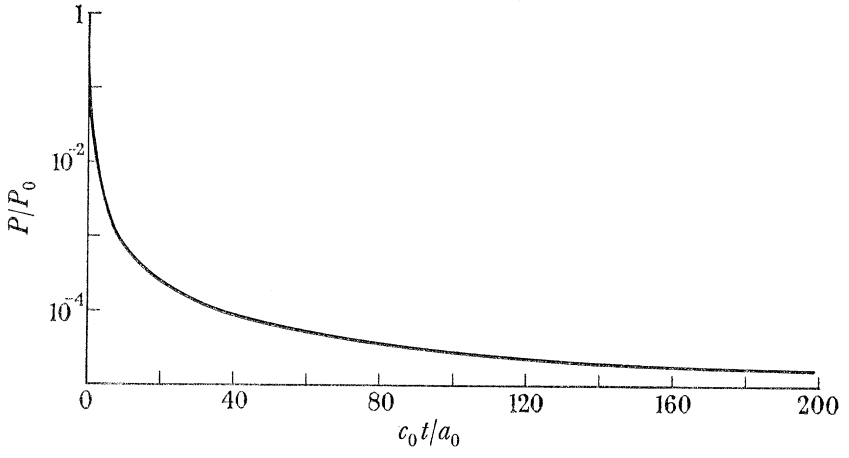

FIGURE 9. Variation of pressure exerted by explosion products of TNT on camouflet surface with time during first expansion phase, according to spherical charge model. Explosion at depth 100 ft. in soil S.

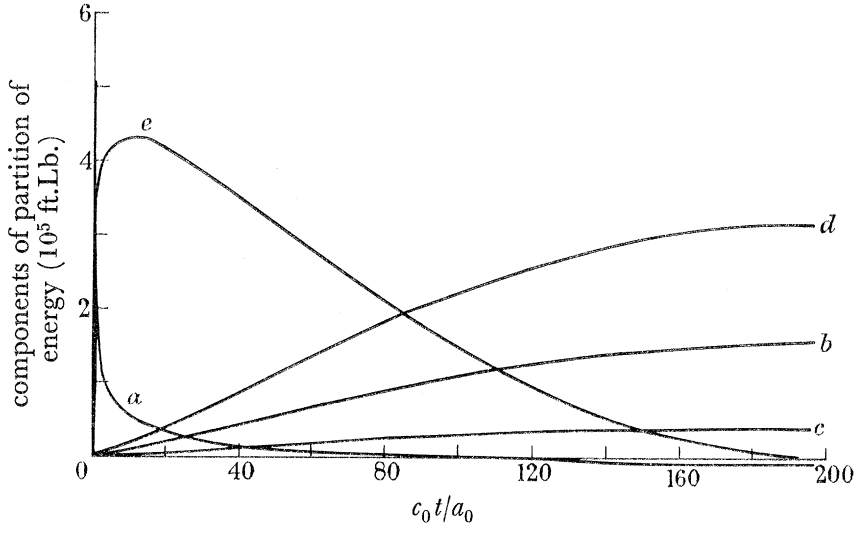

FIGURE 10. Variation of components of partition of energy with time during first expansion phase, according to spherical charge model. Explosion of a one-pound charge of TNT at depth 100 ft. in soil S.

(a) Energy of explosion products ($5{\cdot}09 \times 10^5$ ft. Lb. per pound of TNT available for camouflet formation).
(b) Potential energy stored at infinity.
(c) Total elastic strain energy in soil.
(d) Total plastic work done on soil.
(e) Total kinetic energy of soil.

The variation of the velocity of the camouflet surface with time during the first expansion phase, depicted in figure 8, shows the extremely rapid way in which the motion is generated.

Consider now the extent of the agreement between the point source and spherical charge models during the first expansion phase. These models differ most noticeably in their predictions of the quotient b/a. For the point source model this quotient is constant. For the spherical charge model, as the deformation proceeds, it increases from unity, when plastic deformation first occurs, to a value approximately equal to that predicted by the point source model. However, the detailed numerical results show that this increase takes place mainly during the early stage of the motion. Thus, for example, for a depth of charge burial of 100 ft., figure 7 shows that b/a is close to its final value for the last 99, 80 and 65 % of the duration of the first expansion phase for soils *S*, *P* and *Z* respectively.

TABLE 7. SUMMARY OF RESULTS GIVEN IN TABLES 4, 8, 9 AND 10 AND IN FIGURES 5 TO 10

A, B refer to point source models coupled with assumptions *A* and *B*. C refers to spherical charge model.

location	soil	h (ft.)	model	variables	time range
table 4	*S*, *P*, *Z*	100	A, B	τ_1, a_1/a_0, b/a	—
8	*S*, *P*, *Z*(*MS*)	50, 100, 250, 500	C	τ_1, τ_2, a_1/a_0, $a_{1,e}/a_0$, a_2/a_0, b_1/a_1, d_2/a_2	—
9	*S*, *P*, *Z*	100	C	t_1, t_2, a_1, a_2, b_1, d_2	—
10	*S*, *P*, *Z*	50, 100, 250, 500	C	U_2, U_3, U_4	—
figure 5	*S*, *P*, *Z*	100	A, B, C	τ, a/a_0	$0 \leqslant \tau \leqslant \tau_1$
6	*S*, *P*, *Z*	50, 100, 250, 500	C	τ, a/a_0	$0 \leqslant \tau \leqslant \tau_2$
7	*S*, *P*, *Z*	100	C	τ, b/a	$0 \leqslant \tau \leqslant \tau_1$
8	*S*, *P*, *Z*	100	C	τ, $\dot{a}/c_0$	$0 \leqslant \tau \leqslant \tau_1$
9	*S*	100	C	τ, P/P_0	$0 \leqslant \tau \leqslant \tau_1$
10	*S*	100	C	τ, U_1, U_2, U_3, U_4, U_5	$0 \leqslant \tau \leqslant \tau_1$

Again, for the same depth of charge burial of 100 ft., figure 5 and tables 4 and 8 show the extent of the agreement between the predictions of the two models for certain other features of the motion. It is apparent that the measure of agreement depends considerably on the type of soil: for soil *S* it is good, for *P* only moderate and for *Z* it is poor. Thus the agreement between the two models worsens as the internal friction of the soil increases. The trend of these results is likely to be a consequence in part of the fact that the point source model can be expected to be a good approximation to the spherical charge model only in circumstances where a_0^3 is much smaller than a^3 during the greater part of the motion. This criterion is clearly better satisfied for soil *S* than for soils *P* and *Z*, but it cannot be the only relevant factor, since it does not adequately distinguish between the latter two soils.

The first contraction phase has received attention only for the spherical charge model. The results given in figure 6 and table 8 show that, for soils *P* and *Z*, and over the range of depths of charge burial considered, camouflet motion is practically dead-beat (see § 2·3). In contrast, for the *frictionless* soil *S* this is not so. When $h = 100$ ft. the amplitude of the contraction motion is appreciable, and when $h = 500$ ft. the return motion is practically complete, the first expansion and contraction phases then closely resembling those of the bubble associated with an underwater explosion. This behaviour might be anticipated from the results given in table 10, which shows the energy partition at the end of the first expansion phase. It is noticeable that for soil *S* the proportion of the total energy stored as recoverable energy at this time is large, being about 40 % when $h = 100$ ft. and 70 % when

$h = 500$ ft. Therefore a relatively large fraction of the total energy is available to enforce the compression of the explosion products.

Thus it appears that the internal friction of a soil is of decisive importance in determining the extent of the first contraction phase, and that this is due to the fact that for a frictionless soil a much smaller proportion of the total energy is dissipated during the first expansion phase. Now it can be seen from equations $(5{\cdot}34_2)$ and $(7{\cdot}18)$ that the rate of plastic work per unit volume depends critically upon the value of the quantity $q = \alpha\sigma_r - Y$. When α is

TABLE 8. NUMERICAL VALUES FOR SPHERICAL CHARGE MODEL

τ_1, τ_2, scaled times.
$a_{1,e}/a_0$, a_1/a_0, a_2/a_0, scaled radii of camouflet surface.
b_1/a_1, d_2/a_2, ratios of radii of plastic-elastic boundary and camouflet surface.
Subscripts 1 and 2 refer respectively to the ends of the first expansion and contraction phases.

		depth of charge burial (ft.)			
soil	variable	50	100	250	500
S	τ_1	221·4	197·3	150·2	109·2
	$a_{1,e}/a_0$	1·00013	1·00013	1·00013	1·00013
	a_1/a_0	10·47	9·989	8·933	7·838
	b_1/a_1	13·57	13·57	13·57	13·56
	τ_2	454·3	497·9	458·0	262·3
	a_2/a_0	9·849	8·806	3·165	1·305
	d_2/a_2	6·315	8·313	29·94	64·61
P	τ_1	114·7	94·19	64·19	44·41
	$a_{1,e}/a_0$	1·197	1·197	1·197	1·197
	a_1/a_0	8·005	7·435	6·436	5·600
	b_1/a_1	10·82	9·959	8·442	7·176
	τ_2	125·7	105·0	74·24	53·60
	a_2/a_0	7·993	7·420	6·414	5·569
	d_2/a_2	1·274	1·315	1·385	1·435
Z	τ_1	70·59	52·65	33·58	23·18
	$a_{1,e}/a_0$	1·419	1·419	1·419	1·419
	a_1/a_0	8·297	7·500	6·418	5·637
	b_1/a_1	7·876	6·665	5·192	4·254
	τ_2	92·16	72·02	49·85	37·09
	a_2/a_0	8·199	7·370	6·217	5·355
	d_2/a_2	1·374	1·374	1·372	1·368
MS	τ_1	—	—	137·1	—
	$a_{1,e}/a_0$	—	—	1·040	—
	a_1/a_0	—	—	8·428	—
	b_1/a_1	—	—	12·85	—
	τ_2	—	—	141·2	—
	a_2/a_0	—	—	8·426	—
	d_2/a_2	—	—	1·050	—

TABLE 9. NUMERICAL VALUES FOR SPHERICAL CHARGE MODEL: EXPLOSION OF A 1 LB. SPHERICAL CHARGE (RADIUS 0·137 FT.) AT A DEPTH OF BURIAL OF 100 FT.

t_1, t_2, times (ms).
a_1, a_2, radii of camouflet surface (ft.).
b_1, d_2, radii of plastic-elastic boundary (ft.).
Subscripts 1 and 2 refer respectively to the ends of the first expansion and contraction phases.
c_0, reference velocity (ft./s), see equations (7·39).
Π, initial hydrostatic pressure (Lb./in.^{2}), see equation (5·28).

soil	t_1	a_1	b_1	t_2	a_2	d_2	c_0	Π
S	11·43	1·364	18·51	28·84	1·203	9·999	2358	101·5
P	7·472	1·016	10·11	8·327	1·014	1·333	1722	101·5
Z	7·472	1·025	6·829	10·22	1·007	1·383	962·6	84·14

TABLE 10. ENERGY COMPONENTS FOR SPHERICAL CHARGE MODEL

U_2, potential energy stored at infinity.
U_3, total elastic strain energy in soil.
U_4, total plastic work done on soil.
These components are evaluated at the end of the first expansion phase and expressed as a percentage of the total energy input.

		depth of charge burial (ft.)			
soil	component	50	100	250	500
S	U_2	19·8	30·2	49·6	65·6
	U_3	9·1	7·9	5·7	3·9
	U_4	71·1	61·9	44·6	30·5
P	U_2	9·0	12·7	19·1	24·8
	U_3	4·9	5·0	5·3	5·7
	U_4	86·0	82·2	75·6	69·6
Z	U_2	8·5	10·8	15·4	20·3
	U_3	4·0	4·7	6·0	7·2
	U_4	87·5	84·4	78·6	72·5

exactly zero, q is of the order of Y, but for quite small α, say 0·1, remembering that $|\sigma_r|$ may be of the order of P_0 (which itself is of the order of $10^4 Y$), q is of the order of $10^3 Y$. This suggests that the character of the motion for a slightly frictional soil (i.e. one with a small, but non-zero, value of α) differs radically from that for a frictionless soil ($\alpha = 0$). In order to verify this conjecture, calculations were made for another type of soil, *MS*. This soil has the same properties as soil *S* except that its angle of internal friction is now taken to be 1° (see table 3). Numerical values are given in table 8 for a depth of charge burial of 250 ft., and the comparison of corresponding results for the soils *S* and *MS* confirms the above arguments; it should be noted, however, that the effect on the expansion phase is comparatively small. It seems probable that the *critical value* of α, below which a soil of slight friction is effectively frictionless, is perhaps of the order of 10^{-4}. Now it is not likely that α could ever be so small, since all soils are necessarily frictional to some extent, and, in any event, no meaningful data are obtainable to the implied degree of accuracy. Thus a further conclusion of the present study is that, although camouflet formation is not dead-beat for a frictionless soil, the unlikelihood of the natural occurrence of such a perfect material means that this eventuality is to be wholly discounted for practical purposes. In other words, camouflet formation is sensibly dead-beat under any practical conditions of interest, as predicted by Penney (1954, private communication).

Finally, it should be noted that, as already observed, most of the numerical values derived from the spherical charge model are presented here in dimensionless form, and restrictions of the type discussed in § 6·1·4 must again be borne in mind when they are used to obtain results for specific charge sizes. Now that results are available over a range of depths of charge burial, it is possible to extend the results given in table 5 by expressing the criterion of applicability of the theory in the form

$$h \geqslant mW^n, \tag{7·63}$$

where, from the present results and for $h \leqslant 500$ ft., the parameters m and n have the values given in table 11, W being pounds of TNT and h being depth of charge burial in feet.

TABLE 11. VALUES OF PARAMETERS IN RESTRICTION (7·63) ON CHARGE MASS FOR DEPTHS OF CHARGE BURIAL NOT EXCEEDING 500 FT.

soil	m	n
S	22	0·29
P	18	0·25
Z	15	0·35

7·1·8. *Comparison with experimental data*

Very few experimental data on camouflet formation are available, and the majority of them concern the depth of charge burial necessary to ensure that no major disruption occurs at ground level. It is apparent that this criterion is considerably less restrictive than that given in § 7·1·7, which demands a depth of charge burial supposedly sufficient to ensure spherically symmetric conditions. Experimental work on camouflet formation was undertaken during World War II in order to assist the detection of unexploded bombs. The results obtained show that a depth of charge burial of about 3·5 to 7 $W^{\frac{1}{3}}$ ft. (depending upon the soil type) is necessary if the surface of the ground is not to be ruptured.

So far as camouflet dimensions are concerned, all the available British work has been summarized by Christopherson (1946), who states that only for a few explosions, all in clay, have camouflets been excavated and measured. It is usually found that the cavity is nearly spherical, of volume 9 to 11W ft.^{3} (or diameter 2·5 to 2·7$W^{\frac{1}{3}}$ ft.). This result leaves unspecified the types of clay, and also the depth of charge burial, which presumably is relatively small. For comparison, the results for soil S at a depth of charge burial of 50 ft. lead to a camouflet diameter of 2·9$W^{\frac{1}{3}}$ ft. or, extrapolating to zero depth of charge burial (or rather to a value of Π of 14·7 Lb./in.^{2}), of about 3·0$W^{\frac{1}{3}}$ ft. Thus there appears to be reasonable agreement in this case between predictions of the present camouflet model and experimental data for the dimensions of camouflets.

7·2. *Constitutive equations for large elastic deformations*

The numerical values given in table 8 for a spherical charge model of camouflet formation show that large elastic deformations can occur during the elastic part of the first expansion phase if the soil is frictional. This effect is a consequence of the form of equation (7·16). In § 7·1 the analysis incorporates finite elastic deformation through the use of the convective form of Hooke's stress-strain relations under the condition of incompressibility. Experimental data on the mechanical behaviour of soils at high stress intensities are not available. For infinitesimal elastic deformation the experimental data tend to support the use of Hooke's law, but for finite elastic deformation the choice of suitable stress-strain relations from the wide range of possibilities must largely be governed by considerations of mathematical expediency. For purposes of comparison, a brief discussion will now be given of the analysis (analogous to that of § 7·1·1) which incorporates finite neo-Hookean (in place of convective-Hookean) incompressible elastic deformation. The so-called neo-Hookean solid is a special case of a Mooney solid (see Green & Zerna 1954, pp. 76 and 104–108).

Under spherically symmetric conditions, the relation between stress and displacement for a neo-Hookean incompressible elastic solid gives

$$\sigma_r - \sigma_\theta = \frac{E}{3}\left\{\left(\frac{r_0}{r}\right)^4 - \left(\frac{r}{r_0}\right)^2\right\} \tag{7·64}$$

for a material point with current co-ordinate r and initial co-ordinate $r_0(r)$, where E is a physical constant which, for small strains, is shown later to be Young's modulus. The incompressibility condition requires that

$$r^3-r_0^3=a^3-a_0^3, \tag{7·65}$$

and then equation (7·64) becomes

$$\sigma_\theta-\sigma_r=\frac{E}{3}\frac{(a^3-a_0^3)\,(2r^3-a^3+a_0^3)}{r^4(r^3-a^3+a_0^3)^{\frac{2}{3}}}. \tag{7·66}$$

Since $a\geqslant a_0$, equation (7·66) shows that $\sigma_\theta\geqslant\sigma_r$. If the right-hand side of equation (7·66) is expanded to the first order in $(a^3-a_0^3)/r^3$ and the result compared with the expression for $\sigma_\theta-\sigma_r$ given by the generalized Hooke's law with $\nu=\frac{1}{2}$, then E is seen to be Young's modulus.

The equation of motion is

$$\frac{\partial\sigma_r}{\partial r}+\frac{2(\sigma_r-\sigma_\theta)}{r}=\rho_0\left\{\frac{a^2\ddot{a}+2a\dot{a}^2}{r^2}-\frac{2a^4\dot{a}^2}{r^5}\right\}. \tag{7·67}$$

Therefore, from equations (7·66) and (7·67), σ_r satisfies the equation

$$\frac{\partial\sigma_r}{\partial r}=\rho_0\left\{\frac{a^2\ddot{a}+2a\dot{a}^2}{r^2}-\frac{2a^4\dot{a}^2}{r^5}\right\}+\frac{2E}{3}\frac{(a^3-a_0^3)\,(2r^3-a^3+a_0^3)}{r^5(r^3-a^3+a_0^3)^{\frac{2}{3}}}. \tag{7·68}$$

Integration of this equation subject to the stress boundary condition at infinity (equations (5·27)) shows that

$$\left.\begin{aligned}\sigma_r&=-\Pi-\rho_0\left\{\frac{a^2\ddot{a}+2a\dot{a}^2}{r}-\frac{a^4\dot{a}^2}{2r^4}\right\}+\frac{E}{6}\left\{\frac{(r^3-a^3+a_0^3)^{\frac{1}{3}}\,(5r^3-a^3+a_0^3)}{r^4}-5\right\},\\ \sigma_\theta&=-\Pi-\rho_0\left\{\frac{a^2\ddot{a}+2a\dot{a}^2}{r}-\frac{a^4\dot{a}^2}{2r^4}\right\}+\frac{E}{6}\left\{\frac{5r^6-2(a^3-a_0^3)\,r^3-(a^3-a_0^3)^2}{r^4(r^3-a^3+a_0^3)^{\frac{2}{3}}}-5\right\}.\end{aligned}\right\} \tag{7·69}$$

The stress boundary condition at the camouflet surface (equations (5·27)) shows that a satisfies the equation

$$\rho_0(a\ddot{a}+\tfrac{3}{2}\dot{a}^2)+\frac{E}{6}\left[5-\frac{4a_0}{a}-\left\{\frac{a}{a_0}\right\}^4\right]-P(a)+\Pi=0. \tag{7·70}$$

From equations (7·14) and (7·64), yield first occurs at the camouflet surface when $a=a_{1,e}$, where

$$(1+\alpha)\frac{E}{3}\left[\left\{\frac{a_{1,e}}{a_0}\right\}^2-\left\{\frac{a_0}{a_{1,e}}\right\}^4\right]=Y+\alpha P(a_{1,e}) \tag{7·71}$$

(cf. equation (7·16)). This equation also predicts that, for frictional soils, large elastic strains occur near the camouflet surface prior to yield (see table 12).

The analysis of the motion after the termination of the elastic part of the first expansion phase is similar to that given in § 7·1·1 (*b*) *et seq.* and is not presented here.

7·2·1. *Numerical values*

In table 12, numerical values are given of τ_1, $a_{1,e}/a_0$, a_1/a_0 and b_1/a_1 for the three soils *S*, *P* and *Z* and for the depth of charge burial of 100 ft. It is seen that there is good agreement between the results for the models incorporating convective-Hookean or neo-Hookean elastic deformation, and hence it appears that numerical values are not critically dependent upon the particular choice made of elastic stress-strain relations.

PHILOSOPHICAL TRANSACTIONS OF THE ROYAL SOCIETY A MATHEMATICAL, PHYSICAL & ENGINEERING SCIENCES

TABLE 12. NUMERICAL VALUES FOR SPHERICAL CHARGE MODELS INCORPORATING CONVECTIVE-HOOKEAN OR NEO-HOOKEAN ELASTIC DEFORMATION. DEPTH OF CHARGE BURIAL, 100 FT.

τ_1, scaled time.
$a_{1,e}/a_0$, scaled radius of camouflet surface at onset of plastic yield.
a_1/a_0, scaled radius of camouflet surface at end of first expansion phase.
b_1/a_1, ratio of radius of plastic-elastic boundary to radius of camouflet surface at end of first expansion phase.
C, N refer to assumptions of convective-Hookean or neo-Hookean elastic deformation.

soil	assumption	τ_1	$a_{1,e}/a_0$	a_1/a_0	b_1/a_1
S	C	197·3	1·00013	9·989	13·57
	N	197·3	1·00013	9·989	13·57
P	C	94·19	1·197	7·435	9·959
	N	94·30	1·208	7·443	9·957
Z	C	52·65	1·419	7·500	6·665
	N	52·82	1·440	7·524	6·663

7·3. *Other theories*

The most serious limitation of the spherical charge model of camouflet formation described in § 7·1 is the assumption of elastic incompressibility, and the consequent errors incurred are unlikely to be negligible. If the effects of compressibility in the elastic region were to be included, then the analysis would become more complicated, due primarily to the fact that the elastic wave motion would have to be determined throughout an infinite region bounded internally by a *moving* plastic-elastic boundary. If incompressibility is still assumed in the plastic region, there are difficulties in appropriately matching the elastic and plastic fields at the plastic-elastic boundary, and no satisfactory model of this type has yet been developed. However, if the spherical charge model considered in § 7·1 is discarded, then the logical procedure is to take full account of elastic compressibility effects and to adopt a purely numerical approach *ab initio*. This procedure has not yet been attempted, even for the simpler case of a frictionless soil.

Mention should be made here of a spherical charge model suggested by Hicks (1954, private communication), which is based upon his non-similarity theory (see § 6·2). The camouflet equations of Hicks's theory, together with the initial conditions $a = a_0$ ($\neq 0$), $\dot{a} = 0$ and $b = a_0$ at $t = 0$, do not, except when $\alpha = 0$, lead to a situation of geometrical similarity, in contrast to the system of camouflet equations (6·12) and (6·38) for the point source model of § 6·1 incorporating assumption B. In contrast to the theory developed in § 7·1, Hicks's model takes no account of the elastic deformation which occurs at the beginning of the first expansion phase.

Work has also been done in the Soviet Union on explosions in solid media, particularly porous soils. In this work, which appears to originate with a paper by Kompaneets (1956), the types of ideal soil considered are different from those of the present paper. Extensive developments have been made by Kukudzhanov (1958), Lovetskiĭ (1958, 1959), Romashov, Rodionov & Sukhotin (1958), Andriankin & Koryavov (1959) and Zvolinskiĭ (1960) (see also Kochina & Mel'nikova 1958 who, following work of Sedov 1959, pp. 235 *et seq.*, discuss similarity solutions). Some account of this work is given by Cristescu (1958, pp. 227 *et seq.*; 1960). No attempt is made here to summarize these papers in detail, but as the work of Zvolinskiĭ (1960) is of particular interest, a brief account of it will now be given.

Zvolinskiĭ's (1960) analysis applies to the detonation underground of an explosive charge, spherically symmetric conditions being assumed. The infinite homogeneous region of soil in which the charge is buried is treated as an elastic, perfectly plastic solid. In the elastic range Hooke's law is satisfied. The transition from the elastic to the plastic range is accompanied instantaneously by an increase in density of an assigned amount. In the plastic range the density is constant and a plasticity condition, equivalent to Coulomb's law of failure, is satisfied. This condition follows from a hypothesis concerning the plastic rate of work, and in subsequent analysis only a special case (which corresponds to equation (6·1) with $\alpha = 1$) is treated. Following the initiation of the explosion at the charge centre, the motion of the soil is described in four stages (no detailed account being taken of the motion of the explosion products). During the first stage a shock wave travels outwards from the camouflet surface, compacting the soil through which it passes. As the radius of the shock front increases the shock velocity decreases. The second stage begins when this velocity becomes equal to the compressional elastic wave velocity in the soil, and a compressional elastic wave then detaches itself from the shock front and runs ahead. The shock velocity continues to decrease, and eventually the discontinuity in particle velocity across the front is reduced to zero and the shock wave ceases to exist. This marks the beginning of the third stage, and the boundary between the plastically and elastically deforming regions is now treated as a moving contact discontinuity at which elastic waves continue to be generated. Further plastic deformation occurs, but the plastic-elastic boundary and the camouflet surface are now rapidly brought to rest. Finally, during the fourth stage the motion consists entirely of elastic waves. Since the compacted soil is assumed to be incompressible, the time variable can be effectively eliminated from the analysis and the governing equations reduced to non-linear ordinary differential equations of the first order. Having derived these equations and stated the conditions which their solutions must satisfy, Zvolinskiĭ deduces the salient features of camouflet formation without recourse to detailed computation.

8. Concluding remarks

Studies in the theoretical mechanics of explosion phenomena in soils are necessarily based upon models in which considerable simplifications of the physical situation are assumed, owing to the complex physical characteristics of soils as well as in the interests of mathematical tractability. The model of a deep underground explosion which has been adopted in this paper is believed, however, to provide a realistic account of the large-scale features of camouflet motion. Its main deficiencies are attributable to the neglect of soil compressibility, which eliminates the effects associated with the propagation of elastic and plastic waves, and to the extrapolation of conventional soil behaviour to explosion conditions.

The main predictions of the model studied are as follows. In all cases of practical interest, the initial expansion of the camouflet is large and occurs rapidly, with an extensive region of the surrounding soil undergoing plastic deformation. The amplitudes of any subsequent pulsations are small. The features of the disturbance show much dependence upon the type of soil and upon the depth at which the explosion takes place.

Although models incorporating a soil plasticity theory are certainly not universally appropriate to studies of situations involving large deformations in soils due to explosions,

PHILOSOPHICAL TRANSACTIONS OF THE ROYAL SOCIETY A MATHEMATICAL, PHYSICAL & ENGINEERING SCIENCES

the present study is believed to be realistic and to represent an advance in knowledge of the mechanics of deep underground explosions.

The work described in this paper was commenced in 1956 at Aldermaston (by P. C.) and at Fort Halstead (by A. D. C. and H. G. H.), and the two investigations proceeded independently until detailed computation was first undertaken in 1958. The present paper brings together in a unified presentation the main results of the work done by the three authors.

The authors wish to thank Sir Geoffrey Taylor, F.R.S. and Sir William Penney, F.R.S. for providing the original stimulus for this investigation and for kindly agreeing to the incorporation in this paper of their similarity solution for camouflet formation in soils, previously unpublished. The early stages of the work at Aldermaston benefited much from the interest taken in it by Mr E. P. Hicks and Mr G. C. Scorgie, the former of whom has kindly agreed to the references in this paper to his unpublished extension of the Penney–Taylor theory. At Aldermaston, a large number of preliminary calculations were done on the Deuce computer by Mr B. W. Pearson, and, in later computation carried out on the I.B.M. computers, assistance was given by Dr R. Palmer. Finally, the authors are grateful to Dr L. F. Cooling (Building Research Station, Garston) and Dr R. E. Gibson (Department of Civil Engineering, Imperial College of Science and Technology, London) for their advice on the choice of physical data for soils, and to Professor R. Hill, F.R.S. for his comments on this paper.

Acknowledgement is made to the Controller of H.M. Stationery Office for permission to publish this paper.

References

Andriankin, E. I. & Koryavov, V. P. 1959 *Dokl. Akad. Nauk S.S.S.R.* **128**, 257. English translation: 1960 *Soviet Phys.-Dokl.* **4**, 966.

Biot, M. A. 1941 *a, b* *J. Appl. Phys.* **12**, 155, 426.

Biot, M. A. 1955 *J. Appl. Phys.* **26**, 182.

Biot, M. A. 1956 *a* *J. Appl. Mech.* **23**, 91.

Biot, M. A. 1956 *b,c* *J. Acoust. Soc. Amer.* **28**, 168, 179.

Biot, M. A. & Clingan, F. M. 1941 *J. Appl. Phys.* **12**, 578.

Biot, M. A. & Clingan, F. M. 1942 *J. Appl. Phys.* **13**, 35.

Bishop, A. W. & Eldin, G. 1950 *Géotechnique*, **2**, 13.

Bishop, R. F., Hill, R. & Mott, N. F. 1945 *Proc. Phys. Soc.* **57**, 147.

Chadwick, P. 1959 *Quart. J. Mech. Appl. Math.* **12**, 52.

Chadwick, P. 1962 *Quart. J. Mech. Appl. Math.* **15**, 349.

Christopherson, D. G. 1946 Unpublished Report, Ministry of Home Security.

Cole, R. H. 1948 *Underwater explosions.* Princeton University Press.

Coulomb, C. A. 1773 *Mém. Math. et Phys.* **7**, 343.

Cox, A. D. 1962 *Int. J. Mech. Sci.* **4**, 371.

Cox, A. D., Eason, G. & Hopkins, H. G. 1961 *Phil. Trans.* A, **254**, 1.

Craggs, J. W. 1961 *Progress in solid mechanics*, vol. II (ed. I. N. Sneddon & R. Hill), ch. IV, Plastic waves, p. 143. Amsterdam: North-Holland Publ. Co.

Cristescu, N. 1958 *Dynamic problems in the theory of plasticity* (in Roumanian). Bucharest: Academia Republicii Populare Romîne.

Cristescu, N. 1960 *Plasticity: Proceedings of the Second Symposium on Naval Structural Mechanics* (ed. E. H. Lee & P. S. Symonds), p. 385. Oxford, etc.: Pergamon Press Ltd.

PHILOSOPHICAL TRANSACTIONS OF THE ROYAL SOCIETY A MATHEMATICAL, PHYSICAL & ENGINEERING SCIENCES

Devonshire, A. F. & Mott, N. F. 1944 Unpublished Report, Ministry of Supply.
Drucker, D. C. 1953 *J. Mech. Phys. Solids*, **1**, 217.
Drucker, D. C. & Prager, W. 1952 *Quart. Appl. Math.* **10**, 157.
Gill, S. 1951 *Proc. Camb. Phil. Soc.* **47**, 96.
Glasstone, S. (Ed.) 1962 *The effects of nuclear weapons*, rev. ed. Washington, D.C.: United States Atomic Energy Commission.
Green, A. E. & Zerna, W. 1954 *Theoretical elasticity*. Oxford University Press.
Haythornthwaite, R. M. 1960*a* *Proc. Amer. Soc. Civ. Engrs, J. Soil Mech. Found. Div.* **86**, no. SM5, p. 35.
Haythornthwaite, R. M. 1960*b* *Plasticity: Proceedings of the Second Symposium on Naval Structural Mechanics* (ed. E. H. Lee & P. S. Symonds), p. 185. Oxford, etc.: Pergamon Press Ltd.
Hill, R. 1948 Unpublished Report, Ministry of Supply.
Hill, R. 1950 *The mathematical theory of plasticity*. Oxford University Press.
Hill, R. 1961 *Progress in solid mechanics*, vol. II (ed. I. N. Sneddon & R. Hill), ch. VI, Discontinuity relations in mechanics of solids, p. 247. Amsterdam: North-Holland Publ. Co.
Hill, J. E. & Gilvarry, J. J. 1956 *J. Geophys. Res.* **61**, 501.
Hopkins, H. G. 1960 *Progress in solid mechanics*, vol. I (ed. I. N. Sneddon & R. Hill), ch. III, Dynamic expansion of spherical cavities in metals, p. 85. Amsterdam: North-Holland Publ. Co.
Hopkins, H. G. 1961 *Appl. Mech. Rev.* **14**, 417.
Hunter, S. C. 1958 Unpublished Report, Ministry of Supply.
Jeffreys, H. 1931 *Cartesian tensors*. Cambridge University Press.
Jenike, A. W. & Shield, R. T. 1959 *J. Appl. Mech.* **26**, 599.
Jones, H. & Miller, A. R. 1948 *Proc. Roy. Soc.* A, **194**, 480.
Kochina, N. N. & Mel'nikova, N. S. 1958 *Prikl. Mat. Mekh.* **22**, 3. English translation: 1958 *J. Appl. Math. Mech.* (PMM), **22**, 1.
Koiter, W. T. 1953 *Quart. Appl. Math.* **11**, 350.
Kompaneets, A. S. 1956 *Dokl. Akad. Nauk S.S.S.R.* **109**, 49.
Kukudzhanov, V. N. 1958 *Akad. Nauk Armyan. S.S.R. Izv. Fiz.-Mat. Estest. Tekhn. Nauki*, **11**, 61. English translation: 1960 *United States Joint Publications Research Service*, no. 6103. Washington, D.C.: Office of Technical Services, United States Department of Commerce.
Lewin, L. 1958 *Dilogarithms and associated functions*. London: Macdonald and Co. Ltd.
Lovetskiĭ, E. E. 1958 *Izv. Akad. Nauk S.S.S.R. Otd. Tekhn. Nauk*, no. 1, p. 120.
Lovetskiĭ, E. E. 1959 *Akad. Nauk S.S.S.R. Izv. Mekh. Mashinostroi*, no. 6, p. 36.
Pokrovskiĭ, G. I. & Fedorov, I. S. 1957 *Action of shock and explosion on deformable media* (in Russian). Moscow: Promstroiizdat. English translation: 1962 *UCRL*-TR-777(L). Livermore, Calif.: University of California, Lawrence Radiation Laboratory.
Prager, W. 1953 *J. Appl. Mech.* **20**, 317.
Prager, W. 1955*a* *Proceedings of the Second United States National Congress of Applied Mechanics* (ed. P. M. Naghdi), p. 21. New York: Amer. Soc. Mech. Engrs.
Prager, W. 1955*b* *Proc. Instn Mech. Engrs, London*, **169**, 41.
Rinehart, J. S. & Pearson, J. 1954 *Behavior of metals under impulsive loads*. Cleveland, Ohio: Amer. Soc. Metals.
Romashov, A. N., Rodionov, V. N. & Sukhotin, A. P. 1958 *Dokl. Akad. Nauk S.S.S.R.* **123**, 627. English translation: 1959 *Soviet Phys.-Dokl.* **3**, 1283.
Sedov, L. I. 1957 *Similarity and dimensional methods in mechanics* (in Russian), 4th ed. Moscow: Gosudarstv. Izdat. Tekhn.-Teor. Lit. English translation: 1959. New York: Academic Press Inc.
Shield, R. T. 1955 *J. Mech. Phys. Solids*, **4**, 10.
Skempton, A. W. & Bishop, A. W. 1954 *Building materials: their elasticity and inelasticity* (ed. M. Reiner), ch. X, Soils, p. 417. Amsterdam: North-Holland Publ. Co.

PHILOSOPHICAL TRANSACTIONS OF THE ROYAL SOCIETY A MATHEMATICAL, PHYSICAL & ENGINEERING SCIENCES

Stanyukovich, K. P. 1960 *Unsteady motion of continuous media*. London, etc.: Pergamon Press Ltd.

Taylor, G. I. 1940 Report, Ministry of Home Security. 1958 *The scientific papers of Sir Geoffrey Ingram Taylor* (ed. G. K. Batchelor), vol. 1: *Mechanics of solids*, p. 456. Cambridge University Press.

Taylor, G. I. 1950 *Proc. Roy. Soc.* A, **200**, 235.

Terzaghi, K. 1943 *Theoretical soil mechanics*. New York: John Wiley and Sons, Inc.

Thomas, T. Y. 1961 *Plastic flow and fracture in solids*. New York, etc.: Academic Press Inc.

Thornhill, C. K. 1957 Unpublished Report, Ministry of Supply.

Zvolinskiĭ, N. V. 1960 *Prikl. Mat. Mekh.* **24**, 126. English translation: 1960 *J. Appl. Math. Mech.* (PMM), **24**, 166.

PHILOSOPHICAL TRANSACTIONS OF THE ROYAL SOCIETY A MATHEMATICAL, PHYSICAL & ENGINEERING SCIENCES